Design of the SCOUT II Quadruped with Preliminary Stair-Climbing

Robert F. Battaglia

Department of Mechanical Engineering
McGill University, Montréal, Canada

May 1999

A Thesis submitted to the Faculty of Graduate Studies and Research in partial fulfilment of the requirements of the degree of Master of Engineering.

0-612-50591-X

Dedicato alla mia famiglia

Dedicated to my family

Abstract

Mobile robots are taking an important role in society. They are being used in many industries from entertainment to space exploration. McGill University's Ambulatory Robotics Laboratory recently introduced a new class of quadruped robots - the SCOUT series. These robots feature only one actuated degree of freedom per leg. By keeping the degrees of freedom to a minimum, this class of robots is simpler, less expensive and more reliable than most legged robots built to date. The design and development of the second of these robots, SCOUT II, is the topic of this thesis. Unlike its predecessor SCOUT I, SCOUT II has unactuated prismatic knee joints in addition to the revolute joints, which allow compliant walking, stair-climbing and running gaits to be explored. SCOUT II is a self-contained, autonomous mobile robot whose primary purpose is to serve as the testbed for the various gaits that are being developed. This thesis describes the robot's mechanical design, electrical design, sensors and construction. A preliminary stair-climbing algorithm is developed and simulated. An attempt, though partially unsuccessful, is made to implement this algorithm on SCOUT II. The reasons for the discrepancies between the simulations and the actual system are outlined. This will provide useful insight on modelling parameters, actuator limits and robot dynamics for future stair-climbing, walking and running algorithms that are developed for SCOUT II.

Résumé

Les robots mobiles jouent un rôle de plus en plus important dans la société. On les retrouve dans de nombreuses industries, du divertissement à l'exploration spatiale. Le Laboratoire de Robotique Ambulatoires de l'Université McGill a introduit la série SCOUT, qui est une nouvelle catégorie de robots quadrupèdes dotés d'un seul degré de liberté actionné pour chaque jambe. Le maintien au minimum des degrés de liberté simplifie cette catégorie de robots, en réduit le coût et en augmente la faibilité. La conception du deuxième de ces robots, SCOUT II, est le sujet de la présente thèse. À la différence de SCOUT I son prédécesseur, SCOUT II est équipé d'une articulation de genou prismatique non actionnée en plus d'une articulation rotoïde, ce qui permet l'exploration de la marche souple, de la montée d'escalier et de mouvements de course. SCOUT II est un robot mobile autonome dont le but principal est de servir de banc d'essai pour divers types de mouvements qui sont mis au point. La présente thèse décrit la conception mécanique, la conception électrique, les capteurs et la construction du robot. Nous élaborons et simulons ensuite un algorithme préliminaire de montée d'escalier. Une tentative, quoique partiellement infructueuse, est faite afin d'appliquer cet algorithme à SCOUT II. Les raisons des divergences entre les simulations et le système lui-même sont exposées. Ces explications apporteront une compréhension utile des paramètres de modélisation, des limites des actionneurs et des forces dynamiques du robot pour les futurs algorithmes de montée d'escalier, de marche et de course qui sont élaborés pour SCOUT II.

Acknowledgements

I would like to thank the following people for their assistance through the course of my research.

- Professor Martin Buehler, my supervisor, for his constant support and motivation to me and the project. There were times when we would meet on a daily basis to discuss and iron out details of the design. It is to him that I owe the success of SCOUT II and this thesis.
- The Natural Sciences and Engineering Research Council (NSERC) for their support through a graduate PGS A scholarship.
- Ken Yamazaki, fellow graduate student, for his hard work and dedication to the SCOUT series which served as a benchmark for my work. He was always available to help debug the software and the electronics.
- Dave McMordie for his continuous help with the electronics on SCOUT II. Dave always does more than his share yet he still feels like he hasn't done enough.
- Sami Obaid, fellow ARL Master's student, for his work on the sensors and electronics and for being there whenever I needed help.
- Anca Cocosco for her hard work on developing walking algorithms and for making sure that things were always my fault.
- Geoff Hawker and Marc Leblanc, systems administrators for ARL, for keeping the PC's in tip-top shape and for being there with their support, guidance and advice.

- Mojtaba Ahmadi for his extensive knowledge of robotics.
- Martin de Lasa for his work on getting the RF units operational.
- Joey Mennitto, friend and ex-ARL member, for getting me interested in robotics, for helping with suggestions for SCOUT II, and for reviewing a rough draft of this thesis.
- Joseph Sarkis for helping with the leg design and pinpointing Working Model bugs.
- Nadim El-fata, Research Engineer for ARL, for his work on developing the SPP/SPI system.
- Alois Hueppin, Tony Micozzi, Danen Chellan and Roy Westgate, the technicians in the Mechanical Engineering Machine Shop, for their excellent work on the machined parts for SCOUT II and for not complaining every time I went to see them with a rush job.
- Jan Binder, CIM's system administrator, for keeping the lab's UNIX system up and running, and for being there when I needed help with a Pro/Engineer installation.
- Iyad Abdul-baki, Katja Dauster, Shervin Talebinejad, Didier Papadopoulos and Liana Mitrea, fellow ARL members, for their morale support and for making the lab a great working environment.
- The CIM administrative staff, Marlene Gray, Kathleen VanderNoot, and Ornella Cavaliere, for ensuring that things ran smoothly.
- Terra Aerospace Corp. for helping me determine the specifications for SCOUT II.
- Last but not least, my family, for their constant support even when I didn't quite deserve it. Extra special thanks go out to my sister and her husband for proof reading my thesis and making valuable recommendations.

Contents

List of Figures

List of Tables

Chapter 1

Introduction

1.1 Motivation

Robots have begun to take an important role in today's society. Wheeled and tracked robots are being used for space exploration, bomb disposal, surveillance and in forestry applications. They provide a means of locomotion to a place or situation that may be too dangerous or too inaccessible to a human. However, wheeled and tracked vehicles are often limited to relatively flat terrain. It is the increased dexterity and maneuverability of legged robots that make them appealing. They have a potential to traverse a wide variety of terrain - both natural (mountains, forests) and artificial (stairs, steps, ditches).

Most of the research into legged locomotion thus far has gone towards trying to imitate a human or animal. This has lead to robots with high degrees of freedom which complicates control. In addition, the cost of these complex creatures far exceeded their economic value. The focus of this work has been to develop a legged robot with an agility superior to either wheeled or tracked vehicles, but less complex and less expensive than current legged robots.

1.2 Historical Background

Recently, a tremendous amount of work has gone into developing wheeled, tracked and legged robots that can negotiate a variety of terrains. Some of the more impressive and/or revolutionary robots will be presented. They will be divided by locomotion type: wheeled and tracked robots, and legged robots. Numerous quadrupeds will be discussed, followed by other multi-legged robots that have been successful at climbing steps and crossing rugged terrain.

Wheeled and Tracked Robots

Wheeled and tracked robots are, to this day, the most popular type of robots used in the surveillance, bomb disposal, exploration and entertainment industries. Numerous companies, like Terra Aerospace [68] and IS Robotics [38], and many research institutions are actively developing these types of vehicles. Though these robots are very easy to control and maneuver on flat ground, they have difficulty surpassing obstacles like crevices, logs and stairs. Researchers have tried different solutions to make wheeled and tracked systems more dextrous.

The HELIOS series of robots developed at the Tokyo Institute of Technology, used large wheels and tracks to roll over small obstacles and steps. HELIOS-I (1989) and HELIOS-II (1989) [25, 23, 26] used a track system with little nipples that helped grip the corners of the steps. HELIOS-III (1991) [28] had four custom-made Spring Wheels - wheels composed of a metal rim covered with a coil spring. HELIOS-IV (1995) [27] moved away from the custom-made wheels and used four low pressure tires. Significant improvements were made in the six-wheeled HELIOS-V (1999) [70]. Two central high pressure tires allowed for efficient rolling on flat ground while four low pressure outside tires aided the vehicle in gripping steps and obstacles. In addition, the wheels were connected by active links which increased the maximum obstacle height that the robot could surpass. HELIOS-V successfully negotiated stairs with a rise of 16cm and a run of 30cm. A picture of this robot is provided in Figure 1.1.

Another wheeled robot that was successful at stair-climbing was the Enhanced Wheel System (EWS) by Taguchi (1995) [67] that climbed steps with a rise of 15cm and a run of 35cm (the robot is 110cm long, 57cm high and weighs 35kg). A more impressive, though more complex, example of a wheeled robot is the Amooty [1]. It is a four-wheeled maintenance vehicle where each wheel consists of three robot arms each with a small wheel (see Figure 1.2).

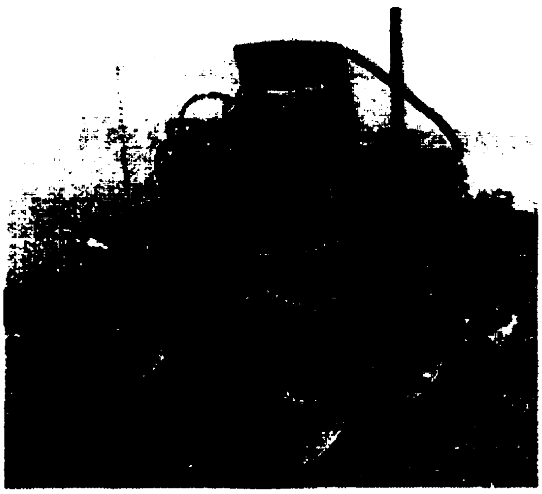

Figure 1.1: *HELIOS-V, 1999 [70].*

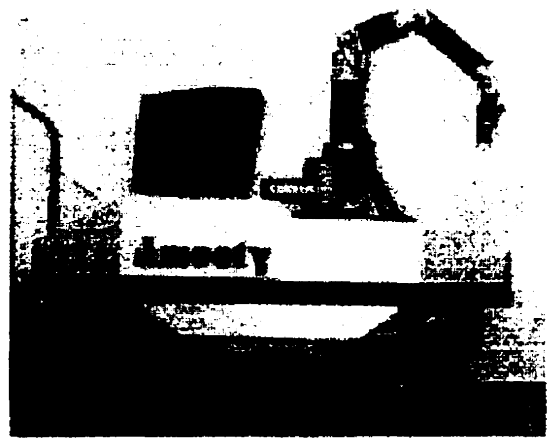

Figure 1.2: *Amooty, 1985 [1].*

Tracked vehicles were thought to be better at climbing steps due to the increased traction that the tracks provided. Merlin [68] is a simple tracked vehicle that uses its robotic arm to get over obstacles and lift itself onto the first step of a staircase (see Figure 1.3). The Scorpion [68] uses two angled aluminum rods to get onto the first step.

Robots like the Variable Configuration Tracked Vehicle (1990) [39] and the entire Andros series [74] use an articulated track systems to negotiate obstacles. The Andros Mark V-A [74], shown in Figure 1.4, can operate on virtually any surface including sand, mud, gravel, grass and snow. It can climb stairs and cross ditches as wide as 0.6 meters.

Some researchers, like Maeda, Tsutani and Hagihara with the MRV-1 [44], used four independent tracks (see Figure 1.5).

Figure 1.3: *Merlin climbing stairs, 1998 [68].*

Figure 1.4: *Andros Mark V-A, 1989 [74].*

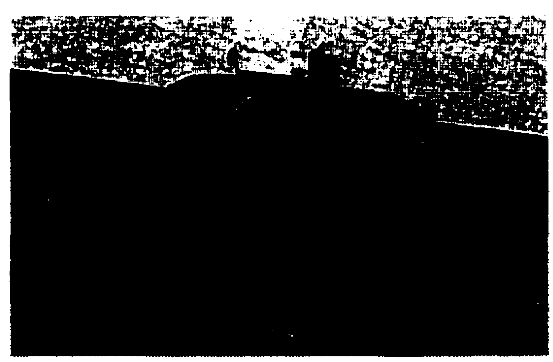

Figure 1.5: *MRV-1, 1985 [44].*

Legged Robots

M. H. Raibert is considered by many to be the pioneer of legged locomotion, particularly when it comes to dynamically stable robots. Some of his robots include two planar robots (a monopod and a biped) and three 3D robots (a monopod, a biped and a quadruped) [63]. Though a lot of information has been published about their running abilities, information on their stair-climbing abilities has been limited [33]. A picture of Raibert's quadruped is provided in Figure 1.6. It has three hydraulically

Figure 1.6: *The MIT Quadruped, 1984 [63].*

actuated degrees of freedom per leg (revolution and abduction at the hip, and prismatic at the knee). With a length of 1.05m and a height of 0.95m, it weighs in at just over 25kg.

Numerous quadrupeds have been developed with a variety of degrees of freedom per leg. Scamper by Furusho, Sano, Sakaguchi and Koizumi [15], has two rotational degrees of freedom per leg each actuated by DC servo motors and a belt-pulley system (see Figure 1.7). It was capable of walking and running using bounce and gallop gaits.

The Exploratores I [7] and Exploratores II [71] are two very lightweight quadrupeds with three degrees of freedom per leg. RC servo motors are used for actuation. A photograph of Exploratores I is provided in Figure 1.8.

The Kimura Laboratory from Japan developed the Collie series of robots. Both

Figure 1.7: *Scamper, 1995 [15].*

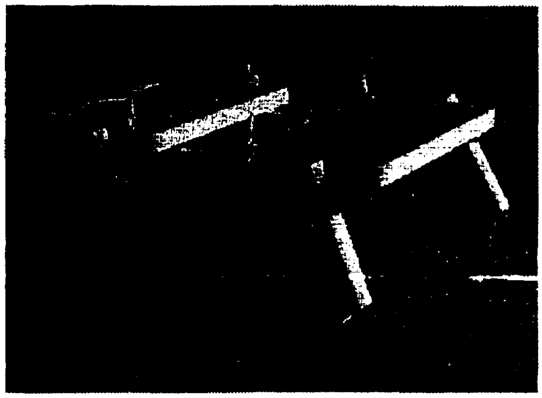

Figure 1.8: *Exploratores I, 1998 [7].*

Collie 1 [49] and Collie 2 [41] have legs with three degrees of freedom about the pitch axis and two about the roll axis. On Collie 1, two pitch axes and one roll axis joints are powered by a DC servo motor. The pitch and roll axis joints located at the ankle are unactuated. On Collie 2, only the roll axis joint at the ankle is unactuated. Both robots are approximately 0.42 meters long, 0.38 meters tall and weight under 7 kg. The slightly larger of the two robots, Collie 2 is shown in Figure 1.9.

Figure 1.9: *Collie 2, 1990 [41].*

Figure 1.10: *Patrush, 1998 [40].*

Another robot from the Kimura Laboratory is the Patrush [40]. Similar in size to the Collie robots, the Patrush has three revolute degrees of freedom about the pitch axis. The two top joints in each leg are actuated by 23W DC servo motors, while the lower ankle joint is unactuated. A spring loaded limb can be added to the passive foot to allow for running gaits. A photograph of the Patrush in its walking configuration is provided in Figure 1.10.

An interesting design was conceived by Cordes, Berns et al. This quadruped's four degree of freedom legs can be converted between reptile-like and mammal-like configurations (see Figure 1.11) [10]. The body of the robot has an additional four degrees of freedom. All degrees of freedom are actuated through ball screws and rare-earth DC servo motors. To this date, the prototype leg has been built and tested.

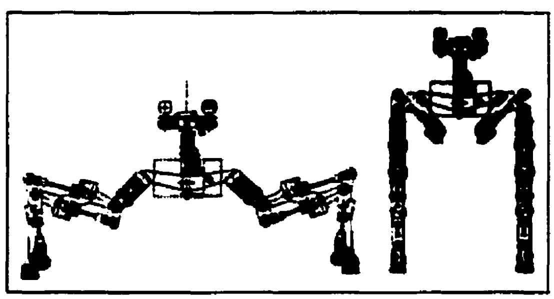

Figure 1.11: *The two leg configurations of the Four-Legged Walking Machine, 1997 [10].*

Two non-conventional six-legged walkers were developed by Ota, Inagaki, Yoneda and Hirose. They are called the ParaWalker-S1 and ParaWalker-II [55, 54], and consist of two three-legged platforms connected via a six degree of freedom parallel manipulator (see Figure 1.12).

As for robots that have proven their ability to traverse rugged terrain, perhaps the most impressive is the eight-legged Dante II [73] robot which descended into the volcano Mount Spurr in Alaska in July of 1994 (see Figure 1.13).

Both MELCRAB-1 and MELCRAB-2 (1986) [43] hexopods successfully climbed stairs. The prototype one-third scale MELCRAB-I has six legs each with two degrees of freedom. These include a prismatic knee joint and a revolute four bar linkage which

Figure 1.12: *ParaWalker-II, 1998 [55, 54].*

Figure 1.13: *DANTE II descending Mount Spurr, 1994 [73].*

produces an approximate straight line motion at the toe. The full size MELCRAB-II incorporates an extra degree of freedom in the body to allow for steering. It weighs 440kg, is 1.276m long, 0.940m wide and 1.940m high. It successfully climbed stairs with a rise of 18cm and a depth of 28cm.

Bipeds that successfully negotiated a stairwell include the SD series robots and, more recently, the Honda P2 [34]. Zheng and Sias developed the SD-1 [17] biped with two degrees of freedom per leg and the SD-2 [76] biped with four degrees of freedom per leg. The SD-1 has only revolution and abduction at the hip, while the SD-2 also has a two degree of freedom ankle joint. These ankle joints were added to help stabilize standing and dynamic walking. The Honda P2 [34] humanoid robot stands over 1.8 meters tall and is capable of walking, turning, climbing stairs, pushing a cart and tightening a nut. It has a total of thirty degrees of freedom in its arms and legs. A picture of the robot is provided in Figure 1.14. The P3 robot is a slighter smaller version of the P2 that makes use of magnesium to reduce its weight (130 kg versus 210 kg for the P2).

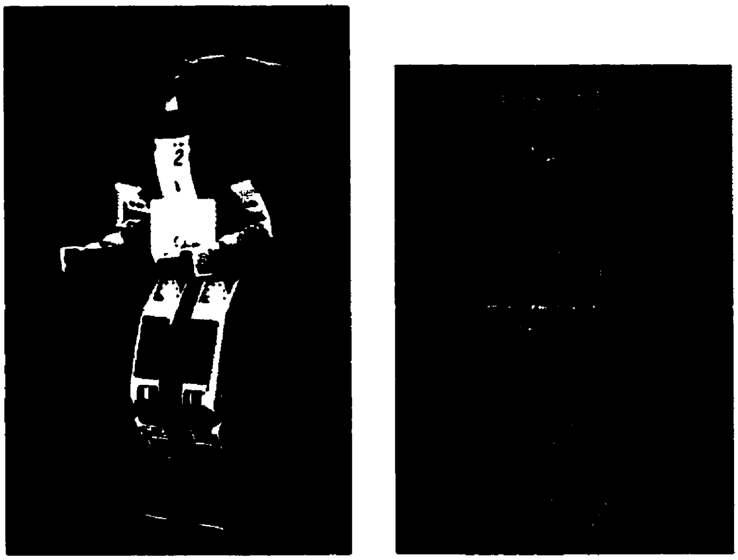

Figure 1.14: *The Honda P2 (left) and P3 (right), 1998 [34].*

Other successful stair-climbing robots include the PV II [22] (see Figure 1.15), TITAN III (1985) [24], TITAN IV (1989) [31] and TITAN VI (1995) [30], all of which have four legs and used a static gait. Figure 1.16 shows the most recent robots in the TITAN series, TITAN VII [32] and TITAN VIII [29].

Figure 1.15: *PV II, 1984 [22].*

An original and impressive design, by Matsumoto et al., is called the Biped Type Leg Wheeled Robot [46] (see Figure 1.17). It is a biped robot with a wheel at each foot. This design takes advantage of both wheeled and legged designs. However, not

Figure 1.16: *TITAN VII, 1997 [32] (left) and TITAN VIII, 1998 [29] (right).*

having a flat foot for support makes stability very difficult. Nonetheless, it successfully negotiated steps with a rise of 6.3cm and a depth of 20cm.

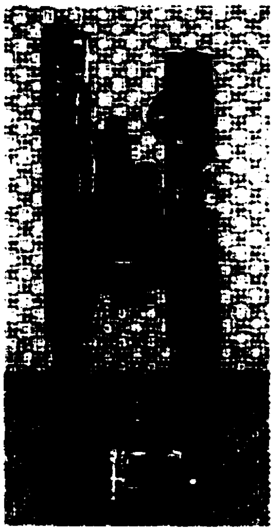

Figure 1.17: *The Biped Type Leg Wheeled Robot, 1998 [46].*

1.3 Progress at the Ambulatory Robotics Laboratory

The work at the Ambulatory Robotics Laboratory (ARL) at McGill's Center for Intelligent Machines (CIM) focuses on developing practical and autonomous legged robots. It was founded in 1991 by Professor Martin Buehler.

The first such robot was the ARL Monopod [19]. This work was similar to that of Raibert with the primary difference of using electric actuation as opposed to hydraulic. The ARL Monopod II [5], shown in Figure 1.18, aimed at reducing power consumption primarily by adding compliance at the hip.

The Compliant Articulated Robotic Leg (CARL) [47, 18] (see Figure 1.19) was then developed as a prototype leg that was to form a four-legged robot. However, the

Figure 1.18: *The Monopod II, 1996 [5].*

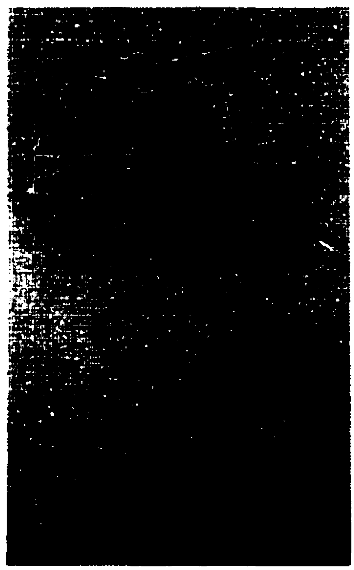

Figure 1.19: *CARL, 1995 [47, 18].*

high cost, complex design and difficulty in controlling the high number of degrees of freedom made a robot with four of these legs unachievable. Hence, the focus turned towards developing complete autonomous systems with simpler legs.

Late in 1996, the idea behind the SCOUT series was born. The plan was to develop a series of robots with only one actuated degree of freedom per leg. This would reduce cost and complexity, and increase reliability. The first robot in the series, SCOUT I [75, 8], can be seen in Figure 1.20. Even with its inherent simplicity, it was shown to be capable of walking, turning, side stepping, sitting and laying down, and step and stair climbing (refer to www.cim.mcgill.ca/~arlweb for more information and videos).

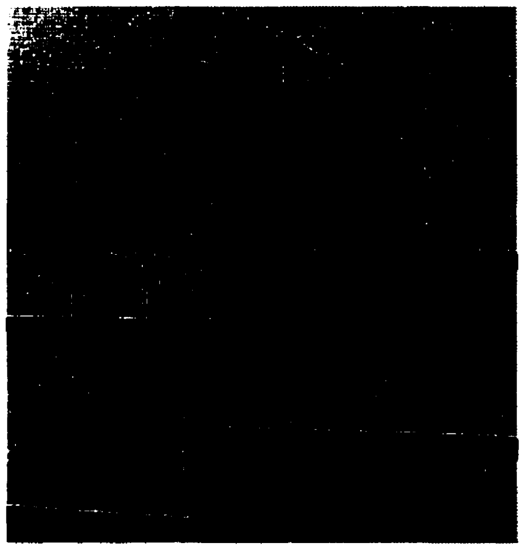

Figure 1.20: *SCOUT I, 1997 [75].*

With the success of SCOUT I, work began on a larger, more robust version that would demonstrate industrial applications. This robot was named SCOUT II and is the primary focus of this thesis. In addition to the one actuated degree of freedom per leg, SCOUT II contains an extra unactuated linear degree of freedom at each leg. This leg compliance allows running and compliant walking gaits to be explored.

Current research at ARL focuses around this robot. Anca Cocosco recently developed stiff-legged walking algorithms while Martin de Lasa is working on compliant walking. Joseph Sarkis and Didier Papadopoulos are working on developing running gaits. Shervin Talebinejad will investigate compliant stair-climbing. Geoff Hawker is working on a new leg design for the SCOUT series that has an unactuated rotational knee joint.

1.4 Author's Contributions

The author's contributions come mainly from the design and development of a quadruped robot that will become a testbed for developing control strategies for walking, running and stair-climbing. More detailed contributions include:

- Mechanical design of the quadruped robot, SCOUT II (with regular consultations with and recommendations from Professor Martin Buehler).
- Sourcing and testing of the motors and gearheads (with the help of Jason Fabro and Graeme Hartlen for the testing).
- Sourcing of numerous sensors and electronic components used on SCOUT II including the PC board, RF units, leg potentiometers, batteries, PWM servo amplifiers, and camera and laser RC servo units.
- Design of the electrical layout and wire routing, and its subsequent implementation (with the help of David McMordie for the high power wiring).
- Development of stair-climbing simulations using Working Model [42].
- Preliminary implementation of these stair-climbing strategies on SCOUT II.

1.5 Organisation of Thesis

The thesis is organised as follows. Chapter 2 discusses the mechanical design and construction of SCOUT II. The sensors and electronics on the robot are discussed in Chapter 3. Chapter 4 primarily discusses stair-climbing, but also describes SCOUT II's walking and running abilities. Lastly, Chapter 5 presents the conclusions and proposed future work and recommendations. The appendices include: Mechanical Drawings (Appendix A), Circuit Diagrams (Appendix B), Stress Analysis (Appendix C), Mass (Appendix D), Cost (Appendix E) and Data Sheets (Appendix F).

Chapter 2

Mechanical Design and Construction

A methodical approach to SCOUT II's design ensured its success. The design process used was similar to the ones outlined in [57, 11, 13] which involve task clarification, conceptual design and embodiment design. Task clarification (Section 2.1) involves the collection of information (Chapter 1), the formulation of the problem (Section 2.1.1) and the specification of the requirements and constraints (Section 2.1.2). In conceptual design (Section 2.2), general design issues are addressed which involve the form and layout of the robot. Embodiment design (Section 2.3) deals with the details of the robot's design. The construction of the robot and the costs associated with it are discussed in Section 2.4 and lastly, Section 2.5 summarizes the mechanical design of SCOUT II by listing relevant dimensions and mechanical properties.

2.1 Task Clarification

2.1.1 Problem Formulation

The plan for SCOUT II was to design and build a larger, more robust version of SCOUT I [75, 8] that could be used to implement and evaluate control strategies for walking, running and stair-climbing with the intention for use in industrial applications. Since this robot is to be used for testing and experimentation, it is of utmost importance that it be adjustable, modular and expandable. The adjustability of parameters like geometry, mass properties and actuator torque/speed characteristics will ensure that the mechanics of the robot will not limit the implementation of the control strategies developed. Modularity will allow for quick repairs and/or replacement of components should they be damaged. It will also allow parts to be changed in order to try new concepts. Lastly, the design should allow for expansion, say, for the addition of sensors.

Though the problem appears quite simple, it involves a significant amount of work. The robot must be light enough to be easily carried (an important feature for commercialisation) yet be sturdy enough to withstand the abuse of testing and experimenting. It must contain a certain amount of sensors in order to sense its environment and for analysis of the experimental runs. Communication through a wireless link with the operator sending directional commands via a Graphical User Interface (GUI) would be advantageous for demonstration purposes.

2.1.2 Specifications

The required specifications for SCOUT II were determined in conjunction with Terra Aerospace Corporation [68], an Ottawa, Ontario based company which develops and sells robots for surveillance and bomb disposal purposes. Their vast experience working with robots for this industry proved to be extremely helpful in determining the specifications for SCOUT II. A summary of the specifications is contained in Table 2.1. Each specification is either listed as an absolute requirement (*Demand*) or as a desired requirement (*Wish*). The minimum requirements for stair dimensions were taken from The Canadian Housing Code (1990) [53] and the National Building Code (1990) [52], and are provided in Table 2.2. The terminology used is defined in Figure 2.1. The run is the distance between two consecutive steps and the tread width is the

Item	*Demand/Wish*
Maximum operational length of 889mm (35")	Demand
Maximum operational width of 508mm (20")	Demand
Maximum mass of 25 kg including operating hardware	Demand
Capable of carrying a 2.5 kg payload	Demand
Simple remote control via directional tele-operator commands	Wish
Robot is stable when stationary	Demand
Speed of 3.6 km/h (1 m/s) on flat terrain	Wish
Capable of operating on sloped ground with +/-20% grade	Demand
Capable of changing direction of travel	Demand
Capable of negotiating stairs with a rise up to 200mm	Demand
Capable of negotiating stairs with a minimum run of 210 mm	Demand
Capable of negotiating spiral staircases	Wish
Capable of starting/stopping on stairs	Demand
Capable of recovering from falls from the up-side-down position	Demand
Minimum of one hour of continuous walking on flat terrain	Demand
Minimum four hour operation in 'surveillance mode'	Demand
Capable of climbing stairs continuously for 30 minutes	Wish
Quick change 24 V DC on-board power supply	Demand
Reliable	Demand
Design simplicity	Demand
Has room for expansion of electronics and sensors	Demand
All components protected from impacts	Demand
Easy accessibility to all components (for repair or replacement)	Demand
Easy assembly/disassembly	Demand
Adjustable leg length	Wish
Adjustable body length	Wish
Adjustable body width	Wish
Low maintenance	Demand
On-board camera	Demand

Table 2.1: *SCOUT II Specification List.*

width of each step.

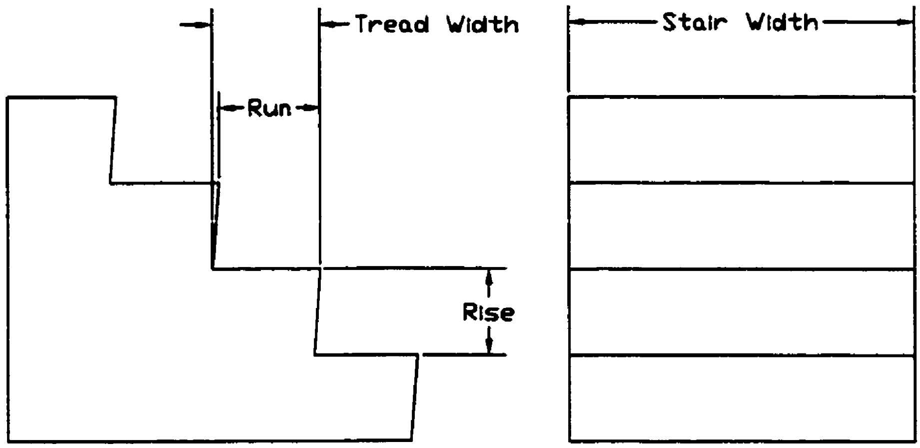

Figure 2.1: *Stair Terminology.*

	Canadian Housing Code (1990)[53]	*National Building Code (1980)*[52]
Maximum rise (mm)	200	200*
Minimum run (mm)	210	210*
Minimum tread width (mm)	235	235
Minimum stair width (mm)	860	860

Table 2.2: *Stair dimensions, from [53, 52]. (*Maximum rise and minimum run are 230 and 200 mm respectively for interior dwelling units to areas used for storage like attics and basements.)*

2.2 Conceptual Design

This section deals with the conceptual design of SCOUT II and is divided into four sub-sections: SCOUT II geometry and kinematics (Section 2.2.1), actuation (Section 2.2.2), layout (Section 2.2.3) and loading (Section 2.2.4).

2.2.1 Geometry and Kinematics

The goal of the SCOUT series is design simplicity. SCOUT I had only one actuated degree of freedom at each of the four legs. This is significantly less than most quadrupeds that have been built to date, which typically have three to four actuated degrees of freedom per leg. Like SCOUT I, SCOUT II also has one actuated degree of freedom per leg. However, it distinguishes itself from its predecessor by having a second unactuated degree of freedom at each leg which allows for leg compliance during walking, running and stair-climbing. Each leg is equipped with a prismatic spring joint. Other important issues with regard to the design of SCOUT II are to make it possible to operate in either compliant or fixed leg mode and permit full 360 degree rotation of its legs.

The factor that determined the overall size of SCOUT II was stair-climbing. Preliminary stair-climbing simulations on Working Model [42] were used to determine the approximate geometry of SCOUT II. In addition, the leg lengths were kept short in comparison to the hip length to facilitate SCOUT's ability to get up from a lying down position. This required the center of mass to be between the toes when all four legs were pointed in one direction.

2.2.2 Actuation

The selection of motors suitable for the task of controlling SCOUT II's legs was the first design task to be addressed. A typical motor's operating characteristics is shown in Figure 2.2. The figure includes plots of speed, efficiency, power and current versus torque. The dashed vertical line represents a typical operating point. The motor efficiency (η_{motor}), is defined as the ratio of (mechanical) output power over (electrical) input power.

$$\eta_{motor} = \frac{P_{mech}}{P_{elec}} = \frac{T \cdot \omega}{V \cdot I},$$

where T is the motor torque [Nm], ω is the motor speed [rad/s], V is the motor voltage [V], and I is the armature current [A]. The maximum efficiency is given by [37] as,

$$\eta_{max} = \left(1 - \sqrt{\frac{I_o}{I_A}}\right)^2$$

where I_o is the no load current [A] and I_A is the starting current [A].

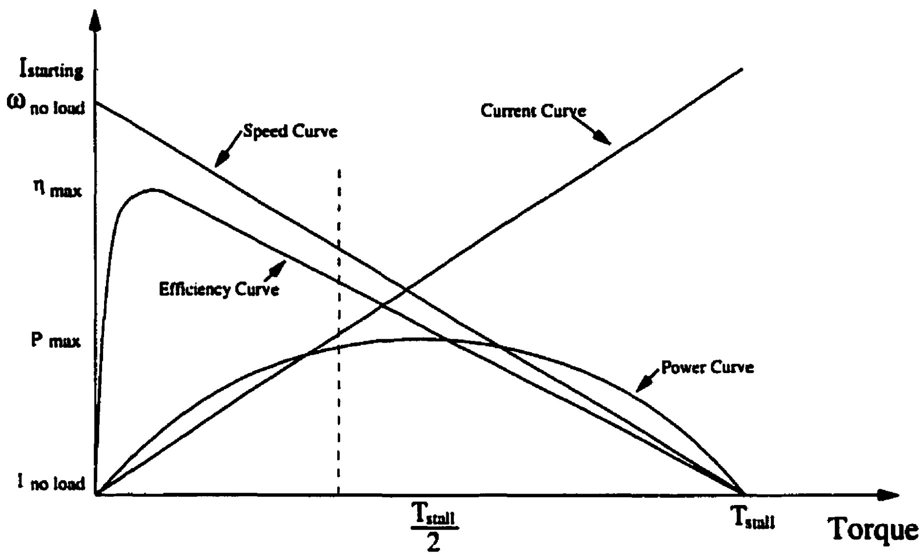

Figure 2.2: *Typical Motor Operating Characteristics, adapted from [37].*

Due to power limitations, there is a trade-off between torque and speed availability. This made it difficult to determine the requirements for SCOUT II's actuators. The nominal operating speed of the motor was determined by the robot's speed, specified to be 1 m/s or 3.6 km/h (see Table 2.1). This corresponds to an operating rotational speed of approximately 35 RPM hence,

$$\omega_{op} = 3.67\, rad/s. \tag{2.1}$$

The ability of SCOUT II to get up from a lying down position was used as a starting point to determine the required stall torque. Figure 2.3 shows a force diagram of SCOUT II. The following assumptions were made:

- The legs are massless and inertia-less.

- Both legs are of equal length, l.
- The entire mass of the robot, M, is concentrated at one point on the body (of length L) at a distance c from leg 1 (see Figure 2.3).
- The robot will use all four legs in order to get up.
- The body remains horizontal hence $\theta_1 = \theta_2 = \theta$.
- For the planar analysis, there are two motors per hip joint since both left and right legs contribute torque (hence the factor of 2 that multiplies the torques, T_1 and T_2, in Figure 2.3).
- Friction and slipping between the toes and the ground are neglected hence the reaction forces N_1 and N_2 are vertical.

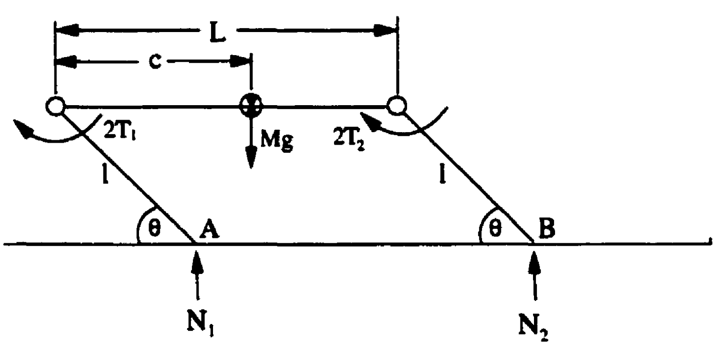

Figure 2.3: *Force Diagram.*

A static force analysis reveals

$$\sum F = 0 = N_1 + N_2 - Mg$$

$$N_1 + N_2 = Mg. \tag{2.2}$$

Taking the sum of the moments about point A, the normal force acting on leg 2 can be determined as

$$\sum M_A = 0 = LN_2 - (-l\cos\theta + c)$$

$$N_2 = \left(\frac{c - l\cos\theta}{L}\right) Mg. \tag{2.3}$$

Using Equations 2.2 and 2.3 the normal force for leg 1 is calculated as,

$$N_1 = Mg - \left(\frac{c - l\cos\theta}{L}\right) Mg. \tag{2.4}$$

In order to keep the robot in a specified position, the torque supplied at the hinge must balance out the normal force,

$$\frac{2T_1}{l\cos\theta} = N_1 \qquad \text{and} \qquad \frac{2\mathrm{T}_2}{\mathrm{l}\cos\theta} = \mathrm{N}_2.$$

Substituting for N_2 and N_1 from equations 2.3 and 2.4 results in

$$T_1 = \frac{Mgl}{2L}(L - c + l\cos\theta)\cos\theta, \tag{2.5}$$

$$T_2 = \frac{Mgl}{2L}(c - l\cos\theta)\cos\theta. \tag{2.6}$$

Equations 2.5 and 2.6 determine the required torques at each leg to hold the robot at a specific leg position. When the robot is standing up straight ($\theta = 90°$) the required torque is 0. When the robot is lying down ($\theta = 0°$) the required torques are at a maximum and have values of

$$T_1 = \frac{Mgl}{2L}(L - c + l), \tag{2.7}$$

$$T_2 = \frac{Mgl}{2L}(c - l). \tag{2.8}$$

Equations 2.7 and 2.8 determine the maximum stall torques that are required at the four leg joints to hold the robot at that position. Obviously, more torque will be required if the robot is to move.

The following approximate values were used to obtain a better understanding of the type and size of motor and transmission system required.

- The mass of the robot (M) was set to 25.0 kg.

- The length of the body (L) was set to 60 cm.
- The length of the legs (l) was set to 27.5 cm.
- The center of mass was at the midpoint of the body (i.e. $c = L/2$).

The front and rear maximum torques can now be calculated from Equations 2.7 and 2.8 as

$$\begin{aligned} T_1 &= \frac{(25.0)(9.81)(0.25)}{2(0.60)}(0.60 - 0.275 + 0.25)\ Nm \;=\; 29.4Nm, \\ T_2 &= \frac{(25.0)(9.81)(0.25)}{2(0.60)}(0.275 - 0.25)\ Nm \;=\; 1.3Nm. \end{aligned} \tag{2.9}$$

The power required was more difficult to estimate since it depended on the efficiency of the transmission system. It was known that the power (P) at the leg is the product of the torque and the rotational speed. Assuming that the system is operating at the motor's maximum power point, the torque will be approximately half the stall torque (the motor's maximum power point occurs at this point - see Figure 2.2). The resulting power required is,

$$\begin{aligned} P_{op} &= T_{op} \cdot \omega_{op} \\ &= \left(\frac{T_{stall}}{2}\right)\omega_{op} \\ &= \left(\frac{29.4Nm}{2}\right)3.67rad/s \\ &= 53.9\ W. \end{aligned} \tag{2.10}$$

The above analysis resulted in a minimum torque of about 30 Nm (Equation 2.9), a rotational speed of about 35 RPM (3.67 rad/s) (Equation 2.1) and a power of about 55 W (Equation 2.10).

Once these minimum requirements were determined, it was time to select the motor and the mode of transmission of power from motor to leg. Three main conceptual designs were considered and are described below. Initial designs had the legs attached directly to the output shaft of the motor or the gearhead. This posed two problems: (1) most commercially available motors and gearheads did not have outputs shafts that could readily handle the impact loads that the leg could transmit to it so additional supporting bearings would have to be added and (2), the motor/gearhead package had to be along the same axis, resulting in a robot that would be very wide.

Some of the options that were originally considered will be discussed in brief, while the final design will be discussed in full afterwards.

Option 1: Using a high torque, low speed motor (direct drive)

Initially a high torque, low speed motor was considered because of its simplistic appeal since no further speed reduction would be required. The leg could be attached directly to the output shaft of the motor, though extra bearings would have to be added to accommodate the impact loads. This design was identical to SCOUT I which had the legs attached directly to RC servos which feature integral gearing (see Figure 2.4). The problem with this design was that high torque, low speed motors are inevitably large in diameter. A motor with the required minimum stall torque would have been about 0.25m in diameter and over 15 kg (*Inland T-7215* [36], for example). Hence this option was discarded.

Option 2: Using an in-line motor with planetary gearhead

This option was also very intriguing due to its simplicity. The problems were with the resulting width of the robot and whether or not extra support would have to be provided to the output shaft. Only one package was found that did not require extra support bearings and at the same time was short enough to comply with the width constraints. This was to use a *Maxon 118776* with a *CGI 17PL1000* gearhead. The problem with this design was threefold. First, the motor and gearhead were not compatible. The motor would have to be shipped to CGI to be custom fitted onto the gearhead. This would have delayed the delivery time (by about 2 weeks) and increased

Figure 2.4: *Picture of SCOUT I showing the leg attached directly to a Hitec servo.*

costs (by about 350 CAN$). Second, the CGI gearhead was very expensive (840 US$ each) - more expensive than other planetary gearheads with the same reduction ratio. The reason for this is because the CGI gearhead had expensive bearings supporting the output shaft and used two stages to get the required reduction ratio, whereas other manufacturers used three. Third, given that the leg was attached directly to the gearhead, there was still the risk that an unexpected fall could transmit loads to it that were beyond its rating of 1780N.

Option 3: Using an in-line motor with an harmonic drive [20, 21]

Harmonic drives are very efficient and are seeing more and more use in robotic applications [47, 66, 34]. The harmonic drive by itself would not be able to support the impact loads, hence extra bearings would have to be added to the output shaft. This, however, would not have been a problem since the motor, harmonic drive and extra bearing package was still short enough that the width of the robot was within the specifications. The main problem with this design was the high cost associated with the purchase of four harmonic drives (844 US$ each).

Due to the problems with the aforementioned designs, the focus changed to coming up with a design that did not have the motors in-line. This involved staggering the two motors and using a toothed pulley and belt system to transmit the power to the leg (see Figure 2.5). Such a system had the following advantages:

- Since the motors were staggered, the minimum width of the robot is the length of one motor/gearhead package as opposed to two.
- The output shaft of the gearhead does not see any of the loads tranferred through the leg.
- Less expensive three stage gearheads without large output bearings could be used.
- The belt allowed for some compliance which would reduce the impact torques on the gearhead.
- Varying the sprocket size changes the gear ratio, thus allowing for more versatility.

The implemented design uses a *Maxon 118777* brushed, 90 Watt DC motor and a *Maxon 110404* three-stage planetary gearhead with a 72.38:1 gear ratio (see Figure 2.6). Appendix F contains the data sheet for the 90W Maxon motor and gearhead. Since SCOUT II was to operate at 24V, two different nominal voltage windings would have been suitable, the 15V and the 30V. The 30V winding was chosen because its higher torque constant (k_T) and lower speed constant (k_n) required a lower gear ratio.

Figure 2.7(a) shows the torque-speed curve specified by the manufacturer. Figure 2.7(c) shows the same torque speed curve but modified to take into account the gearhead ratio at its maximum rated efficiency of 68% (which, according to [37], is measured at maximum continuous torque and nominal speed). Detailed specifications are provided in Table 2.3. Table 2.4 and Figure 2.7(d) show the operating specifications of the SCOUT II system limited by voltage (24 V) and current (12 A). More

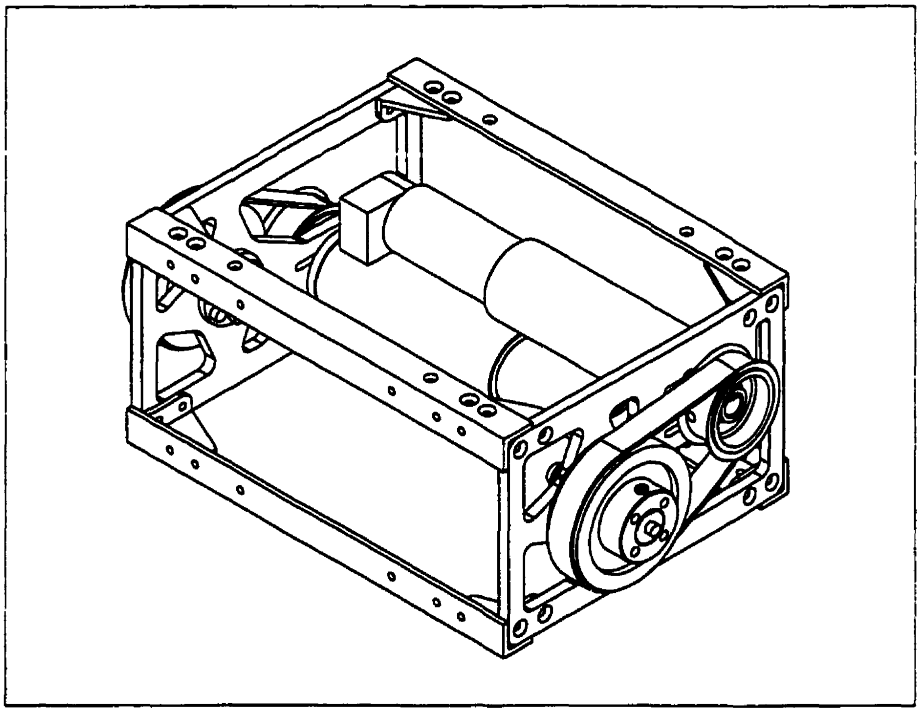

Figure 2.5: *Hip unit with staggered motor units and belt system.*

Figure 2.6: *Maxon 118777 brushed 90W DC motor, the Maxon 110404 gearhead with 72.38:1 ratio and the HP HEDS-5540 encoder.*

Motor Specs	(1)Nominal power	90 W
	(2)Nominal voltage	30 V
	(3)No load speed	7220 RPM
	(4)Stall torque	0.949 Nm
	(5)Maximum permissible speed	8200 RPM
	(6)Maximum continuous current	2.74 A
	(7)Maximum continuous torque	0.107 Nm
	(8)Maximum efficiency	84.1%
	(9)Torque constant	0.0389 Nm/A
	(10)Speed constant	246 RPM/V
	(11)Mass	0.340 kg
Gearhead Specs	(12)Gear ratio	72.38:1
	(13)Maximum permissible speed	5000 RPM
	(14)Maximum continuous torque	14.7 Nm
	(15)Maximum intermittent torque	24.5 Nm
	(16)Maximum efficiency (η)	68%
	(17)Mass	0.720 kg
Package Specs	(18)No load speed [(3)÷(12)]	99.8 RPM
	(19)Stall torque [(4)x(12)x16)] (assuming $\eta_{gearhead} = 68\%$)	46.7 Nm
	(20)Maximum continuous torque [(6)x(9)x(12)x(16)] (assuming $\eta_{gearhead} = 68\%$)	5.27 Nm
	(21)Maximum intermittent torque (limited by gearhead)	24.5 Nm
	(22)Mass	1.060 kg

Table 2.3: *Maxon 118777 brushed 90 Watt DC motor and Maxon 110404 planetary gearhead technical specifications, taken from [37].*

Operating Specifications		
Motor	(23)Operating voltage	24 V
	(24)Maximum current input†	12 A
	(25)Stall torque with 12 A [(24)x(9)]*	0.467 Nm
	(26)No load speed at 24 V [(23)x(10)]*	5904 RPM
Gearhead	(27)Stall torque [(25)x(12)x(16)]*	22.98 Nm
	(28)Continuous torque [(20)]*	5.27 Nm
	(29)No load speed [(26)x(12)]*	81.57 RPM

Table 2.4: *Motor/gearhead specifications with operating voltage of 24 V and operating current limited to 12 A. *Numbers refer to values from Table 2.3. † Current limited by PWM Servo amplifiers (see Section 3.3).*

details about these electrical limitations will be presented in Section 3.3. The pulley system consisted of a HTD toothed timing belt (see Figure 2.12). More information about this design will be provided in Section 2.3.1.

A dynamometer was designed and built for the purpose of testing the motors by two undergraduate students, Jason Fabro and Graeme Hartlen. The dynamometer used a hydraulic Go-Kart brake caliper to supply a load to the motor. Figure 2.8 shows a photograph of this dynamometer. The motor and gearhead units were tested at various operating voltages. Figure 2.9 shows the torque speed curve for a test run at 24V with the current limited to approximately 12A. The graph has four curves. The first is the experimental curve obtained from the dynamometer. The next three are the theoretical curves using gearhead efficiencies of 68%, 85% and 100%. The slight concave shape of the experimental curve confirms that the gearhead efficiency increases as the speed decreases. The experimental stall torque of 29Nm results in a gearhead efficiency at stall close to 85%. Additional data from the testing can be found in [14].

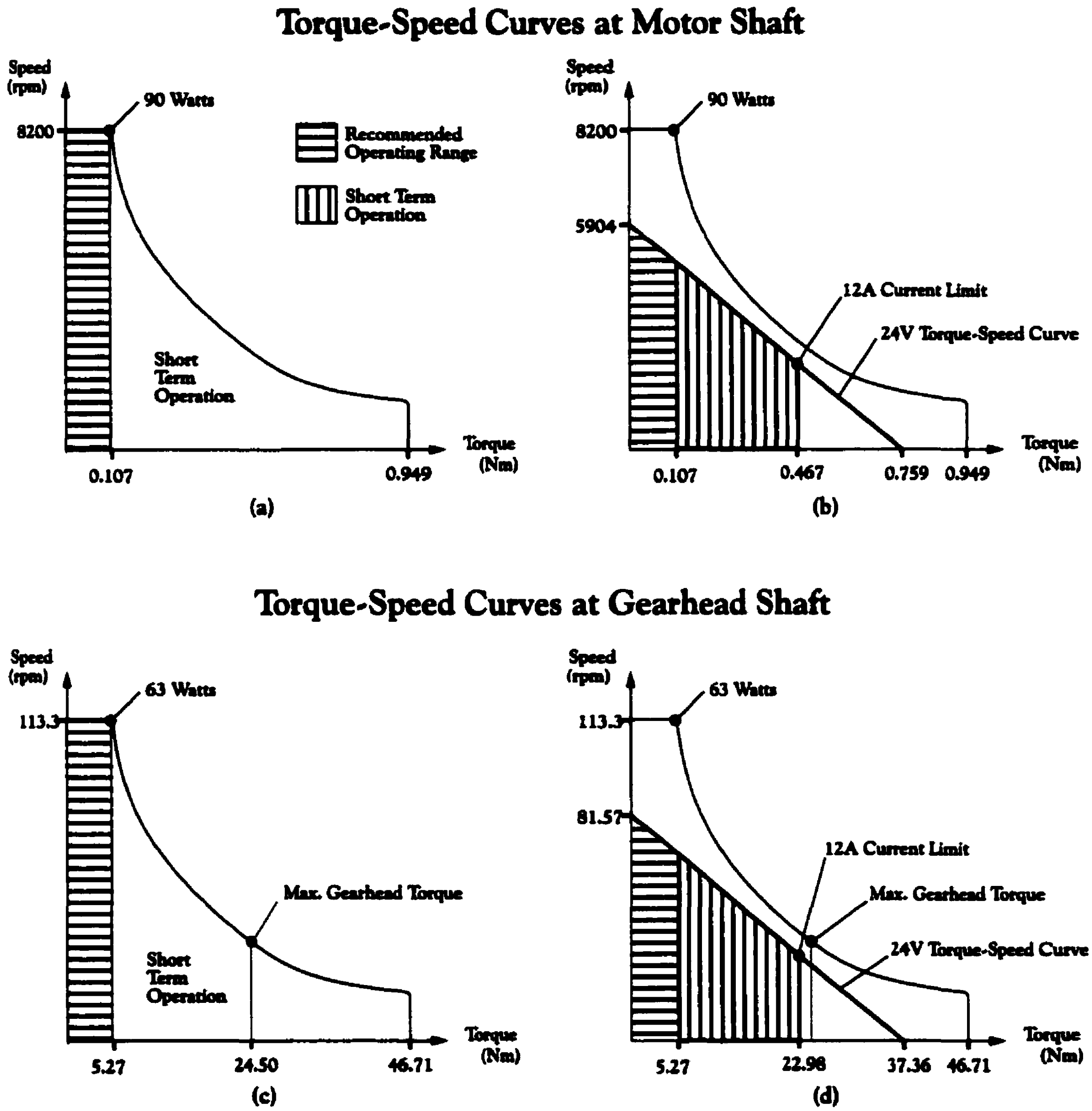

Figure 2.7: *SCOUT II transmission system torque-speed curves, adapted from [37] (a) Maxon 118777 brushed 90W DC motor only, (b) Maxon 118776 brushed 90W DC at operating conditions (24V, 12A max), (c) Maxon 118776 brushed 90W DC with Maxon 110404 gearhead with 72.38:1 ratio using a 68% efficiency and (d) Maxon 118776 brushed 90W DC at operating conditions (24V, 12A max) with Maxon 110404 gearhead with 72.38:1 ratio using a 68% efficiency.*

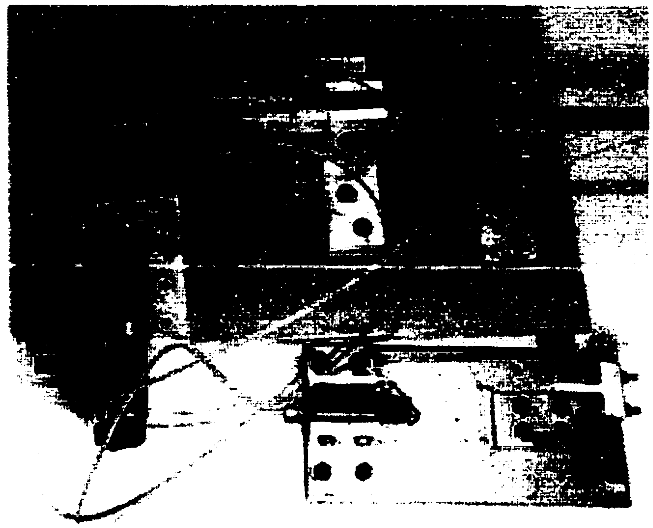

Figure 2.8: *The dynamometer built at ARL for testing motors.*

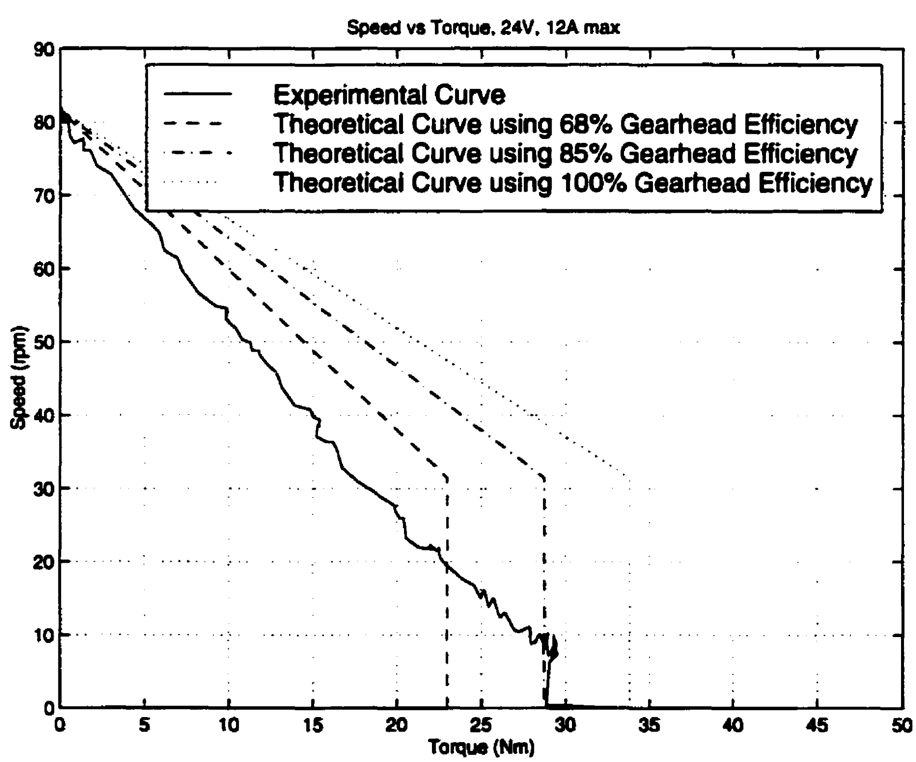

Figure 2.9: *Experimental and theoretical torque-speed graphs for the Maxon 118777 motor and Maxon 110404 gearhead package.*

2.2.3 Layout

In order to keep SCOUT II modular, it is divided into separate sub-systems. Two hip units (one for the front, one for the rear) contain the motors, transmission units, batteries, laser units and the camera. These two units are joined together with simple brackets that also serve as the base for the power and control electronics (see Sections 3.3 and 3.2 respectively). The legs are self-contained units that are fastened to the hip units with bolts.

2.2.4 Loading

Prior to entering the detailed design phase, it was important to analyze the loads and stresses that the robot would encounter. Seeing that this robot's main purpose is to test experimental control theories and software, it is expected to fall and/or roll over. As a result, the robot needs to be capable of withstanding these impacts with little or no damage. During periods of high use and excessive abuse, padding will be added for extra protection.

For most of the stress analyses, the impact loads on the toe at touchdown were assumed to be twenty times the static weight (i.e. 20Gs or, alternately 20mg). Analyses with side loads of 250N applied at the toe were also performed. Impact loads on the body due to accidental fall or impacts were taken to be between 5 and 10Gs. Any stress analysis that required finite element modelling was performed using Pro/Mechanica [60] and the results can be found in Appendix C.

2.3 Embodiment Design

Once a good grasp of the concept was achieved, it was time to begin the detail work. Most of the detail design for SCOUT II was done using Pro/Engineer [59], a 3D CAD/CAM software.

2.3.1 Transmission Design

An exploded view of the complete transmission design can be seen in Figure 2.10. All

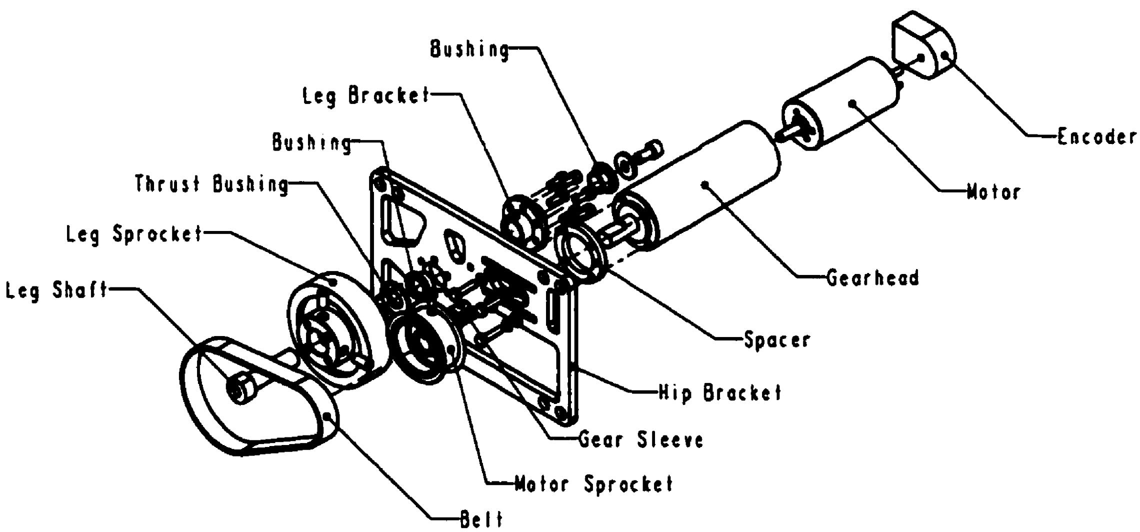

Figure 2.10: *Exploded view of transmission unit.*

four units are identical and the entire transmission system attaches to one bracket in order to keep the system simpler and modular. A HTD timing belt with 70 grooves and a 5 mm pitch (*Stock Drive Products A6R25M070150* [61]) is used. The leg is attached to a 48 groove sprocket (*Stock Drive Products A 6A25M048NF1512* [61]), though larger or smaller sprockets may be used if a different gear ratio is desired. Four holes were tapped into the sprocket allowing the leg to be attached directly onto it. A variety of sprockets ranging from 26 to 34 grooves can be attached to the gearhead shaft. Table 2.5 shows the various sprocket sizes that can be used, and the resulting torque and speed characteristics of each. Figure 2.13 shows the resulting torque and speed using 28 and 34 groove sprockets. Figure 2.11 provides the experimental torque-speed graph for the system with and without the belt transmission system.

The sprockets were modified since they were too wide to attach to the output shaft. The hub was machined off and the set screw hole retapped through the teeth. However, in order to minimize damage to the teeth, a small tap was used (M4).

Number of grooves on small sprocket	34	33	30	28	26
Gear ratio	1.41:1	1.50:1	1.60:1	1.71:1	1.85:1
Efficiency (Approx.)	96				
Number of grooves on belt	70				
Approx. center to center distance (mm)	71.62	73.90	76.15	78.38	80.60
No load speed (RPM)	57.8	54.4	51.0	47.6	44.2
Stall Torque (Nm)	31.1	33.1	35.3	37.8	40.7
Continuous Torque (Nm)	7.1	7.6	8.1	8.6	9.3

Table 2.5: *Possible gear ratio configurations using a 48 groove sprocket at the leg.*

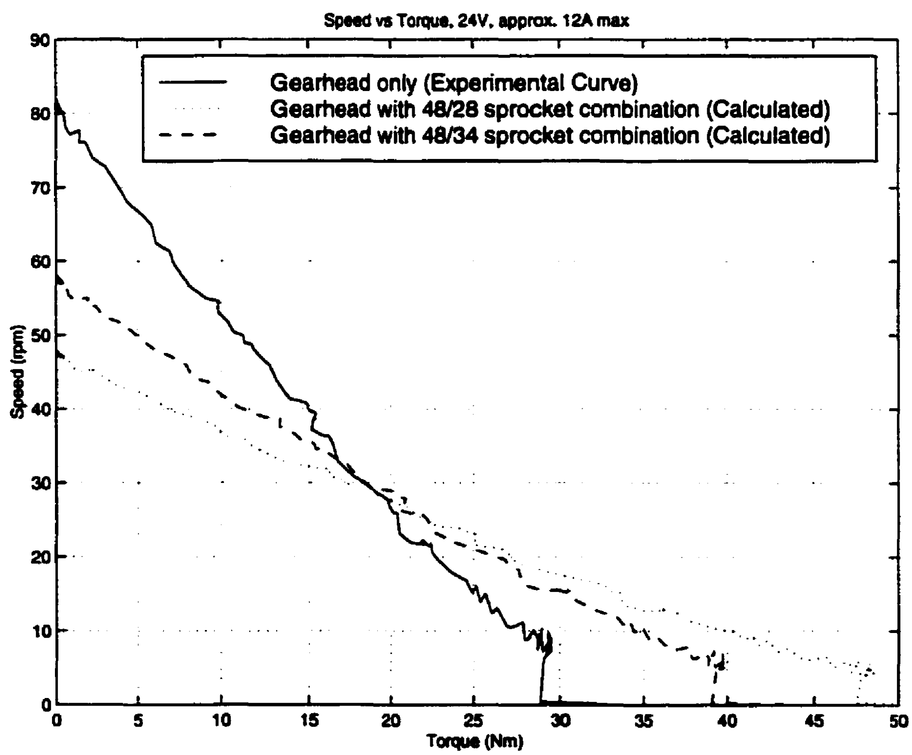

Figure 2.11: *Experimental torque-speed graph for the Maxon 118777 motor and Maxon 110404 gearhead package with and without belt transmission system.*

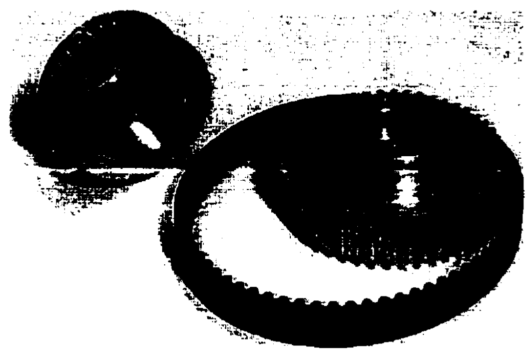

Figure 2.12: *Picture of sprockets and belt used on SCOUT II.*

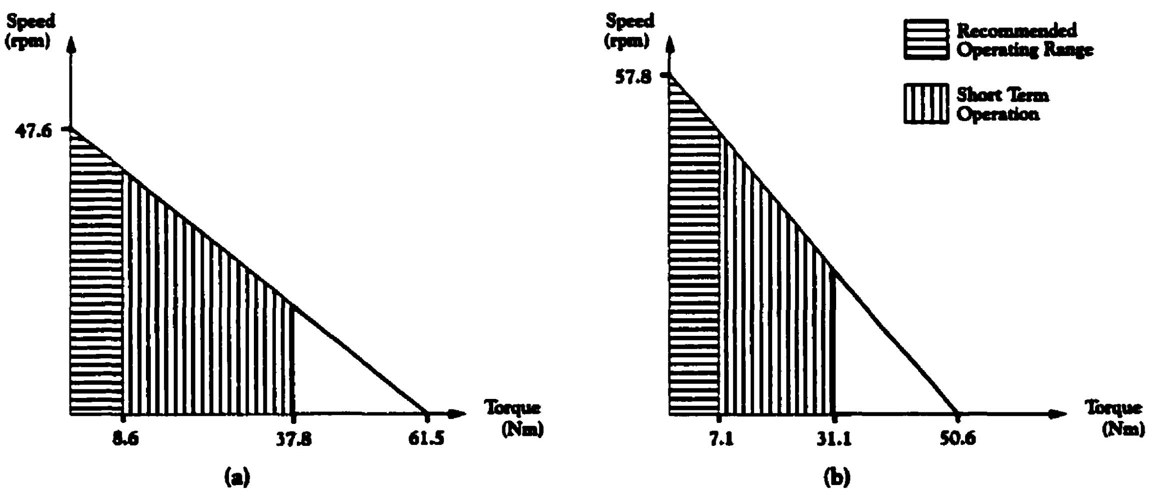

Figure 2.13: *Torque-speed curve of SCOUT II's actuation system using (a) a 48/28 sprocket combination and (b) a 48/34 sprocket combination (using a $\eta_{gearhead} = 68\%$ and $\eta_{belt} = 96\%$).*

This later turned out to be a problem because the high torques transmitted from the gearhead output shaft to the sprocket deformed the set screw and led to play between the two. In order to alleviate this problem, a sleeve (see Figure 2.14) which sits on the gearhead shaft was made to help transmit the torque from the output shaft to the sprocket.

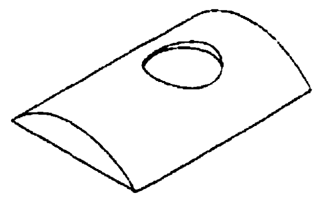

Figure 2.14: *Picture of gear sleeve made to eliminate shaft/sprocket slip.*

Tensioning the belt involves simply pulling the motor/gearhead unit with one hand and tightening the four motor bolts with the other. The belt tension resulting from this 'hand tightening' procedure was enough to avoid tooth hopping but low enough to avoid excessive loads on the shafts.

The leg shaft rotates freely on the motor bracket using two Garlock no-maintenance flanged bushings (*FMB1209DU*) and a thrust bushing (*WC10DU*) [16] which can be seen in Figure 2.15. Though the load capabilities and friction characteristics at high speed make bearings more suitable, the low speed oscillatory motion involved here is more suited to bushings. The leg is attached directly to the large sprocket with four M5 x 20 mm long socket head cap screws. This is a more elegant and robust than using set screws or keys.

All components within the transmission unit were checked to withstand the loading and impacts that would be inflicted upon them. The only part in the transmission unit that was analysed using finite element analysis was the motor bracket because it was under complex loads. The fact that it is such a large component made weight reduction advantageous. The results of the analysis can be found in Appendix C.1.

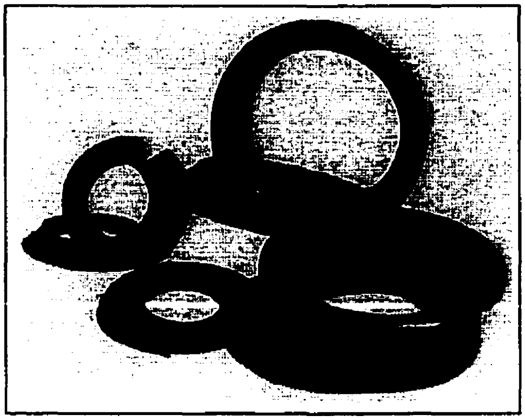

Figure 2.15: *Thrust bushing used at the hip and the flanged bushings used for the hip and legs.*

2.3.2 Hip Design

Figure 2.16 shows the front hip unit. Two transmission units are connected together using angle brackets and stock 3/4" x 3/4" x 1/8" thick aluminium angle. It also houses one of the batteries (see Section 3.3.2) and the laser range finders (see Section 3.1.3). The rear hip unit is identical except that it does not contain the camera unit and is narrower in order to offset the legs so they do not collide.

The laser and camera units are well protected in case of a fall with bent 3.2 mm thick aluminium brackets.

2.3.3 Leg Design

The design for the leg was one of the more challenging tasks. The leg had to be light and compact in order to minimize its mass and inertia, yet sturdy enough to withstand repeated impact loads. It had to accommodate both fixed length operation (for walking and stair climbing) and compliant operation through the use of latex or metal springs (for compliant walking, running and stair-climbing).

An exploded view of the leg is shown in Figure 2.17. Multiple leg lengths are possible by a series of holes on the upper leg that attach to the large sprocket on the

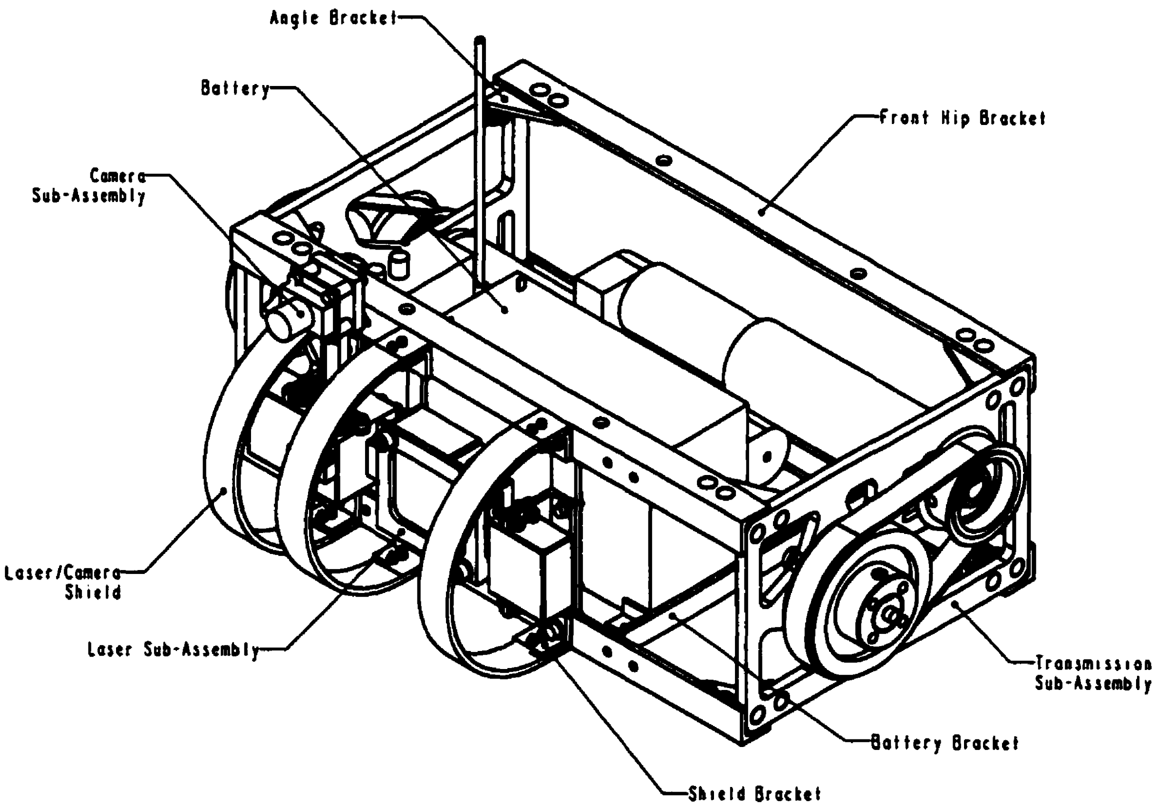

Figure 2.16: *Front hip unit.*

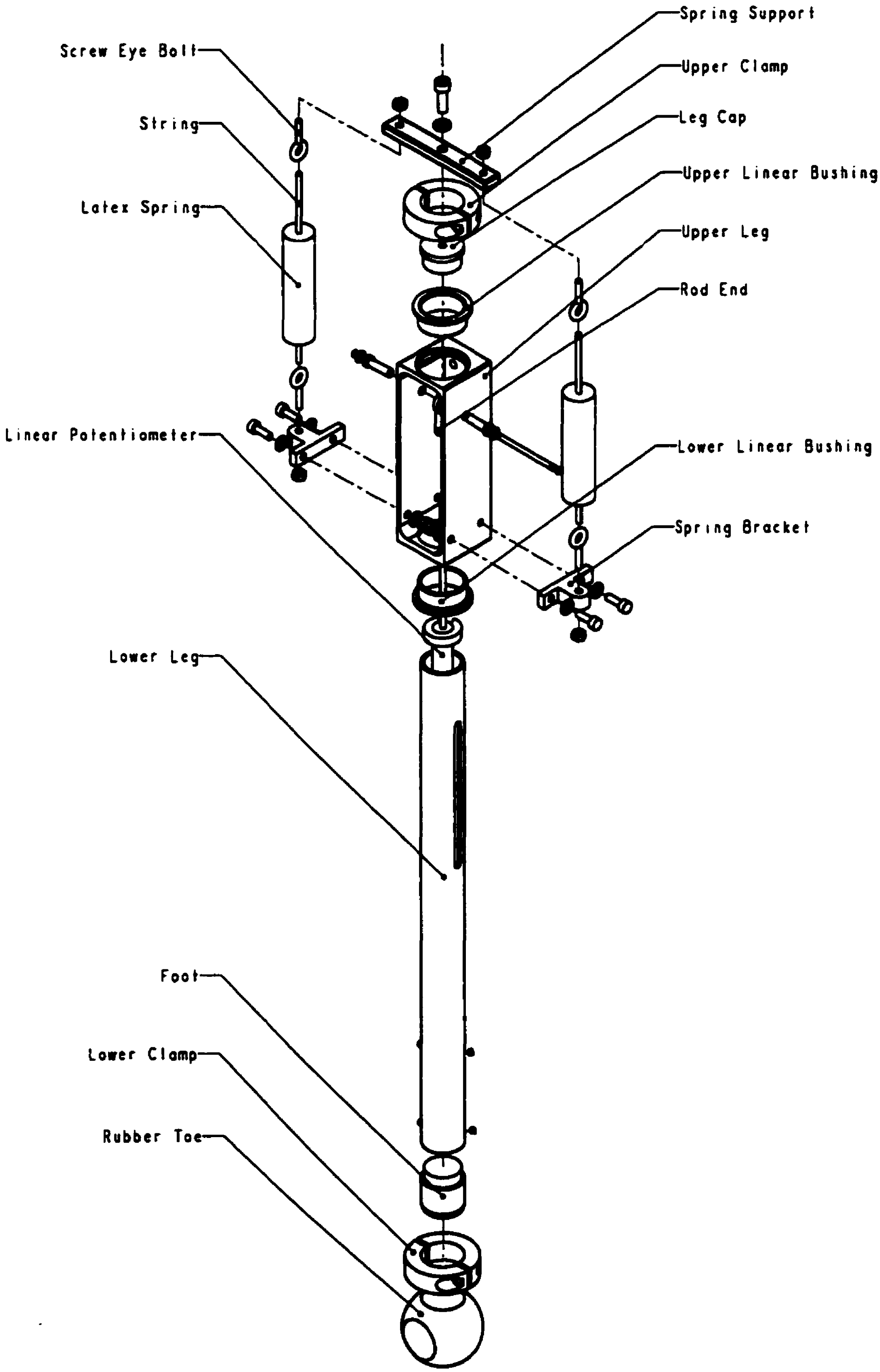

Figure 2.17: *Exploded view of leg.*

transmission unit. For even longer legs, an extension like the one shown in Figure 2.18 is attached to the lower leg. Table 2.6 shows the possible lengths and the corresponding mass and inertia. The design is not limited to these values since the leg extension can be made to any size. The lowest set of holes cannot be used in compliant leg mode since the leg mounting bolts interfere with the spring bracket bolts.

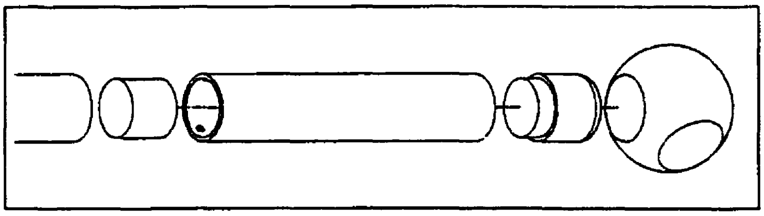

Figure 2.18: *Exploded view of lower leg showing extension.*

A linear potentiometer, used to determine the leg length (see Section 3.1.2), is incorporated in the leg. The potentiometer housing is held to the lower leg with set screws and the shaft is attached to the upper leg with a rod end.

The 1" (25.4mm) diameter steel lower leg slides on the upper leg with two Garlock bushings which are shown in Figure 2.15. A 100mm slot was machined in the leg to allow attachment to the potentiometer rod end.

Leg compliance is provided by either latex or steel springs. The pre-load can be adjusted by tightening or loosening the screw eye bolts. Clamps (*SPAE NAUR part 600-055*) are used to hold the lower leg in place (in fixed leg mode) or to limit the travel of the lower leg to prevent damage to the potentiometer (in compliant leg mode).

A significant amount of work was done in an attempt to source a suitable toe material. It had to have the correct damping characteristics to reduce the impact loads, while not absorbing too much energy which would impede the momentum transfer during touchdown. In addition, it had to have a suitable surface that would minimize slipping. Toy balls from a pet shop turned out to be the best option due their damping and friction characteristics as well as their low cost.

The upper leg was analysed using finite element modelling and the results are provided in Appendix C.2.

	*Mass**	*Leg Length*	*Inertia about pivot†*
	(kg)	*(mm)*	*(gmm^2)*
Without Extension	0.920	255.9‡	12.94
		275.0	14.27
		294.1	16.26
		313.2	18.90
		332.3	22.19
With 150mm Extension	1.057	380.9‡	29.23
		400.0	32.95
		419.1	36.92
		438.2	41.65
		457.3	47.14

Table 2.6: *Possible leg lengths with corresponding mass and inertia. (*Actual measured mass. †Inertia values determined using Pro/Engineer. ‡Configurations not possible in compliant leg mode - see Section 2.3.3.)*

2.3.4 Body Design

The two hip units are held together with four aluminum box extrusions which are connected to the hip units with aluminum brackets. Once again, this design keeps the robot very modular. The aluminum body links can be replaced with longer or shorter ones thus modifying the overall length of the robot. In addition, the hip units can be attached either with the motors on the inside and leg attachment on the outside or vice versa (see Figure 2.19). This will give the robot a much larger moment of inertia which may be advantageous for momentum transfer during leg impact.

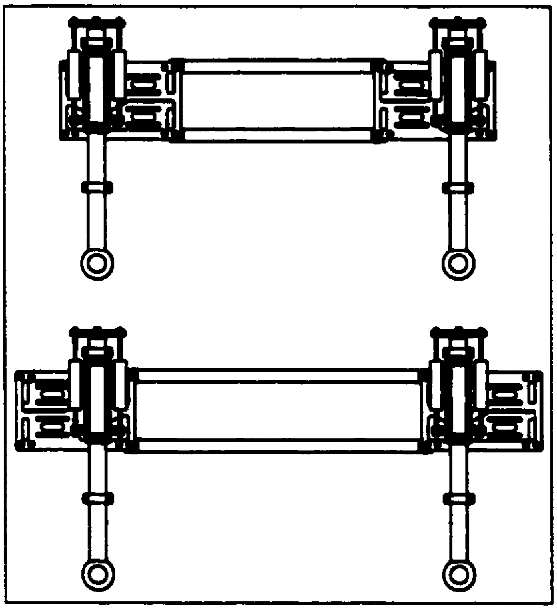

Figure 2.19: *Two possible hip configurations resulting in different body inertias.*

The four body links also serve to hold most of the electronics on the robot. Two Lexan^{TM} plates attached on either side of the robot contain most of the input/output (IO) boards (Figure 2.21). The main electronics plate (Figure 2.20) holds the PWM servo amplifiers, two SPP/SPI multiplexers, laser controllers, two gyroscopes and the PC board. The body links also have brackets attached to them that support the RF unit and the power board (see Chapter 3). A complete exploded view of SCOUT II is provided in Figure 2.22

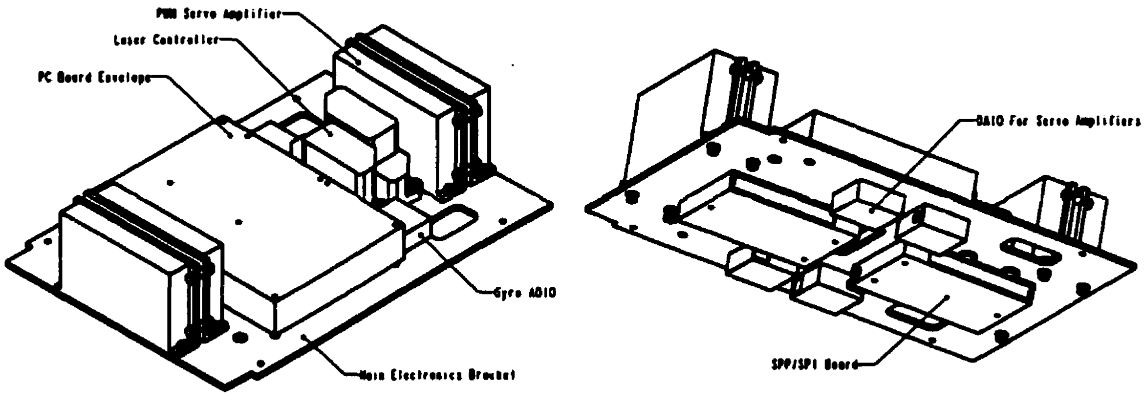

Figure 2.20: *Top and bottom view of main electronics assembly.*

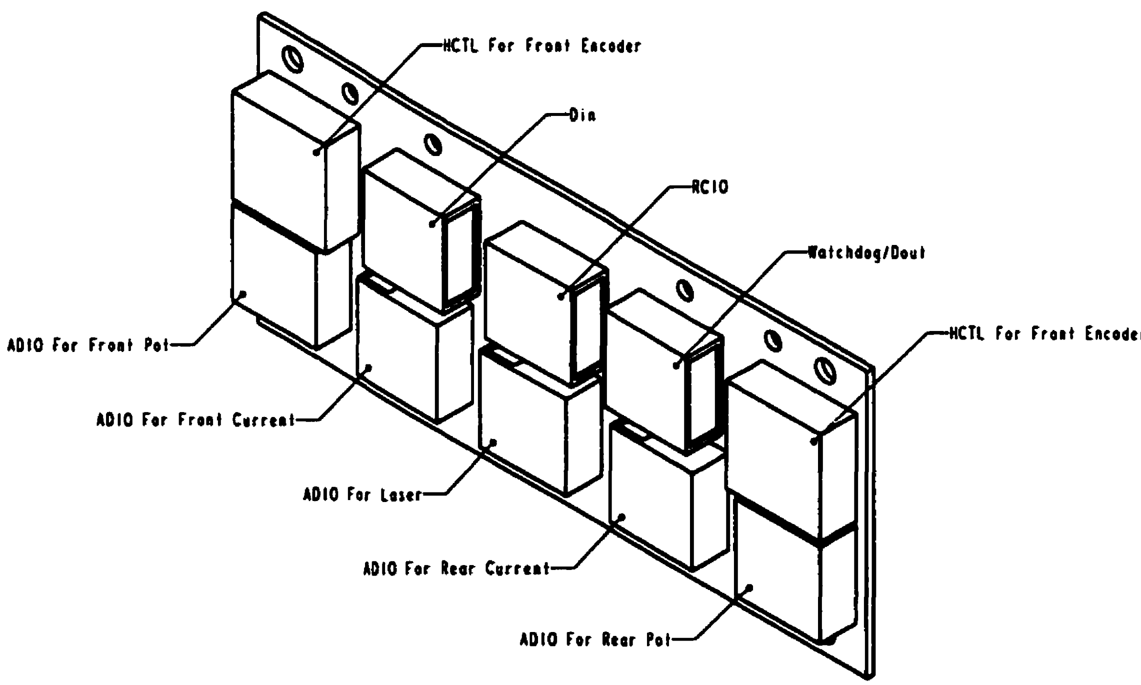

Figure 2.21: *Side electronics assembly.*

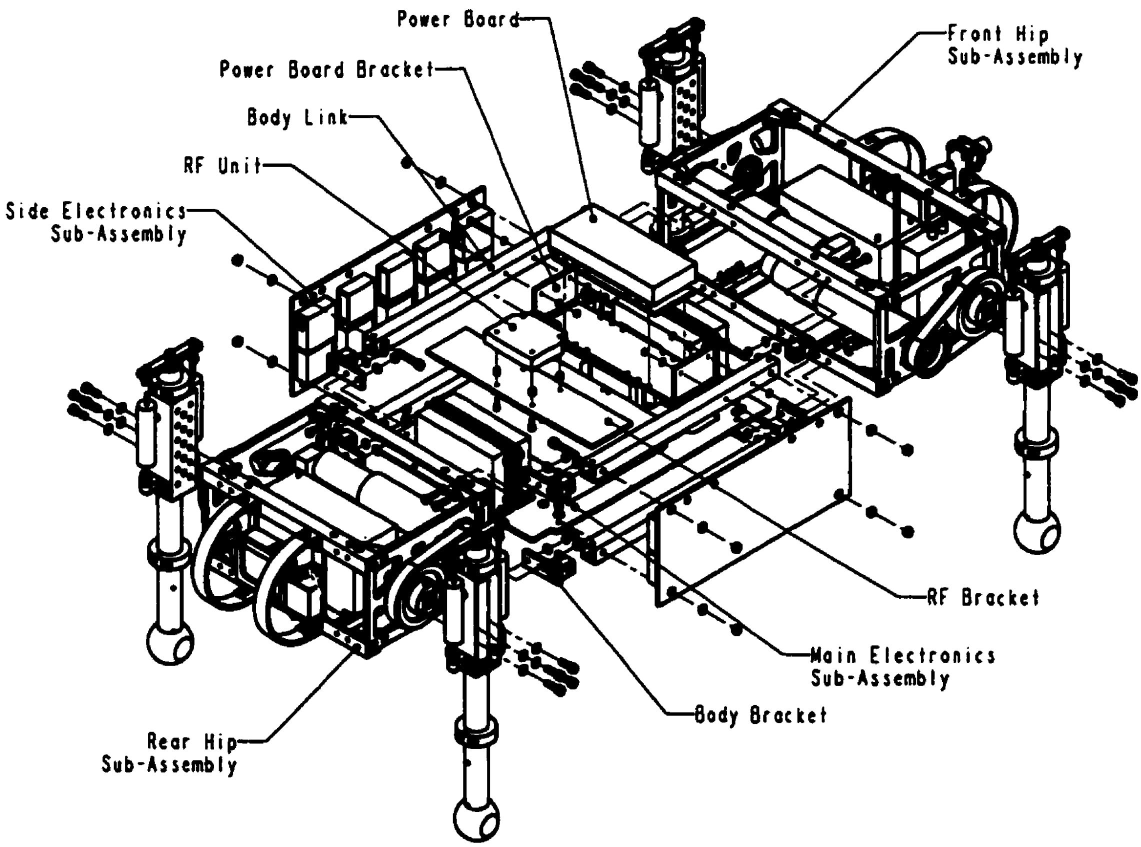

Figure 2.22: *Exploded view of SCOUT II.*

2.4 Construction and Cost

Machining of the various components of the robot began in February 1998 and continued through the summer of 1998. The machining was done in the Mechanical Machine Shop of McGill University either by the experienced staff or the author. Machining costs were in the order of $8500. Assembly was done mostly by the author with the aid of numerous other students working in the Ambulatory Robotics Laboratory. The total cost of the robot was in the order of $25 000. Appendix E has a complete parts list showing all costs associated with the project.

2.5 Summary

A Pro/Engineer drawing of the complete robot is provided in Figure 2.23 and a picture can be seen in Figure 2.24. Table 2.7 details the mechanical specifications of the robot. Complete assembly drawings for SCOUT II can be found in Appendix A while Appendix D has a parts list complete with the mass of all components.

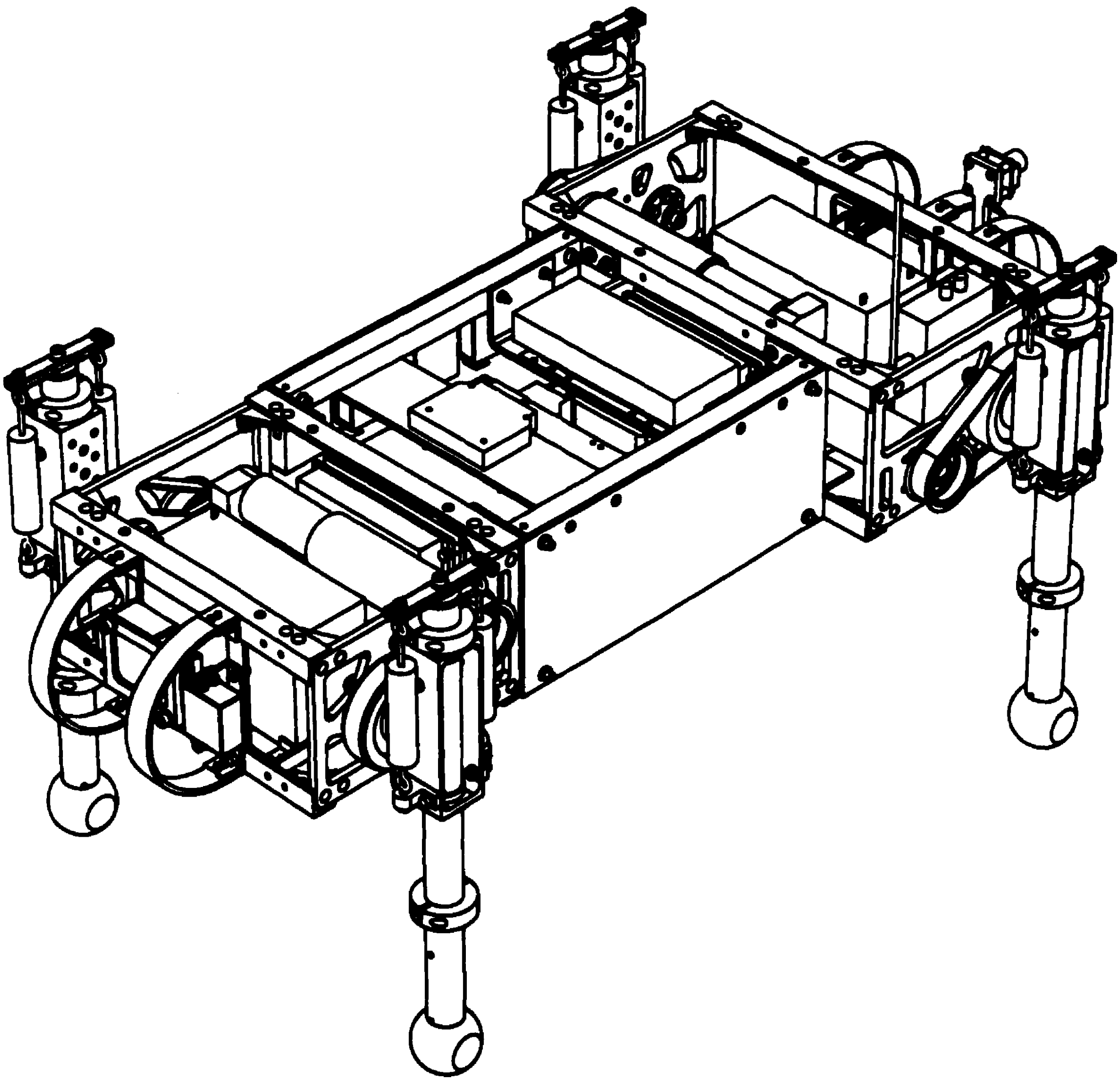

Figure 2.23: *Isometric view of SCOUT II.*

Figure 2.24: *Photograph of SCOUT II.*

Body length		837.0 mm
Body height		126.0 mm
Front hip width		498.0 mm
Rear hip width		413.0 mm
Hip-to-hip length		552.0 mm
Total mass*		23.77 kg
Body mass*		20.09 kg
Body inertia† (about body center)	pitch axis	1.091 kgm^2
	roll axis	0.161 kgm^2
Center of mass location† (from body center)		14.1 mm (in front)
		2.4 mm (to the right)
		3.1 mm (below)
Leg length		255.9-457.3 mm (see Table 2.6)
Leg mass*		0.920 kg
Leg inertia		(see Table 2.6)
No load speed		up to 57.8 RPM (see Table 2.5)
Stall torque		up to 40.7 Nm (see Table 2.5)
Continuous torque		up to 9.3 Nm (see Table 2.5)

Table 2.7: *Mechanical specifications for SCOUT II. (*Actual measured mass. †Values determined using Pro/Engineer.)*

Chapter 3

Sensors and Electronics

SCOUT II is equipped with an electrical system and a number of sensors. Section 3.1 will review all the sensors that are used. Section 3.2 discusses the system used to communicate with and control the robot. The power supply and its distribution system will be discussed in Section 3.3 and, in the final section of the chapter (Section 3.4), the electrical system will be summarized.

3.1 Sensors

Numerous sensors are used on SCOUT II. The purpose of these sensors is:

- To supply feedback to SCOUT II's computer as to the current state of the robot.
- To supply the operator with information on the robot's surroundings.
- To keep track and record data that may be used for debugging and optimising the various controllers being tested.

Each sensor used on SCOUT II is described in Sections 3.1.1 through 3.1.7.

3.1.1 Encoders

The *Maxon 118777* motors are equipped with *Hewlett Packard HEDS 5540 A11* [56] incremental digital encoders which have 500 cycles per revolution (2000 counts per revolution after quadrature encoding). One such encoder, mounted on the motor, is shown in Figure 2.6. The main function of these encoders is to determine leg angle. The data can then be differentiated to obtain angular velocity. One of the shortcomings of using an incremental digital encoder is that it does not have a zero position. Hence, when starting a run, the encoders have to be 'zeroed' so that all subsequent readings were taken from a calibrated, absolute angle. Hall effect sensors are used for this purpose (see Section 3.1.5).

3.1.2 Leg Potentiometers

In order to measure varying leg length in compliant leg mode, it was necessary to put linear potentiometers in the leg. *Midori LP-100FP* 5kΩ [48] potentiometers are used because of their small diameter and suitable stroke length (100mm). Their 50Gs shock rating is well above anticipated shock loads.

These potentiometers turned out to serve a useful purpose in both fixed and compliant leg mode. In fixed leg mode, they are used to detect foot touchdown. This is accomplished by leaving a few millimeters of play in the leg. When the leg is compressed these few millimeters, it means that it is in contact with the ground and therefore in stance. When the leg is fully extended, it is in flight. This provides a second method of determining foot states (the primary method is using the laser range finders and will be described in Section 3.1.3). In compliant mode, the potentiometers are used both to measure leg length and to detect touchdown. Figure 3.1 shows a picture of the potentiometer.

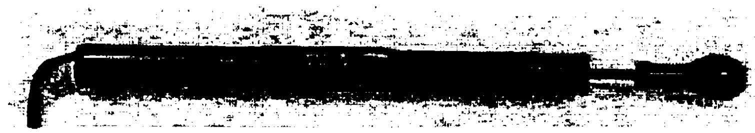

Figure 3.1: *Midori LP-100FP 5kΩ potentiometer [48].*

3.1.3 Laser Range Finders

Two *Aromat ANR12261 LM10-250* [6] laser range finders are mounted on SCOUT II - one at each end. These lasers have a range between 100 and 400 mm with a resolution of 0.15mm. Figure 3.2 shows one such sensor. In order to make these lasers even more

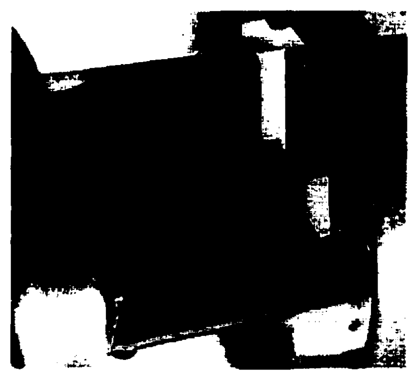

Figure 3.2: *Aromat ANR12261 LM10-250 laser range finder [6].*

versatile, they are mounted on a tilting platform that is powered by a *Futaba 3003* [69] R/C servo actuator. Figure 3.3 shows an exploded view of the laser assembly unit. These servos, which are normally used in radio controlled aircraft, were suitable for this task because of their simplicity, low cost (under 20 CAN$) and easy interfacing.

The lasers units serve numerous purposes. These include:

- Scanning the terrain ahead of SCOUT II.
- Determine body angle and body angular velocity. This can be achieved using either the two lasers or one laser and one stance leg.
- Detect foot touchdown. This is achieved by using the information from the laser in conjunction with the motor encoders and leg potentiometers.

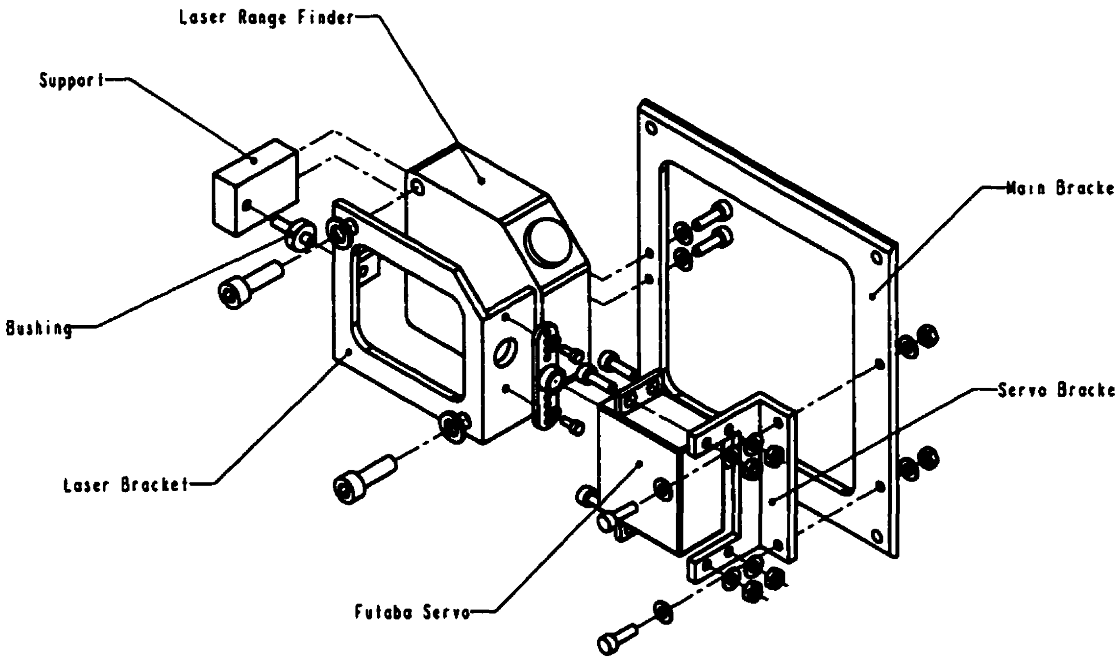

Figure 3.3: *Exploded view of laser assembly.*

- Determine body height and vertical velocity.
- Determine body horizontal distance and velocity.

The equations for determining the above items were developed by Sami Obaid. More information concerning the laser range finders, their function and performance characteristics can be found in [51].

3.1.4 Gyroscopes

Two *Murata ENC-05EA* [50] solid state gyroscopes (see Figure 3.4) are mounted on SCOUT II's body to measure angular velocity - one in the pitch direction, the other in the roll direction. Although they are rated by the manufacturer to ±80 deg/s, they were found to be accurate up to ±450 deg/s with an absolute error of less than 9 deg/s at maximum angular velocity. All testing on the gyroscopes was performed by Sami Obaid. The corresponding pitch and roll angles are determined by integrating the signal. In order to reduce the effect of drift, the signal is reset when the body angle could be determined more accurately (for example, when all legs are on the ground) or by using the laser range finders. More information on the gyroscopes can be found in [51] and on the web at www.cim.mcgill.ca/~arlweb/sensorsfrm.htm.

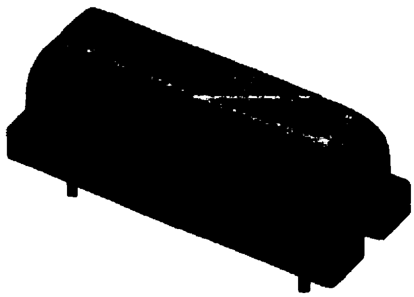

Figure 3.4: *Murata ENC-05EA solid state gyroscope [50].*

3.1.5 Hall Effect Sensors

Since the motor encoders are only capable of supplying relative position, it was necessary to determine a method of 'zeroing' the leg. The digital hall effect sensors shown in Figure 3.5 are used for this purpose. They are manufactured by Honeywell (part number *SS21PE MICRO*) [35]. A sensor is mounted on each motor bracket and a magnet is attached to the sprocket at each leg. The point at which the sensors trigger was experimentally measured and entered into the run-time code as the calibration angle for the legs. Upon commencing a run, the legs rotate until the hall effect sensors are triggered whence the encoders are set to the previously determined angles.

3.1.6 Motor Current Measurement

It was determined that logging the motor current would be advantageous for debugging. The *Advanced Motion Controls 12A8E* [4] PWM servo amplifier that was used to control the motors is equipped with current feedback. This information turned out to be very useful during testing since it gave the operator valuable information on the motor performance and, perhaps more importantly, allowed the operator to ensure

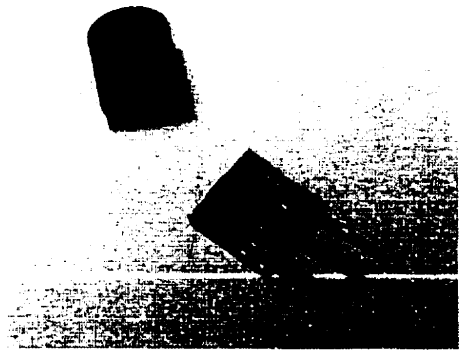

Figure 3.5: *Hall effect sensor and magnet [35].*

that the motor's thermal limit was not surpassed. More information on these servo amplifiers will be presented in Section 3.3.1.

3.1.7 Camera

In order to supply the operator of SCOUT II with visual feedback of the robot's surroundings, a small black and white digital camera (*Marshall Electronics V-X007-PCB [45]*) is used. In addition, the camera is mounted on a pan/tilt system using two *Futaba S3003* [69] R/C servos like the ones used for the lasers. The camera, along with the *TV Genie TR-200* UHF transmitter can be seen in Figure 3.6, while the pan/tilt unit assembly drawing is shown in Figure 3.7.

3.1.8 Summary

Table 3.1 summarizes all of the sensors used on SCOUT II along with their function.

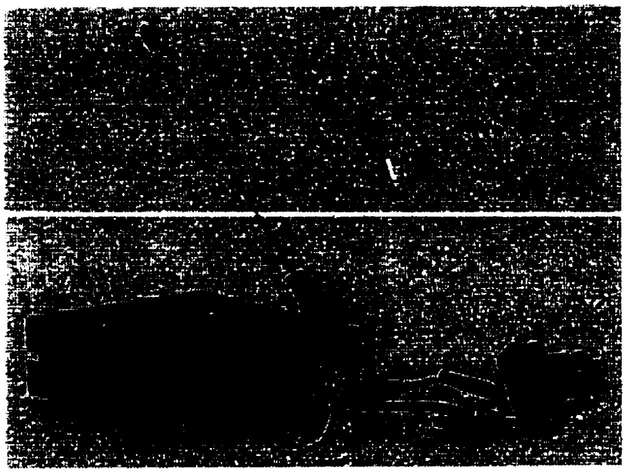

Figure 3.6: *Camera and transmitter.*

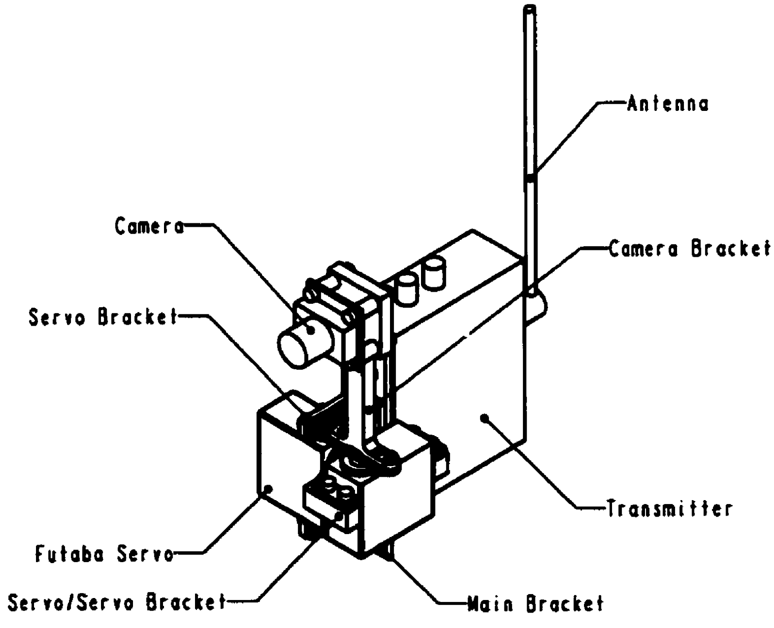

Figure 3.7: *Isometric view of SCOUT II's camera pan/tilt unit.*

Sensor	Qty	Function(s)
Encoder	4	Measure leg angle and angular velocity
Motor current	4	Measure motor current
Leg pots	4	Measure leg length Determine foot touchdown
Lasers	2	Measure body angle and angular velocity Determine foot touchdown Scan terrain and stairs Body height and vertical velocity Body horizontal distance and velocity
Gyroscope	2	Measure pitch velocity and angle Measure roll velocity and angle
Hall effect	4	Zero legs at startup
Camera	1	Visual feedback for operator

Table 3.1: *Sensors used on SCOUT II.*

3.2 Control Electronics

3.2.1 The SPP/SPI System

SCOUT II's motors, sensors and R/C servos were interfaced using a SPP/SPI (Standard Parallel Port/Serial Periferal Interface) system. The system was designed by Nadim El-fata and developed by David McMordie and Kenneth Yamazaki. The system consists of a multiplexer which allows up to 8 inputs and 8 outputs to be read and driven through a standard, bi-directional PC parallel port. Numerous Input/Output (I/O) modules can be connected to the multiplexer with RJ-11 telephone type connectors. The different types of I/O modules used include:

- ADIO (Analog to Digital Input Output Module): This module was designed to read an analog voltage input with 12 bits of resolution and convert it to a digital signal. It is used mainly to read the various sensors.

- HCTL (Digital Encoder Input Module): This module was designed to read quadrature inputs from a digital encoder. (The acronym HCTL comes from the main chip on board - a *Hewlett Packard HCTL-2016 quadrature decoding IC* [56].)
- DAIO (Digital to Analog Input Output Module): This module was designed to drive an analog voltage output signal. It is used to drive the PWM servo amplifiers.
- DIN (Digital INput Module): This module was designed to read up to ten high/low digital inputs. It is used to read the hall effect sensors.
- RCIO (R/C Servo Input Output Module)/DOUT (Digital OUTput Module): This module was developed to drive up to two R/C servos and eight digital high/low outputs. It is used to control the R/C servos for the camera and laser units and as a watchdog to enable the motors.

SCOUT II used a total of 24 I/O modules including 17 inputs and 7 outputs. Table 3.2 summarizes all the I/O modules and their function.

The 17 inputs would require three SPP/SPI multiplexers. However, due to limitations on the number of parallel ports available on the on-board PC board (see Section 3.2.2), only two SPP/SPI multiplexers were used. This meant that only 16 out of the 17 inputs could be read at any one time. This was not a problem since 4 current inputs were being used mainly for debugging purposes and hence could be removed. In the case where the current readings were required, the roll gyroscope could be removed. Figure 3.8 shows the two SPP/SPI multiplexers and 4 DAIO's mounted on SCOUT II. Circuit diagrams for each of the boards can be found in [75].

3.2.2 PC Board

SCOUT II is equipped with an *Adastra VNS-486* [3] embedded PC board. It is a self-contained PC with an AMD DX5 motherboard, 133MHz processor speed, 64MB

	Module	Function	Qty		
Inputs	ADIO	Leg pots	4	12	17
		Lasers	2		
		Motor current	4		
		Gyroscopes	2		
	HCTL	Encoders	4	4	
	DIN	Hall effect	1	1	
Outputs	DAIO	Servo amplifiers	4	4	7
	RCIO	Camera and laser units	2	2	
	DOUT	Watchdog	1	1	

Table 3.2: *Summary of I/O modules used on SCOUT II.*

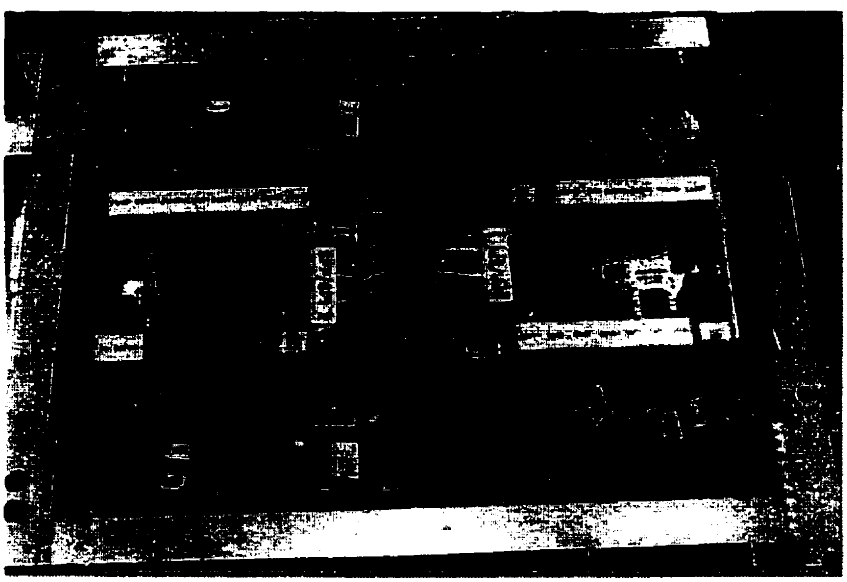

Figure 3.8: *SPP/SPI multiplexer boards and 4 DAIOs mounted on SCOUT II.*

of RAM and a 8MB Flash Solid State disk. It also has full ethernet capabilities, four serial ports and two enhanced parallel ports (hence the limit of two SPP/SPI multiplexers). Its small size (146mm x 203mm x 32mm) and low weight (397g) made it an ideal canditate for SCOUT II. The 8Mbyte solid state disk is large enough for the operating system and the run-time code, while the 64M of RAM can be used to log data.

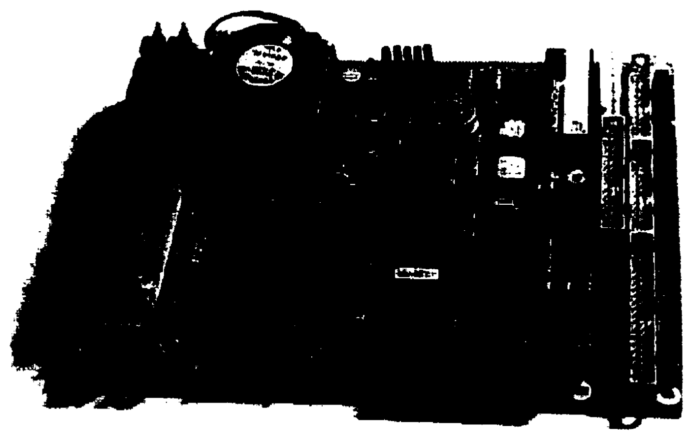

Figure 3.9: *Adastra VNS-486 PC board.*

3.2.3 Communications with SCOUT II

Communication with SCOUT II can be done in several ways. Each option is briefly explained below.

Option 1: Desktop PC only

The method used most often for testing purposes was a desktop PC with parallel ports connected directly to the SPP/SPI multiplexers on SCOUT II. The PC was a Pentium 100MHz running the QNX realtime operating system [62]. This is the simplest method of communicating with SCOUT II since it does not require the embedded PC board or the RF unit. The disadvantage is the two parallel cable tethers between the computer and SCOUT II that are required.

Option 2: Desktop PC with ethernet connection to SCOUT II

In this case, a desktop PC is connected to the embedded PC via an ethernet cable. The embedded board has the run-time code (once again using QNX) and is connected to the two SPP/SPI multiplexers. In this case, the desktop PC is reduced to the role of serving simply as a user interface. This method has the advantage of replacing the two bulky parallel cables with one ethernet cable.

Option 3: Embedded PC with wireless link

The prefered method is through a wireless RF link with the run-time code running on the embedded PC. The RF unit is a *Abacom RTcom-RS232* [2] and is capable of up to 19200 bps (bits per second) at half duplex with a range of 200 meters. A desktop or laptop PC acts as the user interface. The RF unit had not been operational at the time of writing. Martin de Lasa is actively working on getting the system functioning.

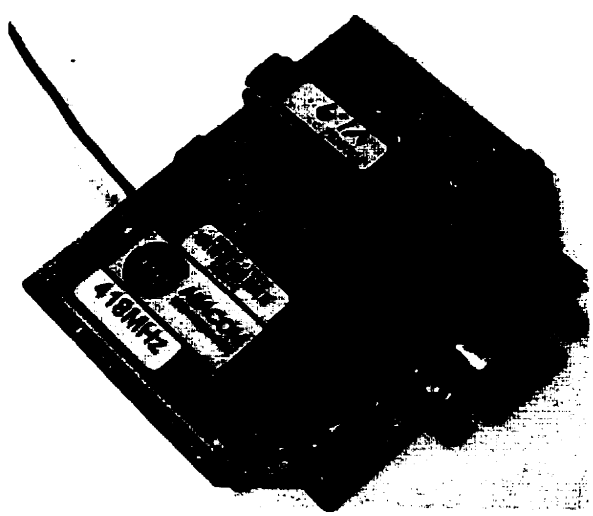

Figure 3.10: *Abacom RTcom-RS232 radio modem.*

Figure 3.11 summarizes the control system including the three methods available for interfacing. A more detailed diagram is included in Appendix B.

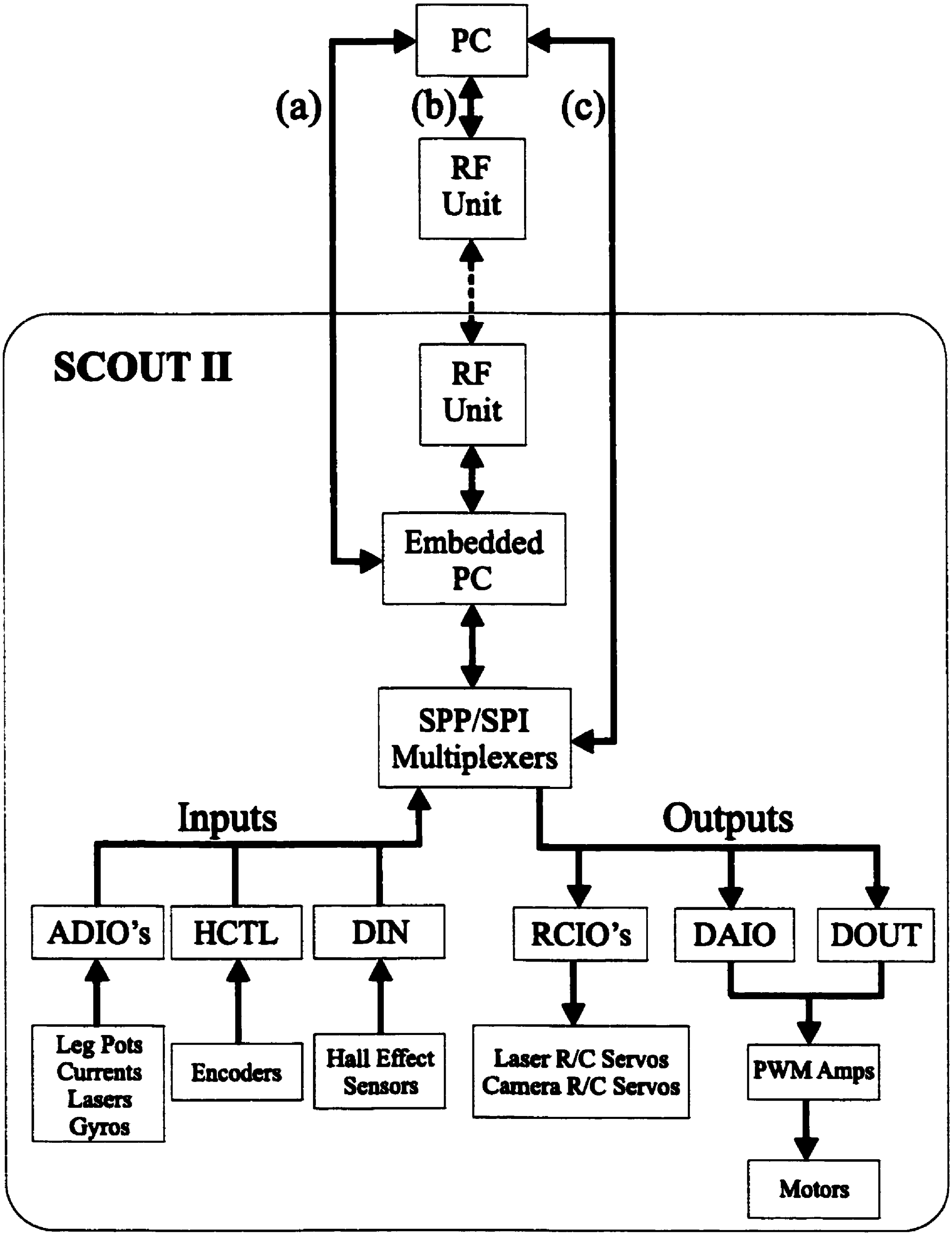

Figure 3.11: *SCOUT II's control system showing three methods of interfacing; (a) ethernet cable to PC board, (b) wireless RF link, and (c) two parallel cables to SPP/SPI multiplexers.*

3.3 Power Electronics

3.3.1 PWM Servo Amplifiers

SCOUT II uses four *Advanced Motion Controls 12A8E* [4] brush type, Pulse Width Modulation (PWM) servo amplifiers. Figure 3.12 is a picture of one such unit. They have a peak current of 12A (hence the limitation on the motor in Section 2.2.2) and a maximum continuous current of 6A. They can operate in numerous modes including open-loop, voltage, IR compensation, velocity, current (torque), analog position loop and digital position loop. SCOUT II normally operated in current (torque) mode which meant that a reference input voltage to the servo amplifier commanded a proportional torque output.

Other features of these servo amplifiers include an inhibit pin, which is used to enable them, and current feedback pins. ARL's past experience using these servo amplifiers made them an easy choice for SCOUT II.

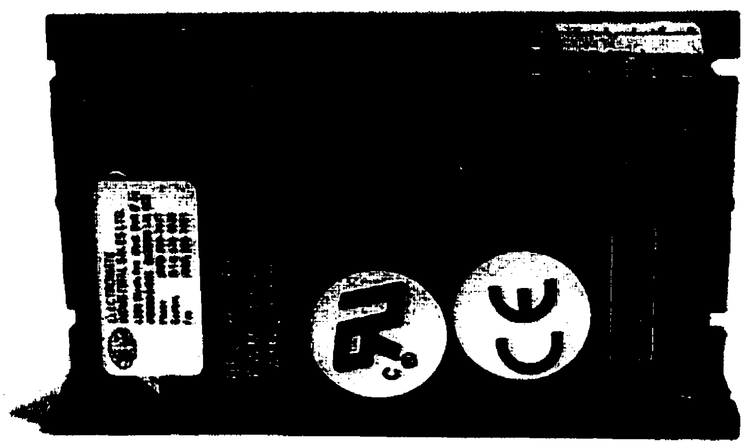

Figure 3.12: *Advanced Motion Controls 12A8E PWM servo amplifier [4].*

3.3.2 Power Supply

When wireless operation is desired, SCOUT II gets its power from on-board batteries. Two *Panasonic LCR 12V7.2P* [58] high capacity, 12V batteries are used. Each one has a rated capacity of 7.2Ah (at 20 hour discharge rate) and weighs in at just under 2.5 kg. During testing, when a wireless connection is not required, a 24 V external power supply can be used.

3.3.3 Power Distribution

The PWM servo amplifiers (and therefore the motors) are directly connected to the power supply (whether batteries or external). Also connected is the power distribution board which was designed and built by David McMordie. Its function is to convert the incoming 24V to the necessary voltages and distribute it to the various components. A *Vicor VI-JW0-CY* [72] DC-DC converter supplies the RF unit, camera and transmitter with 12V. A *Vicor VI-JW1-CY* [72] supplies the embedded PC, multiplexers, and R/C servos with 5V. The individual IO modules get their power from the SPP/SPI multiplexer hence they need not be connected to the power distribution board. A picture of the board is provided in Figure 3.13 and its circuit diagram can be seen in Appendix B. A general diagram of the complete power system on SCOUT II is shown in Figure 3.14.

Figure 3.13: *Power distribution board on SCOUT II (designed and built by David McMordie).*

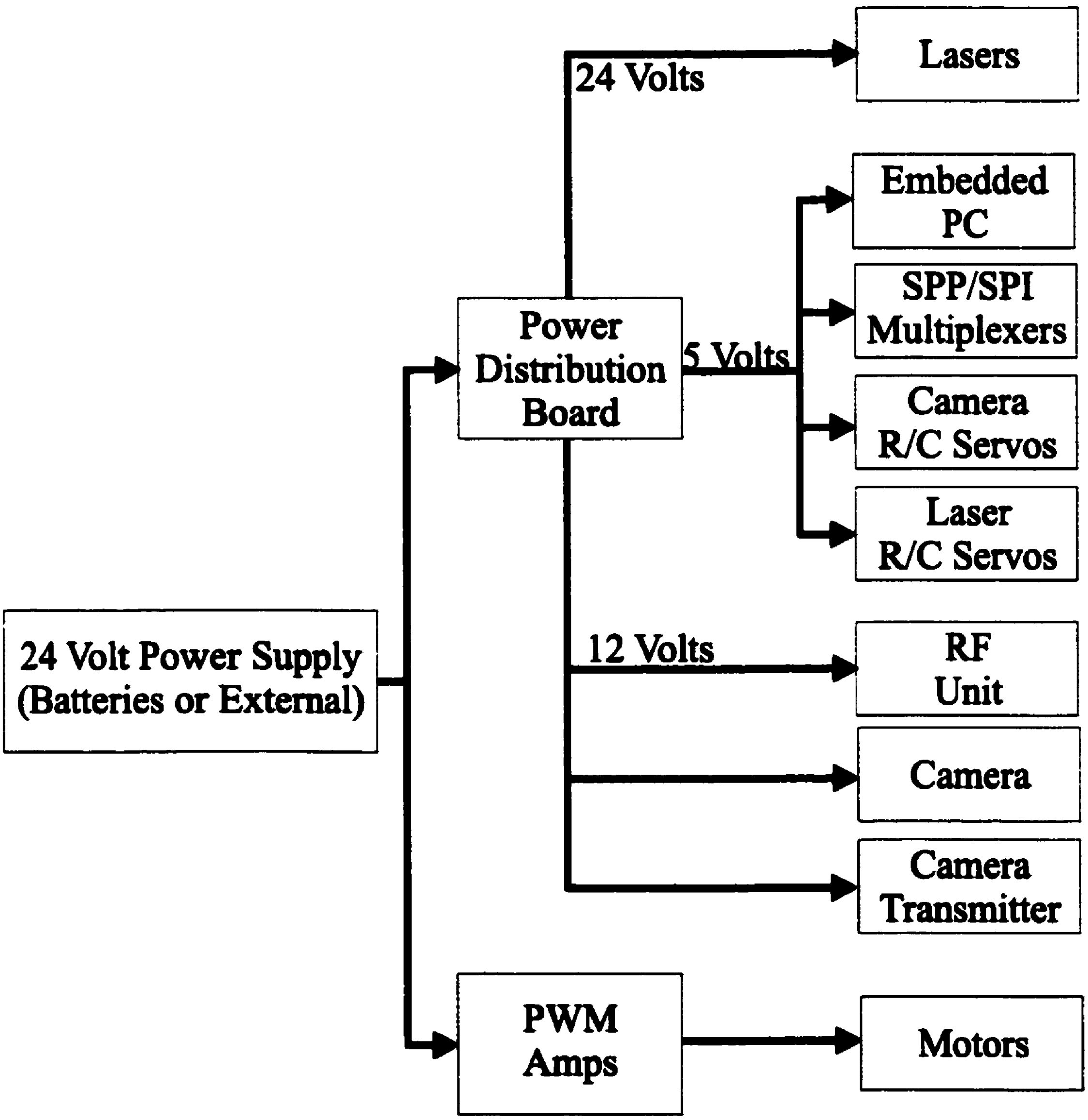

Figure 3.14: *SCOUT II's power network.*

3.4 Summary

Table 3.3 summaries the electrical specifications of SCOUT II.

Power	Source	2 Panasonic LCR 12V7.2P 12V Lead Acid Batteries
	Capacity	7.2 Ah (20hr rate)
Control	Source	Adastra VNS-486 PC board
	Iteration rate	1 kHz
Endurance	Continous operation	20 min. (estimated)
	Standby mode	1 hr. (estimated)

Table 3.3: *SCOUT II's electrical specifications.*

As with SCOUT II's mechanical design, the electrical system was designed to be modular and allow room for expansion. A variety of sensors are available, some of whom give redundant data (lasers or gyroscope to determine body angle, lasers or potentiometers to determine touchdown). This allows the different methods to be compared and the best one determined or, at least, determine which method works better for which instances.

Chapter 4

Stair-Climbing

This chapter begins by presenting the nomenclature for defining SCOUT II's geometry (Section 4.1). Section 4.2 reviews the walking and running algorithms that were implemented on SCOUT II by Anca Cocosco and Joseph Sarkis. Next, Section 4.3 focuses on stair-climbing simulations that were run using Working Model 2D [42]. The implementation of a stair-climbing algorithm is presented in Section 4.4. Lastly, Section 4.5 summarizes the results and presents some open issues which can be used as a starting point for future stair-climbing algorithms.

4.1 Nomenclature

Figure 4.1 and Table 4.1 define the nomenclature used for SCOUT II in fixed leg mode. A description of the nomenclature in compliant mode is provided in [64].

4.2 Walking and Running

SCOUT II's main purpose is to serve as an implementation tool to develop walking, running and stair-climbing algorithms.

This section briefly discusses the walking and running algorithms that have thus

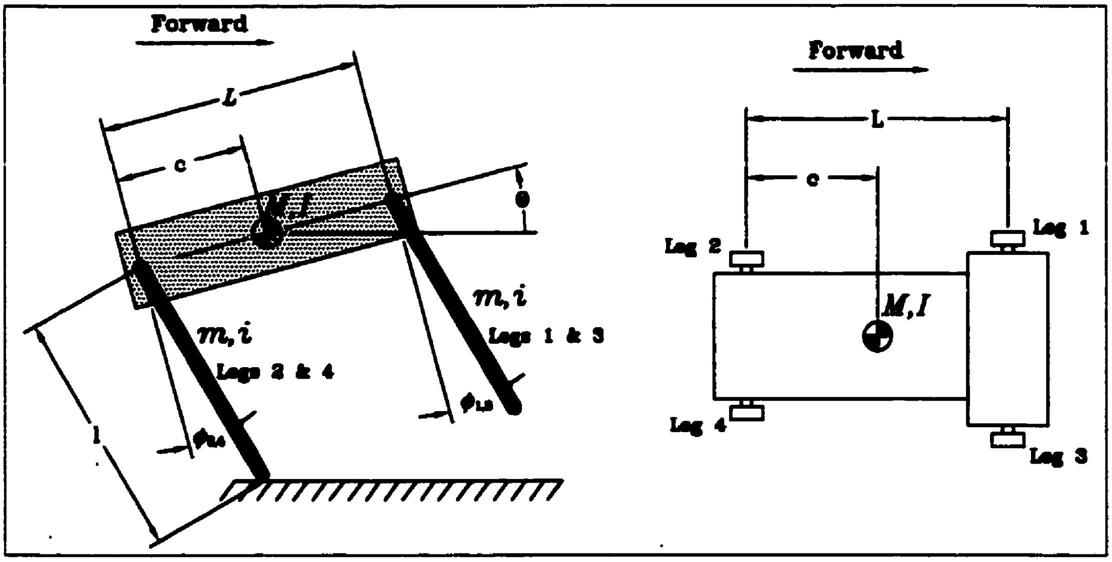

Figure 4.1: *SCOUT II nomenclature. (Side view at the left, top view at the right).*

Parameter	*Description*
L	Hip-to-hip length
c	Distance of center of mass from rear legs
$l_{1,2,3,4}$	Leg lengths
θ	Body angle wrt horizontal (ccw positive)
$\phi_{1,2,3,4}$	Leg angles wrt body (zero with legs perpendicular to body, ccw positive)
$\phi_{1_d,2_d,3_d,4_d}$	Desired leg angles

Table 4.1: *SCOUT II nomenclature description.*

far been implemented on SCOUT II. Anca Cocosco developed and successfully implemented two types of walking controllers on SCOUT II, the "Ramp Controller" and the "Saturated Ramp Controller". Both controllers kept the front legs at a fixed angle and relied on the momentum transfer when the non-elastic legs hit the ground. Figure 4.2 shows a picture playback of SCOUT II walking with the Ramp Controller. More detailed information on these algorithms can be found in [9].

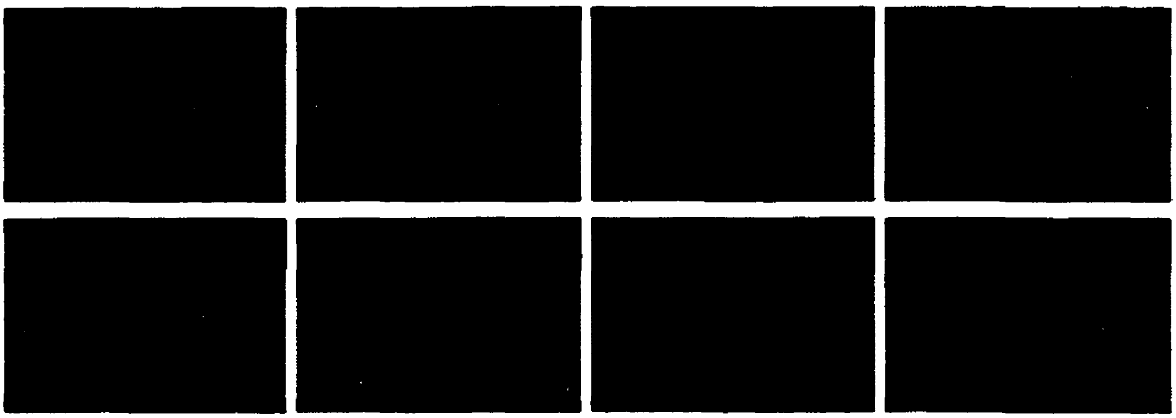

Figure 4.2: *Playback of SCOUT II taking two steps using the Ramp Controller [9].*

Joseph Sarkis developed a running controller for SCOUT II with compliant legs [64] based on Raibert's three-part controller [63]. Though the controller has not yet been successfully implemented on SCOUT II, preliminary runs have proven that SCOUT II can serve as a useful tool for testing running gaits with compliant legs as well.

4.3 Stair-Climbing Simulations

This section outlines the development of a stair-climbing algorithm for SCOUT II. Both the simulation software and the model will be described, and the results presented.

4.3.1 The Model

Stair-climbing simulations were run using the Working Model 2D [42] software package. The advantage of using such a package is that the user need not calculate the equations of motions. Instead, the software integrates the forces and moments acting on the bodies over a finite time period and determines the resulting motions. Numerous actuators and constraints are available to include in the model. The simulation can also take properties like friction and elasticity into account, something that is more difficult to do using classical Newtonian or Lagrangian methods.

Numerous simplifying assumptions were made for the simulations. These include:

1. The motion is planar.
2. Both front and rear legs of the quadruped move together and are hence modelled as single bodies with twice the mass and inertia.
3. Though the torques applied at the actuators are limited to the maximum stall torque available, they do not take into account the torque-speed characteristics of the actual motors.
4. The hip joints are frictionless.
5. Coefficients of friction are high enough to prevent slip between the toes and ground.
6. All impacts are inelastic.
7. All bodies are rigid.

In hindsight, some of these simplifying assumptions, in particular numbers 3 and 5, contribute to the considerable mismatch between the simulations and experiments - Section 4.4.1 will address this issue.

The model used for the simulations can be seen in Figure 4.3. The model consists of three rigid bodies: the body and two legs. Each leg features a circular toe which

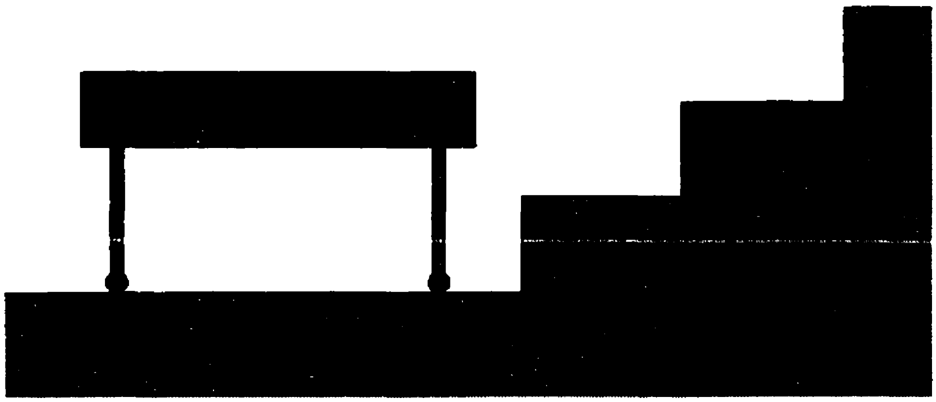

Figure 4.3: *SCOUT II in Working Model 2D [42].*

was considered as part of the leg rigid body. A torque actuator is placed between the body and each leg. A PD controller determines the torque based on the error between the desired and actual angles,

$$\tau = K_p \cdot e + K_d \cdot \dot{e} \tag{4.1}$$

where τ is the commanded actuator torque, K_p is the proportional gain (stance or flight), K_d is the derivative gain (stance or flight), and $e = \phi - \phi_d$.

Working Model parameters that were set include the animation time step, the integrator error and the integrator type. The animation time step represented the rate at which the screen was updated. The integrator error defined the accuracy of the simulation. At each step, the integrations were performed using the animation time step. If the resulting error was larger than the preset integrator error, the time step was halved and the integrations repeated. This process continued until the resulting error is below the values set for the integrator error.

Table 4.2 defines all of the parameters used for the simulations and their numerical values. All values used in the simulations represented the actual SCOUT II parameters.

Item	*Value*
Physical Properties	
Body length (L)	0.552 m
Body center of mass location (c)	0.262 m
Leg length (l)	0.313 m
Body mass (M)	20.09 kg
Leg mass (m)	1.720* kg
Toe mass	0.12* kg
Body inertia (I)	1.09 kgm^2
Leg inertia (wrt center of mass) (i)	0.028* kgm^2
Toe inertia (wrt center of mass)	0.0000003* kgm^2
Actuator properties	
Type	Torque
$\tau_{1,2}$	Actuator torques
Maximum torque (τ_{max})	75* Nm
PD controller gains	
Proportional flight gain (K_{p_f})	120 Nm/rad
Derivative flight gain (K_{d_f})	6.5 Nm s/rad
Proportional stance gain (K_{p_s})	1000 Nm/rad
Derivative stance gain (K_{d_s})	15 Nm s/rad
Body interaction properties	
Static friction coefficients for all bodies	100
Dynamic friction coefficients for all bodies	100
Elasticity coefficient for all bodies	0
Working Model Parameters	
Animation time step	0.005 s
Integrator type	5th order Runge Kutta
Integrator error	0.00001 m

Table 4.2: *Parameters used on Working Model. (* Values doubled to take into account a pair of legs.)*

4.3.2 The Algorithm

The stairs used for the simulations had a rise of 16.3 cm and a run of 27.5 cm. To simplify matters, the tread width was set equal to the run. These dimensions were chosen as they are similar to the actual dimensions of the stairs in the McConnell Engineering building at McGill University.

The algorithm developed can be seen in Figure 4.4. It was decided to use the corner of the step in order to reduce the possibility of the front toes slipping. This way the front foot can be wedged into the corner and thus, minimize slipping. The rear foot landed at approximately the quarter tread width. This was enough to ensure that the center of mass of the body was within the support region set by the feet. Numerous leg lengths were tested and it turned out that using a length of 313.2 mm would be advantageous. The various phases of the algorithm will be briefly described.

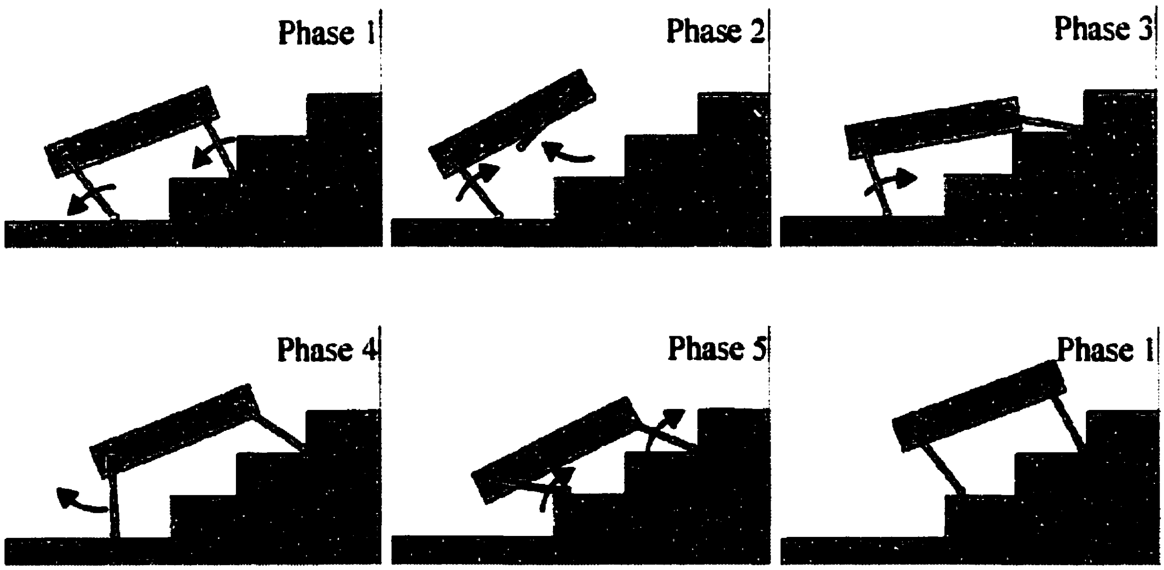

Figure 4.4: *Stair-climbing algorithm.*

Phase 1: Lean back

In this phase the rear leg angle (ϕ_2) increases thus allowing the body to lean back to the point where the center of mass is almost over the rear foot. The front leg applies no torque.

Phase 2: Launch 1

The rear leg is rotated clockwise launching the body up and forward. The front leg is rotated clockwise to an angle that will allow it to land at the corner of the step.

Phase 3: Launch 2

Zero torque is applied at the front leg while the rear leg is rotated clockwise until it is nearly vertical. This allows the body to gain the required forward and vertical momentum that will lift off the rear leg.

Phase 4: Lift off

This phase is actually divided into numerous parts. At first, the front leg it rotated counter-clockwise to help convert the forward momentum of the body into a rotational momentum that further raises the rear leg. When the rear leg lifts off, it is commanded to rotate clockwise to an angle where it hits the next step at the quarter tread width point. When the body reaches its apex, the front torque is reversed to further help lift up the body. Shortly after, the front leg is made to rotate clockwise with respect to the body to ensure that the rear leg hits the ground at the correct point and instant.

Phase 5: Lean forward

Both legs are rotated clockwise thus allowing the robot to return to the initial conditions of phase 1.

The algorithm was completely open loop, meaning that no feedback as to the current and past state of the robot was being used. The legs were simply being commanded to angle set-points and given a certain amount of time to get there. The final desired angles for all the phases, as well as the time required to get there, were determined experimentally. In all cases, the legs were commanded to the final desired angle using a linear trajectory. Its form was as follows,

$$\phi_t = \frac{\phi_{final} - \phi_{initial}}{t_{final} - t_{start\,motion}} * (t - t_{start\,motion} - t_{start\,phase}) + \phi_{initial} \tag{4.2}$$

where ϕ_t is the desired leg angle at time t, ϕ_{final} is the final leg angle, $\phi_{initial}$ is the initial leg angle, $t_{start\,phase}$ is the start time for the phase, $t_{start\,motion}$ is the start time for the motion, and t_{final} is the final time for the phase.

4.3.3 Results/Potential Problems

The algorithm discussed in Section 4.3.2 was coded in Working Model 2D and the set-points for each phase were tweaked. SCOUT II successfully climbed four steps before errors due to the open loop nature of the controller accumulated enough to hamper its continuation. Though significantly more time could have been spent fine-tuning the controller (and perhaps also making use of some feedback), it was decided to attempt implementation of the current algorithm. This way, the differences between the simulations and the real system could be determined. The next section covers the implementation process.

4.4 Stair-Climbing Implementation

Seeing as the simulations were run using an actuator torque of 75Nm, the 48/28 sprocket combination (which, according to Table 2.5 produces 37.8Nm of torque per motor) was used. A PD controller, as defined in Equation 4.1, was used to control the legs. Linear trajectories, similar to the ones in Equation 4.2, were used for the angles.

4.4.1 Data and Results

With minor modifications to the set-points, SCOUT II successfully achieved phases 1 and 2 of the algorithm. One modification was the lean back angle for the rear leg

($\phi 2_{final}$) at the end of phase 1. In the simulations, the leg went from 17° to 20° in 0.43 seconds. Experimentally, the same change in angle took more time (by approximately 25%) due to actuator speed limitations, hence the final angle was adjusted to 25°. In phase 2, if the final front leg angle was kept at -290° (or, alternately 70° if the angles are reset at every revolution), the body would hit the step (mainly due to leg overshoot caused by gearhead backlash, belt compliance and rubber toe compliance). Hence the angle was changed to -305° (55°) and the rear leg angle adjusted accordingly. Table 4.3 provides a comparison between the simulation set-points and the implemented ones for these two phases.

Parameter	*Simulation*	*Experimental*
Phase 1		
$\phi 1_{initial}$	-2°	-2°
$\phi 1_{final}$	zero torque	zero torque
$t1_{start\ motion}$	0 s	0 s
$t1_{end\ motion}$	0.43 s	1.5 s
$\phi 2_{initial}$	17°	17°
$\phi 2_{final}$	20°	25°
$t2_{start\ motion}$	0 s	0 s
$t2_{end\ motion}$	0.43 s	1.5 s
Phase 2		
$\phi 1_{final}$	-290° (70°)	-305° (55°)
$t1_{start\ motion}$	0 s	0 s
$t1_{end\ motion}$	0.23 s	0.23 s
$\phi 2_{final}$	7°	20°
$t2_{start\ motion}$	0 s	0 s
$t2_{end\ motion}$	0.27 s	0.25 s

Table 4.3: *Set-points for Phases 1 and 2.*

Phases 3 and 4 were significantly more difficult to implement. When first attempted with the simulation set-points, SCOUT II's rear legs barely got off the ground. The body had to be held to allow the rear legs to complete phase 4. Figure 4.5 displays the data for the leg angles for both simulation and experimentation. Phase 3, which

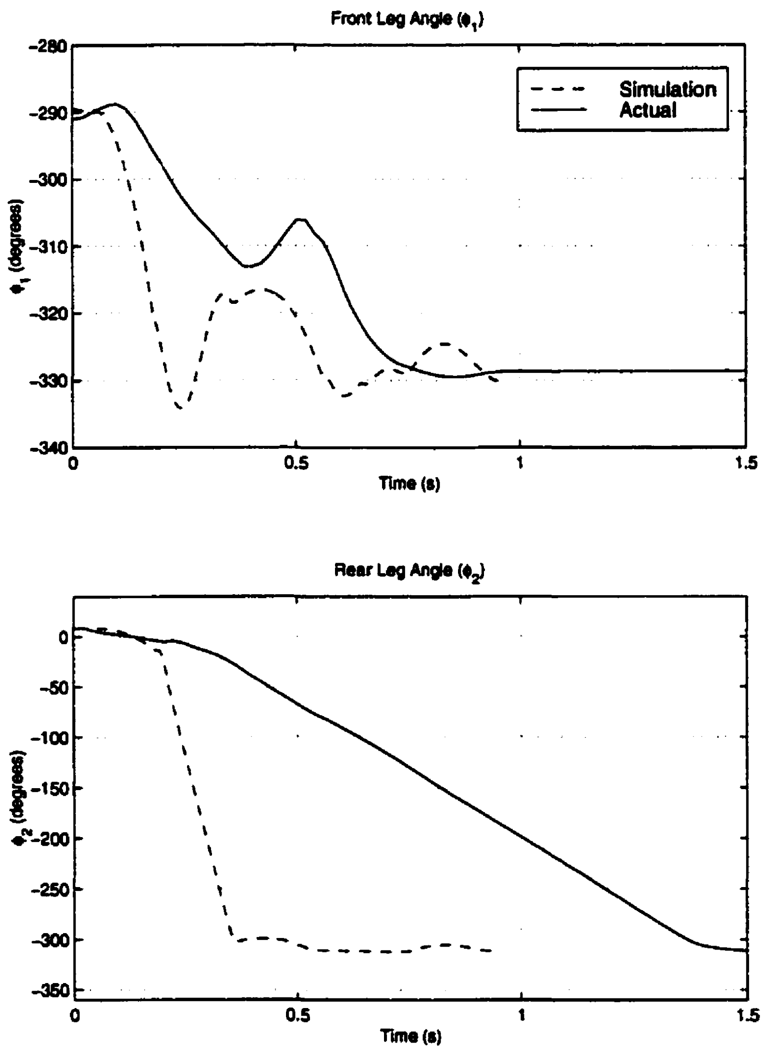

Figure 4.5: *Leg angles during phases 3 and 4.*

took 0.13 seconds in the simulation, took 0.25 seconds with the real system. Phase 4 took 0.2 seconds in the simulation (though it did not have to take quite that long to be successful), while the actual robot took 1.2 seconds. Analysis of the data (through feedback from the sensors and slow motion video footage) provided the following information as to the reasons for the discrepancies.

Toe slip

It was difficult to ensure that the front feet were totally in the corner of the step. Not being right up against the vertical section allowed the feet to slip during phase 3. This caused a significant amount of delay and lost energy.

Joint friction

As was stated in the assumptions, the simulations did not take joint friction into account. In phase 3, zero torque is applied to the front legs, while the rear legs rotate clockwise. Since the real system had friction in the front, a significant amount of energy was lost in this critical pushing phase. Hence the phase took longer to reach completion and the resulting body speed at the end was significantly lower than the simulations had predicted.

Speed limitations

It was originally believed that the leg speed would be a problem in phase 4. However, it turned out to be more of a problem in phase 3. Due to the limited leg speed, by the end of the phase, the velocity of the body was much lower.

The lack of body momentum by the end of phase 3 can be seen in Figure 4.5. In the simulations, the body gains enough forward and vertical speed that the front leg angles ($\phi_{1,3}$) reach -335° (25°). In the actual implementation, the front legs only reach -315° (45°).

Numerous modifications were made to the algorithm to try to improve its effectiveness. The primary change was to increase ϕ_2 at the beginning of phase 3. This allowed more time for the rear leg to sweep which gave the body more momentum. The initial conditions and set-points were modified until the rear legs reached their maximum velocity at the end of phase 3. Though the results improved significantly, SCOUT II was still unsuccessful. About 1.2 seconds was required to give the legs enough time to get onto the next step. At best, the rear feet were in the air for about 0.7 seconds.

Attempts at increasing ϕ_2 at the beginning of phase 3 too much had adverse effects. It lead to SCOUT II having most of its weight over the rear legs resulting in the front legs lifting off the ground.

Changing the gear ratio from the 48/28 sprocket configuration to the 48/34 configuration was also considered. This would have resulted in about 20% more speed. The loss of torque, however, would then have been a problem.

4.4.2 Improvements to Algorithm

Though time limited the amount of work that was done in attempting to improve the algorithm, preliminary results from it are quite pessimistic. This algorithm has most of the weight of the robot on the rear legs and relies on torque and speed from the actuators to get through phases 3 and 4. This may not be the optimal way to achieve stair-climbing. An algorithm similar to the one implemented on SCOUT I [75] may be more successful. The algorithm gets the rear legs on the next step by rocking the body onto the front legs. This, however, will require having both feet on one step which may pose some geometric and stability issues.

4.5 Summary

Though implementation of the developed stair-climbing controller was unsuccessful, it provides useful insight about SCOUT II and its abilities, or, more precisely, its limitations. It gives an understanding about the importance of the assumptions made in the simulations. The stair-climbing data received from these experiments allows for improvements to be made to the simulations. This preliminary information will undoubtably prove useful to further stair-climbing research at ARL and subsequent implementation on SCOUT II.

Chapter 5

Conclusion

The design and construction of the most recent robot in the SCOUT series, SCOUT II, was presented. This series of quadrupeds is distinguished by having only one actuated degree of freedom per leg. This is a substantial reduction from most of quadrupeds that incorporate three to four degrees of freedom per leg. Unlike SCOUT I, SCOUT II has a second degree of freedom which is unactuated. This passive joint allows compliant walking, running and stair-climbing gaits to be explored. SCOUT II was built to demonstrate that even with a simple design, a high maneuverability can be achieved.

This thesis commenced by detailing the specifications for the robot as well as preliminary calculations required for the selection of a suitable actuation system. Next, a complete description of the mechanical design and construction was presented. Chapter 3 presented the electronics and sensor systems. The first part of Chapter 4 (Section 4.2) presented information on preliminary walking and running algorithms that were developed and implemented on SCOUT II by Anca Cocosco and Joseph Sarkis respectively. The following sections discussed a preliminary stair-climbing controller that was developed, simulated on Working Model 2D [42] and partially implemented on SCOUT II.

The result of this work produced a fully autonomous mobile robot with a high level of modularity. This will ensure that the robot's current specifications do not limit the algorithms developed. All of the mechanical and electrical specifications outlined in Table 2.1 were met. SCOUT II weighs in at under 24kg, is 0.837m long and 0.498m wide. The highly adjustable actuation system can produce torques of up to 40.7Nm and speeds up to 57.8 RPM. The robot has fully adjustable leg lengths. The body length and width can be modified by replacing very simple components.

SCOUT II's performance specifications, on the other hand, are still a work in progress. Though stiff-legged walking was successfully demonstrated, SCOUT II has yet to run and stair-climb. Even though the stair-climbing algorithm presented in Chapter 4 was unsuccessful, it highlighted useful information about the robots limitations and the modelling parameters used in the simulations.

Even though this small part of this work was not totally successful, the project thus far has been a great success. The important thing is that the Ambulatory Robotics Laboratory now has a tool to test the control algorithms being developed.

Future Work

The focus of this work was to develop the tool for the implementation of various gaits. Hence, a lot of the work on the development and implementation is yet to be done. As for the robot itself, very little work remains. Martin de Lasa is actively working on getting the RF unit operational and Geoff Hawker is ironing out some bugs with the embedded PC board. Once these two items are complete, SCOUT II will be fully autonomous.

The work presented on stair-climbing requires a significant amount of refining for it to succeed. Perhaps, the primary task is to modify the model used in the simulations to account for toe slipping, non-frictionless hip joints and actuator torque-speed characteristics. This will produce more realistic simulations that have a greater chance of being successfully implemented. Using the actual robot as a guide, the Working Model parameters can be tuned to mimic the real life situation.

As for the stair-climbing algorithm itself, its success is questionable with the current actuators. A controller similar to the one developed for SCOUT I, should prove to be more successful. Shifting the robot's center of mass onto the front legs will make it significantly easier for the rear legs to move up a step. Obviously, using SCOUT II in compliant leg mode may also aid in the implementation of an algorithm.

Numerous graduate students from the Ambulatory Robotics Laboratory are developing controllers for SCOUT II. Of notable importance is Martin de Lasa's compliant walking controller. This algorithm should drastically improve the current stiff-legged walking controller by producing a quicker and smoother walking motion. Didier Papadopoulos will attempt to implement a modified version of Joseph Sarkis' running controller.

The work does not end with successful walking, running and stair-climbing. For SCOUT II to prove its usefulness, it must be able to get up from a laying down position and be able to turn (both while walking and on the spot).

Modifications to the leg design may also improve SCOUT II's maneuverability and, therefore, its success. Geoff Hawker is looking to replace the unactuated prismatic knee joints with unactuated revolute joints. This will allow trotting gaits to be investigated, not to mention the tremendous improvement that it will make to stair-climbing.

Though the development may take years, the final result should produce a simple, reliable quadruped robot that is more maneuverable in rugged terrain than wheeled and tracked robots.

Bibliography

[1] Amooty, a stair climbing intelligent maintenance robot. *Nuclear Engineering International*, 30(367), Apr. 1985.

[2] Abacom Technologies, Etobicoke, ON, Canada. 1996.

[3] Adastra Systems, Hayward, CA. *VNS-486 User's Manual*, 1997, www.adastra.com.

[4] Advanced Motion Controls, Camarillo, CA. *PWM Servo Amplifiers Catalogue*, 1992, www.a-m-c.com.

[5] M. Ahmadi. *Stable Control of a One-Legged Robot Exploiting Passive Dynamics*. PhD thesis, McGill University, Montréal, QC, Canada, March 1998.

[6] Aromat Corporation, Etobicoke, ON, Canada. *Aromat Catalogue*, 1997, www.aromat.com.

[7] R. Brunner, A. Molnár, L. Varga, and Z. Vámossy. Exploratores, quadruped robot. In K. Dobrovodsk, editor, *Proc. of 7th International Workshop of Robotics in Alpe-Adria-Danube Region - RAAD '98 (Slovak Academy of Sciences)*, pages 215–220, Bratislava, Slovakia, 1998.

[8] M. Buehler, R. Battaglia, A. Cocosco, G. Hawker, J. Sarkis, and K. Yamazaki. SCOUT: A simple quadruped that walks, climbs and runs. In *Proc. IEEE Int. Conf. Robotics and Automation*, pages 1707–1712, Leuven, Belgium, May 1998.

[9] A. E. Cocosco. Control of walking in a quadruped robot with stiff legs. Master's thesis, McGill University, Montréal, QC, Canada, Jul 1998.

[10] S. Cordes, K. Berns, M. Eberl, W. Ilg, and Peter Buhrle. On the design of a four-legged walking machine. In *Proc. Int. Conf. Advanced Robotics*, pages 65–70, Monterey, CA, July 1997.

[11] N. Cross. *Engineering Design Methods.* John Wiley and Sons, New York, NY, second edition, 1994.

[12] E. Oberg, F. D. Jones, H. L. Horton and H. H. Ryffel. *Machinery's Handbook.* Industrial Press Inc., New York, NY, twenty-fourth edition, 1992.

[13] A. Ertas and J.C. Jones. *The Engineering Design Process.* John Wiley and Sons, New York, NY, second edition, 1996.

[14] J. Fabro and G. Hartlen. Mechanical Laboratory Final Report: DC Motor Testing. Technical report, McGill University, Montréal, QC, Canada, Apr. 1998.

[15] J. Furusho, A. Sano, M. Sakaguchi, and E. Koizumi. Realization of bounce gait in a quadruped robot with articular-joint-type legs. In *Proc. IEEE Int. Conf. Robotics and Automation*, pages 697–702, May 1995.

[16] Garlock Bearings Inc, Thorofare, NJ. *DU Self-Lubricating Bearings*, 1987, www.garlockbearings.com.

[17] J. Golden and Y. Zheng. Gait synthesis for the SD-2 biped robot to climb stairs. *International Journal of Robotics and Automation*, 5(4):149–159, 1990.

[18] P. Grégoire, T. Marincic, and O. Payant. CARL: Compliant Articulated Robotic Leg. Design v final report, McGill University, Montréal, Canada, Apr. 1994.

[19] P. Gregorio. Design, control and energy minimization strategies for an electrically actuated legged robot. Master's thesis, McGill University, Montréal, QC, Canada, Aug. 1994.

[20] Harmonic Drive, Wakefield, MA. *Cup and Pancake Component Gear Sets*, 1989, www.harmonic-drive.com.

[21] HD Systems, Inc., Hauppauge, NY. *Cup Type HDUC and HIUC Component Sets*, 1994, www.hds.co.jp.

[22] S. Hirose. A study of design and control of a quadruped walking vehicle. *Int. J. Robotics Research*, 3(2):113–133, 1984.

[23] S. Hirose, S. Aoki, and J. Miyake. Terrain adaptive quadru-track vehicle HELIOS-II. In *Int. Symp. on Industrial Robots*, pages 235–243, Tokyo, Japan, Oct. 1989.

[24] S. Hirose, T. Masui, H. Kikichiand, Y. Fukuda, and Y. Umetani. TITAN III a quadruped walkig vehicle - its structure and basic characteristics. In *Int. Symp. Robotics Research*, pages 325–331, 1985.

[25] S. Hirose, J. Miyaki, and S. Aoki. Terrain adaptive tracked vehicle HELIOS-I. In *Proc. Int. Conf. Advanced Robotics*, pages 676–687, 1989.

[26] S. Hirose, J. Miyaki, and S. Aoki. Development of terrain adaptive quadru-track vehicle HELIOS II. In *Jour. of RSJ*, pages 283–291, 1992.

[27] S. Hirose and A. Rattipat. Design of a stair-climbing vehicle. In *Proc. of the 13th Ann. Conf. RSJ*, pages 153–154, 1995.

[28] S. Hirose, M. Usa, and S. Aoki. Development of terrain adaptive quadru-track vehicle HELIOS III. In *Proc. of the 9th Ann. Conf. RSJ*, pages 305–306, 1991.

[29] S. Hirose and K. Yoneda. TITAN-VIII, 1999, mozu.mes.titech.ac.jp/research/walk/TITAN8/TITAN8.htm.

[30] S. Hirose, K. Yoneda, K. Arai, and T. Ibe. Design of a quadruped walking vehicle for dynamic walking and stair climbing. *Advanced Robotics*, 9(2):107–124, 1995.

[31] S. Hirose, K. Yoneda, R. Furuya, and T. Takagi. Dynamic and static fusion control of quadruped walking vehicle. In *Proc. IEEE/RSJ Int. Conf. Intelligent Systems and Robots*, pages 199–204, 1989.

[32] S. Hirose, K. Yoneda, and H. Tsukagoshi. TITAN-VII: Quadruped walking and manipulating robot on a steep slope. In *Proc. IEEE Int. Conf. Robotics and Automation*, pages 494–500, Albuquerque, NM, 1997.

[33] J. Hodgins and M. Raibert. Adjusting step length for rough terrain locomotion. *IEEE Trans. Robotics and Automation*, 7(3):289–298, June 1991.

[34] Honda Motor Co., Ltd. Humanoid Robot, 1999, www.honda.co.jp/english/technology/robot/index.html.

[35] Honeywell, 1999, www.honeywell.com.

[36] Inland Motor - Kollmorgen Corporation, Radford, VA. *Direct Drive DC Motors*, 1985, www.kollmorgen.com.

[37] Interelectric AG, Sachseln, Switzerland. *Maxon Motor Catalogue*, 1997/98, www.maxon.com.

[38] IS Robotics, Somerville, MA. *www.isr.com.*

[39] T. Iwamoto and H. Yamamoto. Mechanical design of variable configuration tracked vehicle. *Mechanical Design*, 112(3):289–294, Sept. 1990.

[40] H. Kimura. Realization of dynamic walking and running of the quadruped using neural oscillator. In *5th Int. Conf. on Simulation of Adaptive Behavior (SAB98), Workshop on Biological Inspired Walking*, pages 7–15, Zurich, 1998.

[41] H. Kimura and I. Shimoyama ad H. Miura. Dynamics in the dynamic walk of the quadruped. *Proc. Int. Conf. Advanced Robotics*, 4(3):283–301, 1990.

[42] Knowledge Revolution. *Working Model 2D Version 4.0.* San Mateo, CA, 1996, www.krev.com.

[43] N. Koyachi, H. Adachi, and E. Nakano. Design and basic control of stair-climbable fixed gait hexapod walking machines. In *Proc of the USA Jpn Symp. on Flexible Autom. Crossing Bridges Adv in Flexible Autom and Rob.*, pages 673–680, 1986.

[44] Y. Maeda, S. Tsutani, and S. Hagihara. Prototype of multifunctional robot vehicle. In *Proceedings of '85 International Conference on Advanced Robotics*, pages 421–428, Japan, Sept.2 1985.

[45] Marshall Electronics, Culver City, CA.

[46] O. Matsumoto, S. Kajita, M. Saigo, and K. Tani. Dynamic trajectory control of passing over stairs by a biped type leg-wheeled robot with nominal reference of static gait. In *Proc. IEEE/RSJ Int. Conf. Intelligent Systems and Robots*, pages 406–412, Victoria, BC, Canada, Oct. 1998.

[47] G. Mennitto. Compliant articulated robot leg with antagonistic LADD actuation. Master's thesis, McGill University, Montréal, QC, Canada, Feb. 1995.

[48] Midori America Corp., Fullerton, CA. *Green Pot Potentiometers*, 1997, www.thomasregister.com/midori.

[49] H. Miura, I. Shimoyama, M. Mitsuishi, and H. Kimura. Dynamical walk of quadruped robot (Collie-1). In H. Hanafusa and H. Inoue, editors, *Int. Symp. Robotics Research*, pages 317–324. MIT Press, Cambridge, 1984.

[50] Murata Electronics North America Inc., Smyrna, GA, www.murata.com.

[51] S. Obaid. Sensing for dynamic locomotion. Master's thesis, McGill University, Montréal, QC, Canada, Apr. 1999.

[52] Associate Committee on the National Building Code. *National Building Code of Canada (1980).* National Research Council of Canada, Ottawa, ON, Canada, 1980.

[53] Associate Committee on the National Building Code. *Canadian Housing Code (1990).* National Research Council of Canada, Ottawa, ON, Canada, 1990.

[54] Y. Ota, Y. Inagaki, K. Yoneda, and S. Hirose. Development of a six-legged walking robot with parallel mechanism. In *Proc. TITech COE/Super Mechano-Systems workshop '98*, pages 105–114, 1998.

[55] Y. Ota, Y. Inagaki, K. Yoneda, and S. Hirose. Research on a six-legged walking robot with parallel mechanism. In *Proc. IEEE/RSJ Int. Conf. Intelligent Systems and Robots*, pages 241–248, Victoria, BC, Canada, Oct. 1998.

[56] Hewlett Packard, 1999, www.hp.com.

[57] G. Pahl and W. Beitz. *Engineering Design.* Design Council, London, 1984.

[58] Panasonic. *Sealed Lead-Acid Batteries Technical Handbook.* Osaka, Japan, 1999, www.panasonic.com.

[59] Parametric Technology Corporation. *Pro/Engineer Release 20.0.* Waltham, MA, 1998, www.ptc.com.

[60] Parametric Technology Corporation. *Pro/Mechanica Release 20.0.* Waltham, MA, 1998, www.ptc.com.

[61] Stock Drive Products. *Handbook of Timing Belts, Chains and Friction Drives.* New Hyde Park, NY, d210-2 edition, www.sdp-si.com.

[62] QNX Software Systems LTD. QNX Operating System v4.2, 1996, www.qnx.com.

[63] M. H. Raibert. *Legged Robots That Balance.* MIT Press, Cambridge, MA, 1986.

[64] J. Sarkis. Control of running in a quadruped robot with actuation only at the hips. Master's thesis, McGill University, Montréal, QC, Canada, Mar. 1999.

[65] J. E. Shigley and C. R. Mischke. *Mechanical Engineering Design.* McGraw-Hill Inc., New York, NY, fifth edition, 1989.

[66] H. D. Taghirad. *Robust Torque Control of Harmonic Drive Systems.* PhD thesis, McGill University, Montréal, QC, Canada, March 1999.

[67] K. Taguchi. Enhanced wheel system for step climbing. *Advanced Robotics*, 9(2):137–147, 1995.

[68] Terra Aerospace Corporation. Ottawa, ON, Canada, www.smarteod.com.

[69] Tower Hobbies, Champlain, Il. *Tower Hobbies Catalogue*, 1998.

[70] Y. Uchida, K. Furuichi, and S. Hirose. Fundamental performance of 6 wheeled off-road vehicle "HELIOS-V". In *Proc. IEEE Int. Conf. Robotics and Automation*, Detroit, MI, May 1999.

[71] Z. Vámossy, A. Molnár, R. Brunner, and L. Varga. EXPLORATORES II, the Four-Legged Mobile Robot. In Y. Baudoin, editor, *Proc. of International Symposium on Climbing and Walking Robots - CLAWAR '98*, Brussel, Belgium, 1998.

[72] Vicor, 1999, www.vicr.com.

[73] D. Wettergreen and H. Pangels. Behaviour based gait execution for the DANTE II walking robot. In *Proc. IEEE/RSJ Int. Conf. Intelligent Systems and Robots*, pages 274–279, Pittsburg, PA, Aug. 1995.

[74] J. White, J. Coughlan, M. Harvey, R. Upton, and K. Walker. Taking Andros for a walk. *Nuclear Engineering International*, 34(415):52–53, Mar. 1989.

[75] K. S. Yamazaki. The design and control of SCOUT I, a simple quadruped robot. Master's thesis, McGill University, Montréal, QC, Canada, Feb. 1999.

[76] Y. F. Zheng and Jr. F. R. Sias. Design and control of practical biped robots. *Int. J. of Robotics and Automation*, 3(2):70–77, 1988.

Appendix A

SCOUT II Assembly Drawings

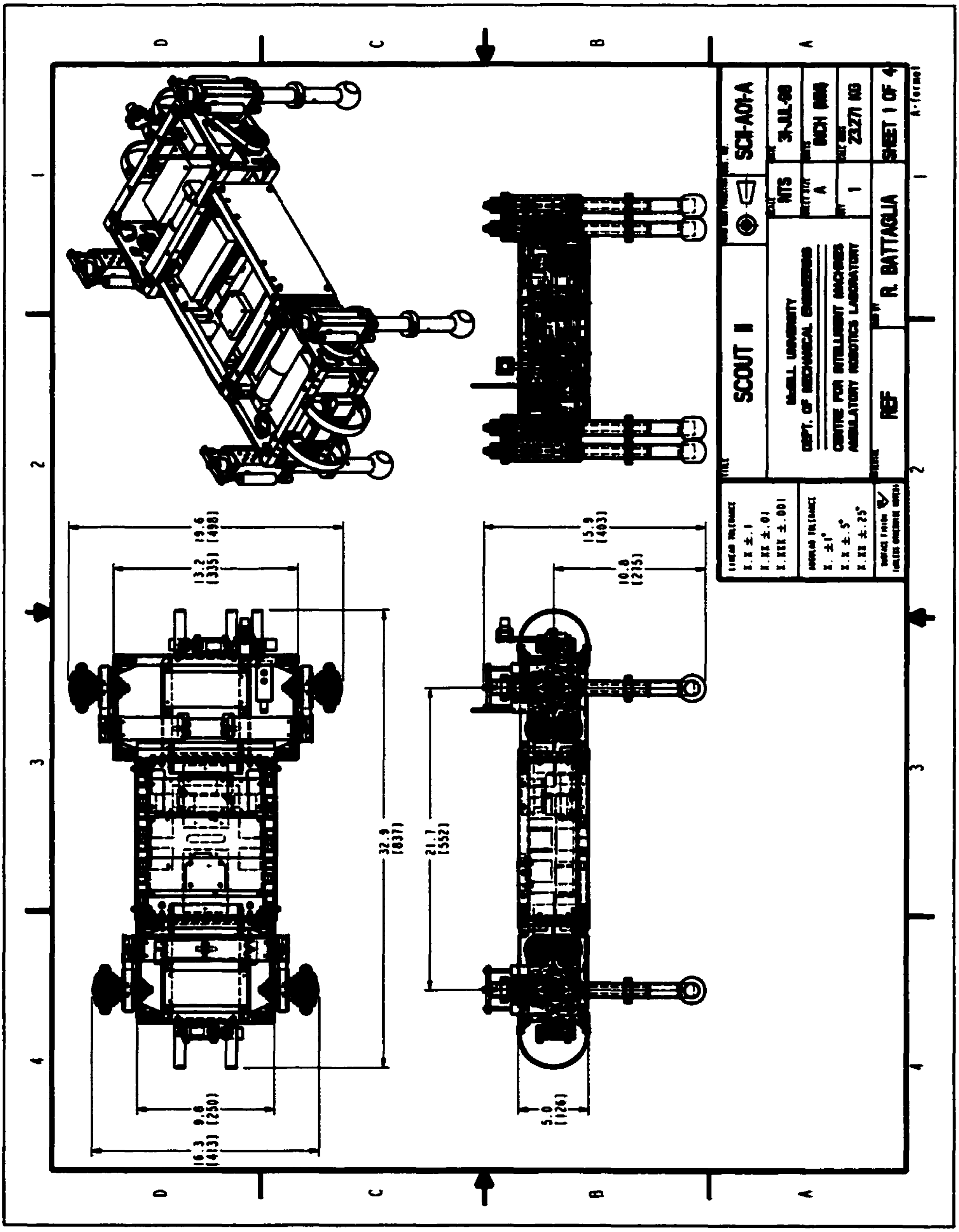
SCOUT II
McGILL UNIVERSITY
DEPT. OF MECHANICAL ENGINEERING
CENTRE FOR INTELLIGENT MACHINES
AMBULATORY ROBOTICS LABORATORY
SCII-A01-A
NTS
A
1
R. BATTAGLIA
REF
SHEET 1 OF 4
32.9 [837]
21.7 [552]
15.9 [403]
10.8 [275]
5.0 [126]

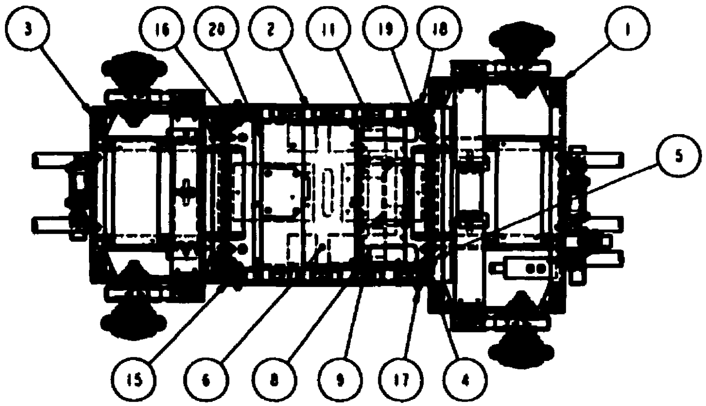

BILL OF MATERIALS					
INDEX	NAME	DESCRIPTION	MATERIAL	QTY	DWG NUMBER
1	FRONT_HIP_LEG	FRONT HIP SUB-ASSEMBLY	REF	1	SCII-A03-A
2	BODY_LINK	BODY SHAFT	AL-6061-T6	4	SCII-011-A
3	REAR_HIP_LEG	REAR HIP SUB-ASSEMBLY	REF	1	SCII-A04-A
4	WASHER_M4	4MM WASHER	STEEL	20	REF
5	SHCS_M4X16	M4X16 SHCS	STEEL	16	REF
6	BOTTOM_ELEC	BOTTOM ELECTRONICS SUB-ASSEMBLY	REF	1	SCII-A07-A
7	SHCS_M4X10	M4X10 SHCS	STEEL	4	REF
8	POWER_BOARD_BRACKET	POWER BOARD BRACKET	AL-6061-T6	1	SCII-044-A
9	POWER_BOARD	POWER BOARD	REF	1	REF
10	WASHER_M3	3MM WASHER	STEEL	4	REF
11	NUT_M3	M3 NUT	STEEL	4	REF
12	SHCS_M3X30	M3X20 SHCS	STEEL	4	REF
13	SIDE_ELEC	SIDE ELECTRONICS SUB-ASSEMBLY	REF	2	SCII-A09-A
14	RF	RF UNIT	REF	1	REF
15	BODY_BRACKET	BODY SHAFT BRACKET	AL-6061-T6	8	SCII-021-B
16	WASHER_M5	5MM WASHER	STEEL	8	REF
17	SHCS_M5X30	M5X30 SHCS	STEEL	8	REF
18	NUT_M5	M5 NUT	STEEL	8	REF
19	NUT_M4	M4 NUT	STEEL	16	REF
20	RF_BRACKET	FR UNIT BRACKET	LEXAN	1	SCII-045-A
21	SPACER_3_5X6X5	METRICAM PARTS 56000 3.5X6X10	PLASTIC	4	REF

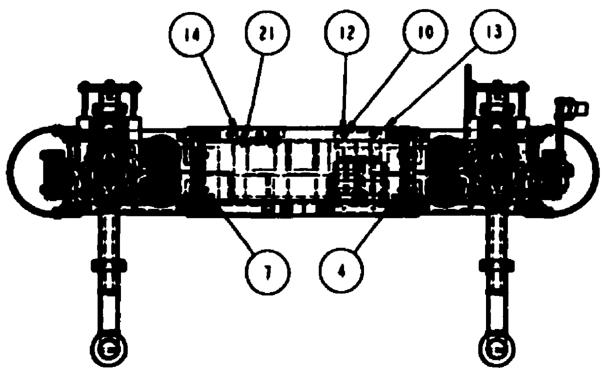

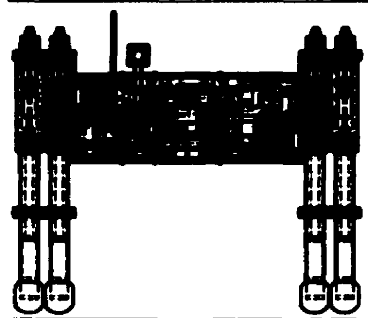

LINEAR TOLERANCE
X.X ±.1
X.XX ±.01
X.XXX ±.001

ANGULAR TOLERANCE
X. ±1°
X.X ±.5°
X.XX ±.25°

SURFACE FINISH (UNLESS OTHERWISE NOTED)

SCOUT II

SCII-A01-A

McGILL UNIVERSITY
DEPT. OF MECHANICAL ENGINEERING

CENTRE FOR INTELLIGENT MACHINES
AMBULATORY ROBOTICS LABORATORY

NTS | 30-DEC-98
A | INCH (MM)
1 | 23.271 KG

REF | R. BATTAGLIA | SHEET 3 OF 4

A-format

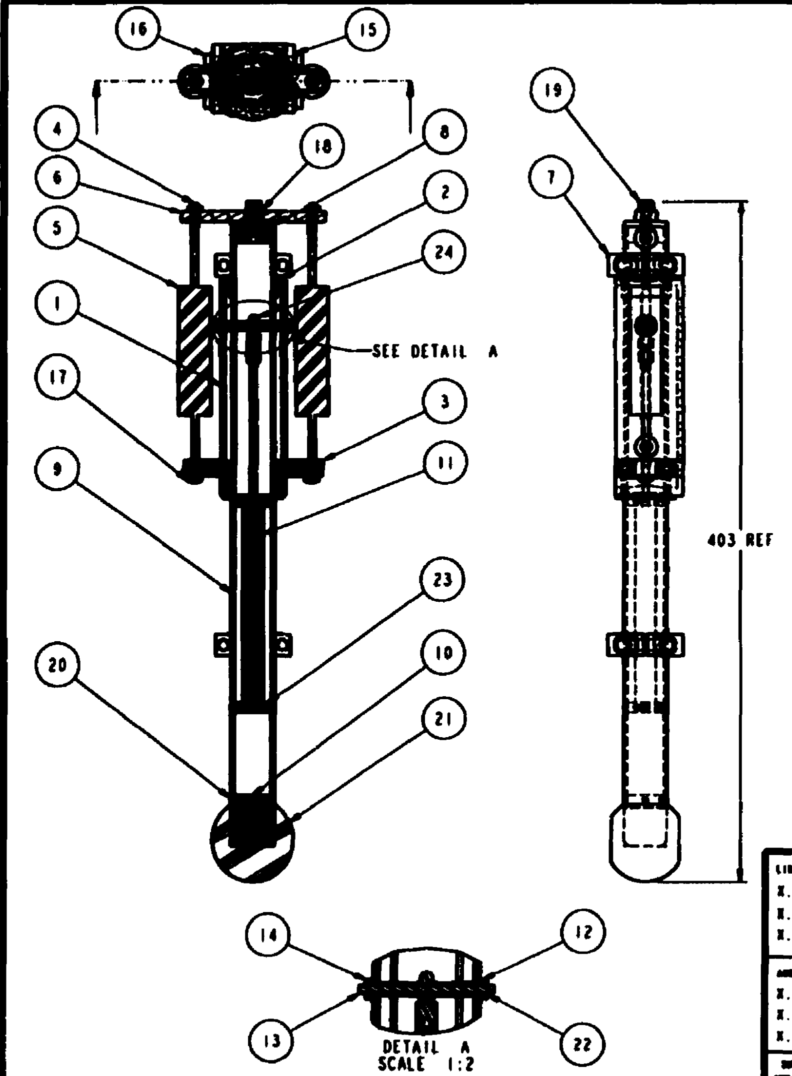

BILL OF MATERIALS					
INDEX	NAME	DESCRIPTION	MATERIAL	QTY	DWG NUMBER
1	UPPER_LEG	UPPER LEG	AL-6061-T6	1	SC11-012-A
2	LEG_BUSHING	GARLOCK PART# 16DU08	REF	2	REF
3	SPRING_BRACKET	SPRING BRACKET	AL-6061-T6	2	SC11-013-A
4	HOR_SCREW_EYE	METRICAN PART#17420 M4x15x6	STEEL	4	REF
5	RUBBER_SPRING	LATEX RUBBER SPRING	LATEX RUBBER	2	REF
6	SPRING_SUPPORT	SPRING SUPPORT	AL-6061-T6	1	SC11-014-A
7	LEG_CLAMP	SPAE-NAUR PART# 600-055	STEEL	2	REF
8	LEG_TOP_BUSHING	LEG CAP	AL-6061-T6	1	SC11-015-A
9	LOWER_LEG	LOWER LEG	STEEL	1	SC11-016-A
10	FOOT	FOOT	AL-6061-T6	1	SC11-017-A
11	POT	MIDORI PART# LP-100FP	REF	1	REF
12	POT_BUSHING	POT BUSHING	STEEL	2	SC11-018-A
13	POT_SHAFT	POT SHAFT	STEEL	1	SC11-019-A
14	WASHER_M3	3MM WASHER	STEEL	2	REF
15	WASHER_M4	4MM WASHER	STEEL	8	REF
16	SHCS_M4X12	M4x12 SHCS	STEEL	4	REF
17	NUT_M4	M4 NUT	STEEL	4	REF
18	WASHER_M5	5MM WASHER	STEEL	1	REF
19	SHCS_M5X16	M5x16 SHCS	STEEL	1	REF
20	SS_M3X3	M3x3 SET SCREW	STEEL	4	REF
21	TOE	RUBBER BALL	RUBBER	1	SC11-022-A
22	RR_M3	3MM RETAINING RING	STEEL	2	REF
23	POT_CLAMP	POT CLAMP	AL-6061-T6	2	SC11-020-A
24	POT_ROD_END	AURORA PART# CW-M3	STEEL	1	REF

LINEAR TOLERANCE
X.X ±.1
X.XX ±.01
X.XXX ±.001

ANGULAR TOLERANCE
X. ±1°
X.X ±.5°
X.XX ±.25°

SURFACE FINISH

TITLE: LEG SUB-ASSEMBLY

SC11-A02-A

McGILL UNIVERSITY
DEPT. OF MECHANICAL ENGINEERING

CENTRE FOR INTELLIGENT MACHINES
AMBULATORY ROBOTICS LABORATORY

SCALE: NTS
DATE: 15-DEC-98
SHEET SIZE: A
UNITS: MM
QTY: 4
CALC MASS: 0.920 KG

MATERIAL: REF
DRAWN BY: R. BATTAGLIA
SHEET 1 of 2

A-format

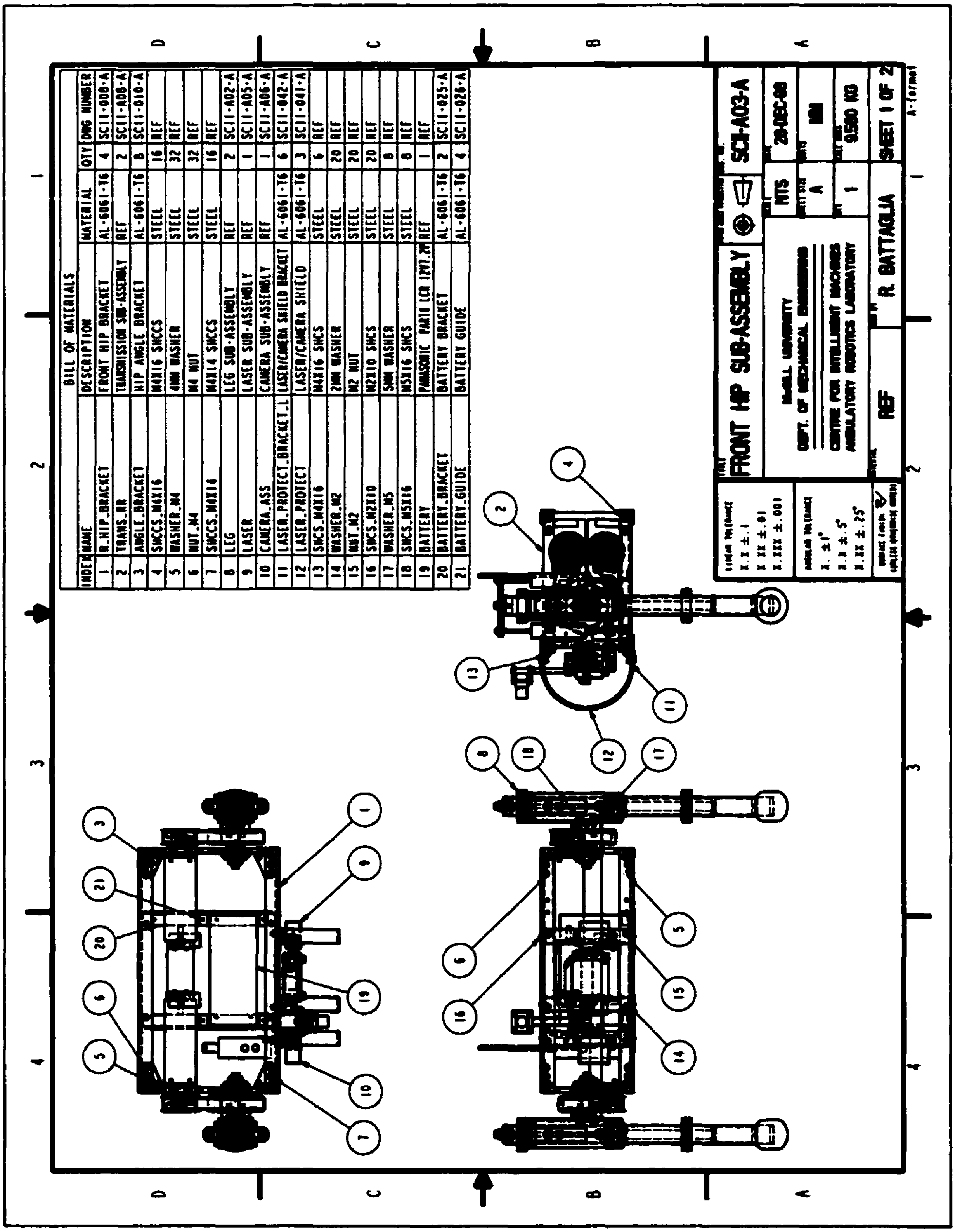
BILL OF MATERIALS
INDEX NAME DESCRIPTION MATERIAL QTY DWG NUMBER
1 R_HIP_BRACKET FRONT HIP BRACKET AL-6061-T6 4 SCII-008-A
2 TRANS_RR TRANSMISSION SUB-ASSEMBLY REF 2 SCII-A08-A
3 ANGLE_BRACKET HIP ANGLE BRACKET AL-6061-T6 8 SCII-010-A
4 SHCCS_M4X16 M4X16 SHCCS STEEL 16 REF
5 WASHER_M4 4MM WASHER STEEL 32 REF
6 NUT_M4 M4 NUT STEEL 32 REF
7 SHCCS_M4X14 M4X14 SHCCS STEEL 16 REF
8 LEG LEG SUB-ASSEMBLY REF 2 SCII-A02-A
9 LASER LASER SUB-ASSEMBLY REF 1 SCII-A05-A
10 CAMERA_ASS CAMERA SUB-ASSEMBLY REF 1 SCII-A06-A
11 LASER_PROTECT_BRACKET_L LASER/CAMERA SHIELD BRACKET AL-6061-T6 6 SCII-042-A
12 LASER_PROTECT LASER/CAMERA SHIELD AL-6061-T6 3 SCII-041-A
13 SHCS_M4X16 M4X16 SHCS STEEL 6 REF
14 WASHER_M2 2MM WASHER STEEL 20 REF
15 NUT_M2 M2 NUT STEEL 20 REF
16 SHCS_M2X10 M2X10 SHCS STEEL 20 REF
17 WASHER_M5 5MM WASHER STEEL 8 REF
18 SHCS_M5X16 M5X16 SHCS STEEL 8 REF
19 BATTERY PANASONIC PART# LCR 12V7.2P REF 1 REF
20 BATTERY_BRACKET BATTERY BRACKET AL-6061-T6 2 SCII-025-A
21 BATTERY_GUIDE BATTERY GUIDE AL-6061-T6 4 SCII-026-A
FRONT HIP SUB-ASSEMBLY
SCII-A03-A
McGILL UNIVERSITY
DEPT. OF MECHANICAL ENGINEERING
CENTRE FOR INTELLIGENT MACHINES
AMBULATORY ROBOTICS LABORATORY
NTS
28-DEC-98
A
MM
1
9.580 KG
REF
R. BATTAGLIA
SHEET 1 OF 2
X.X ±.1
X.XX ±.01
X.XXX ±.001
X. ±1°
X.X ±.5°
X.XX ±.25°
A-format

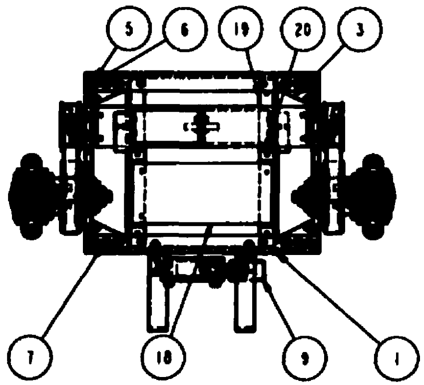

BILL OF MATERIALS					
INDEX	NAME	DESCRIPTION	MATERIAL	QTY	DWG NUMBER
1	F_HIP_BRACKET	REAR HIP BRACKET	AL-6061-T6	4	SC11-009-A
2	TRANS_RR	TRANSMISSION SUB-ASSEMBLY	REF	2	SC11-A08-A
3	ANGLE_BRACKET	HIP ANGLE BRACKET	STEEL	8	SC11-010-A
4	SHCCS_M4X16	M4X16 SHCCS	STEEL	16	REF
5	WASHER_M4	4MM WASHER	STEEL	32	REF
6	NUT_M4	M4 NUT	STEEL	32	REF
7	SHCCS_M4X14	M4X14 SHCCS	REF	16	CREF
8	LEG	LEG SUB-ASSEMBLY	REF	2	SC11-A02-A
9	LASER	LASER SUB-ASSEMBLY	REF	1	SC11-A05-A
10	LASER_PROTECT_BRACKET_L	LASER/CAMERA SHIELD BRACKET	AL-6061-T6	6	SC11-042-A
11	LASER_PROTECT	LASER CAMERA SHIELD	AL-6061-T6	3	SC11-041-A
12	SHCS_M4X16	M4X16 SHCS	STEEL	4	REF
13	WASHER_M2	2MM WASHER	STEEL	16	REF
14	NUT_M2	M2 NUT	STEEL	16	REF
15	SHCS_M2X10	M2X10 SHCS	STEEL	16	REF
16	WASHER_M5	5MM WASHER	STEEL	8	REF
17	SHCS_M5X16	M5X16 SHCS	STEEL	8	REF
18	BATTERY	PANASONIC PART# LCR 12V7.2P	REFF	1	REF
19	BATTERY_BRACKET	BATTERY BRACKET	AL-6061-T6	2	SC11-025-A
20	BATTERY_GUIDE	BATTERY GUIDE	AL-6061-T6	4	SC11-026-A

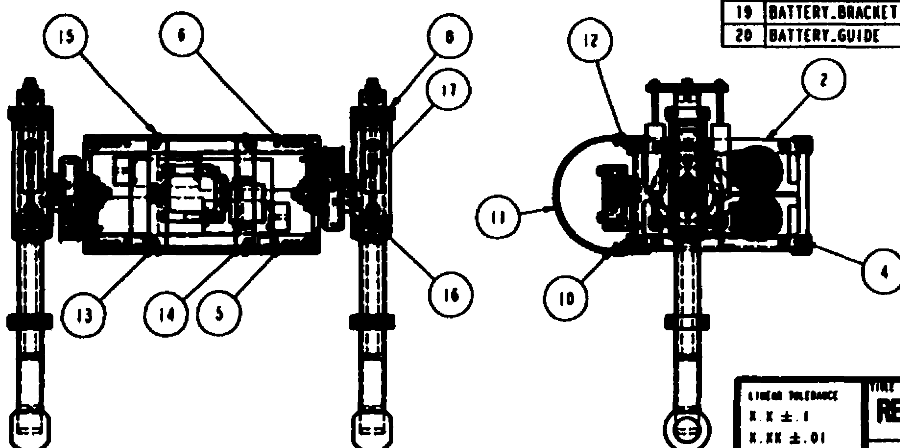

LINEAR TOLERANCE
X.X ±.1
X.XX ±.01
X.XXX ±.001

ANGULAR TOLERANCE
X. ±1°
X.X ±.5°
X.XX ±.25°

TITLE: REAR HIP SUB-ASSEMBLY

DWG. NO.: SCII-A04-A

McGILL UNIVERSITY
DEPT. OF MECHANICAL ENGINEERING

CENTRE FOR INTELLIGENT MACHINES
AMBULATORY ROBOTICS LABORATORY

SCALE: NTS | DATE: 28-DEC-98
SHEET SIZE: A | UNITS: MM
QTY: 1 | CALC MASS: 8.990 KG

MATERIAL: REF | DRAWN BY: R. BATTAGLIA | SHEET 1 OF 2

A-format

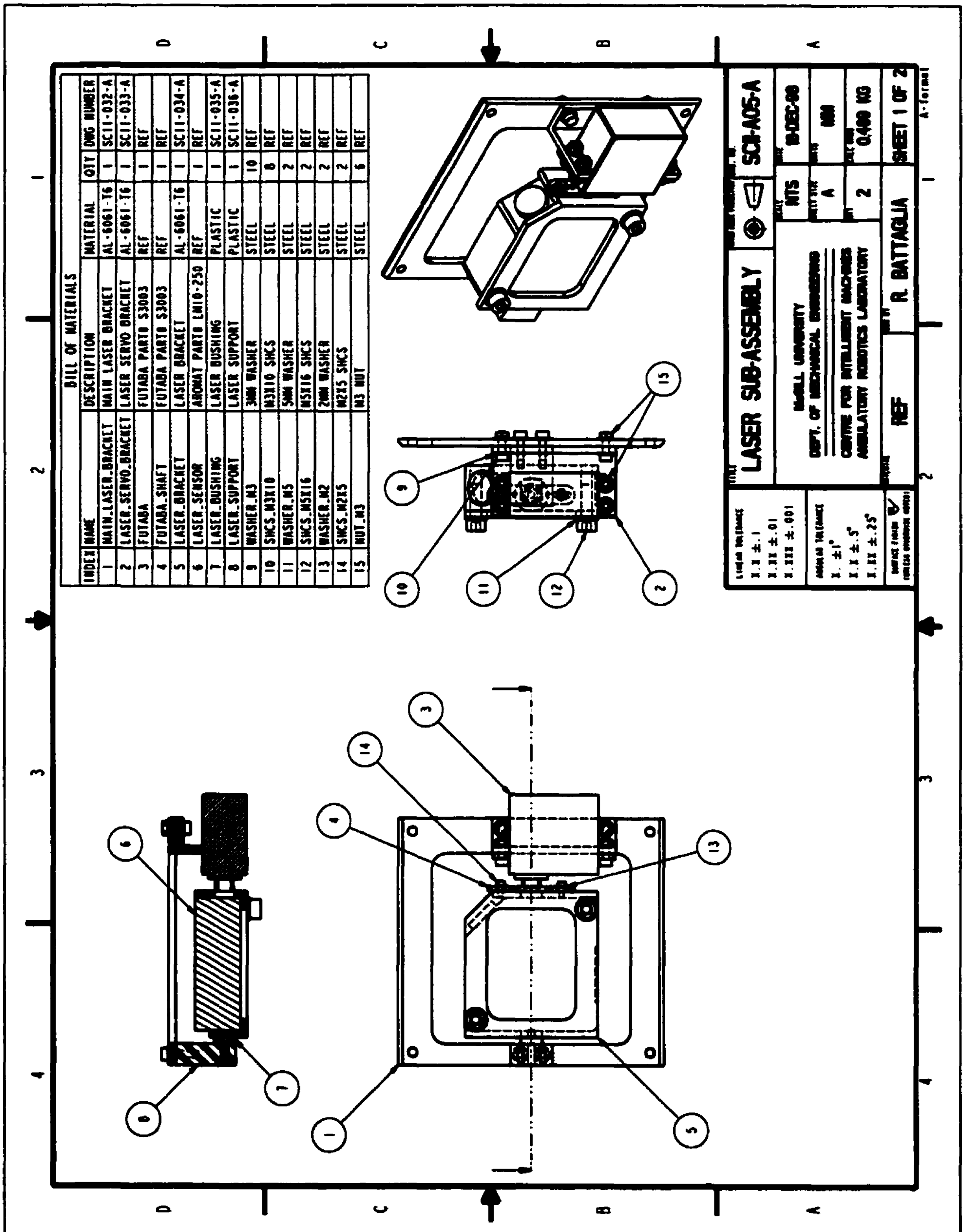

INDEX	NAME	DESCRIPTION	MATERIAL	QTY	DWG NUMBER
1	MAIN.LASER.BRACKET	MAIN LASER BRACKET	AL-6061-T6	1	SC11-032-A
2	LASER.SERVO.BRACKET	LASER SERVO BRACKET	AL-6061-T6	1	SC11-033-A
3	FUTABA	FUTABA PARTO S3003	REF	1	REF
4	FUTABA.SHAFT	FUTABA PARTO S3003	REF	1	REF
5	LASER.BRACKET	LASER BRACKET	AL-6061-T6	1	SC11-034-A
6	LASER.SENSOR	AROMAT PARTO LM10-250	REF	1	REF
7	LASER.BUSHING	LASER BUSHING	PLASTIC	1	SC11-035-A
8	LASER.SUPPORT	LASER SUPPORT	PLASTIC	1	SC11-036-A
9	WASHER.M3	3MM WASHER	STEEL	10	REF
10	SHCS.M3X10	M3X10 SHCS	STEEL	8	REF
11	WASHER.M5	5MM WASHER	STEEL	2	REF
12	SHCS.M5X16	M5X16 SHCS	STEEL	2	REF
13	WASHER.M2	2MM WASHER	STEEL	2	REF
14	SHCS.M2X5	M2X5 SHCS	STEEL	2	REF
15	NUT.M3	M3 NUT	STEEL	6	REF

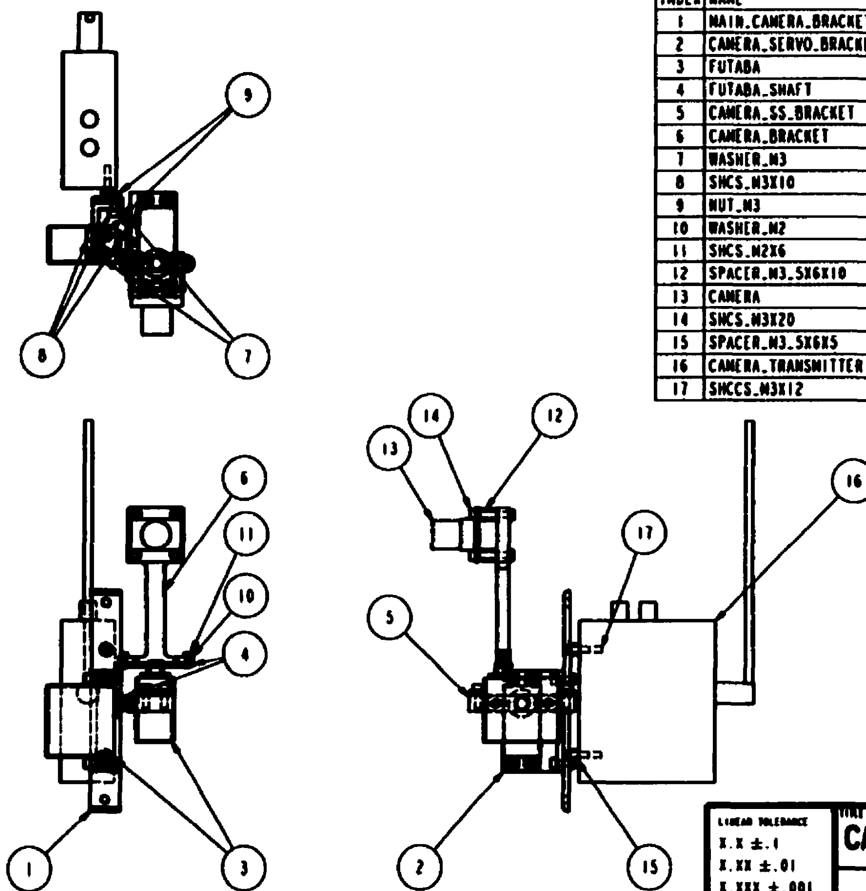

BILL OF MATERIALS

INDEX	NAME	DESCRIPTION	MATERIAL	QTY	DWG NUMBER
1	MAIN_CAMERA_BRACKET	MAIN CAMERA BRACKET	AL-6061-T6	1	CII-037-A
2	CAMERA_SERVO_BRACKET	SERVO BRACKET	AL-6061-T6	1	SCII-038-A
3	FUTABA	FUTABA PART# S3003	REF	2	REF
4	FUTABA_SHAFT	FUTABA PART# S3003	REF	2	REF
5	CAMERA_SS_BRACKET	SERVO/SERVO BRACKET	AL-6061-T6	1	SCII-039-A
6	CAMERA_BRACKET	CAMERA BRACKET	AL-6061-T6	1	SCII-040-A
7	WASHER_M3	3MM WASHER	STEEL	8	REF
8	SHCS_M3X10	M3X10 SHCS	STEEL	10	REF
9	NUT_M3	M3 NUT	STEEL	10	REF
10	WASHER_M2	2MM WASHER	STEEL	4	REF
11	SHCS_M2X6	M2X6 SHCS	STEEL	4	REF
12	SPACER_M3_5X6X10	METRICAN PART# 56800 3.5X6X10	PLASTIC	4	REF
13	CAMERA	CAMERA	REF	1	REF
14	SHCS_M3X20	M3X20 SHCS	STEEL	4	REF
15	SPACER_M3_5X6X5	METRICAN PART# 56800 3.5X6X5	PLASTIC	2	REF
16	CAMERA_TRANSMITTER	TRANSMITTER	REF	1	REF
17	SHCCS_M3X12	M3X12 SHCCS	STEEL	2	REF

LINEAR TOLERANCE
X.X ±.1
X.XX ±.01
X.XXX ±.001

ANGULAR TOLERANCE
X. ±1°
X.X ±.5°
X.XX ±.25°

SURFACE FINISH (UNLESS OTHERWISE NOTED)

TITLE: CAMERA SUB-ASSEMBLY

DWG. NO. SCII-A06-A

McGILL UNIVERSITY
DEPT. OF MECHANICAL ENGINEERING

CENTRE FOR INTELLIGENT MACHINES
AMBULATORY ROBOTICS LABORATORY

SCALE: NTS
DATE: 23-DEC-98
SHEET SIZE: A
UNITS: MM
QTY: 1
WEIGHT: 0.447 KG
MATERIAL: REF
DRAWN BY: R. BATTAGLIA
SHEET 1 OF 2

A-format

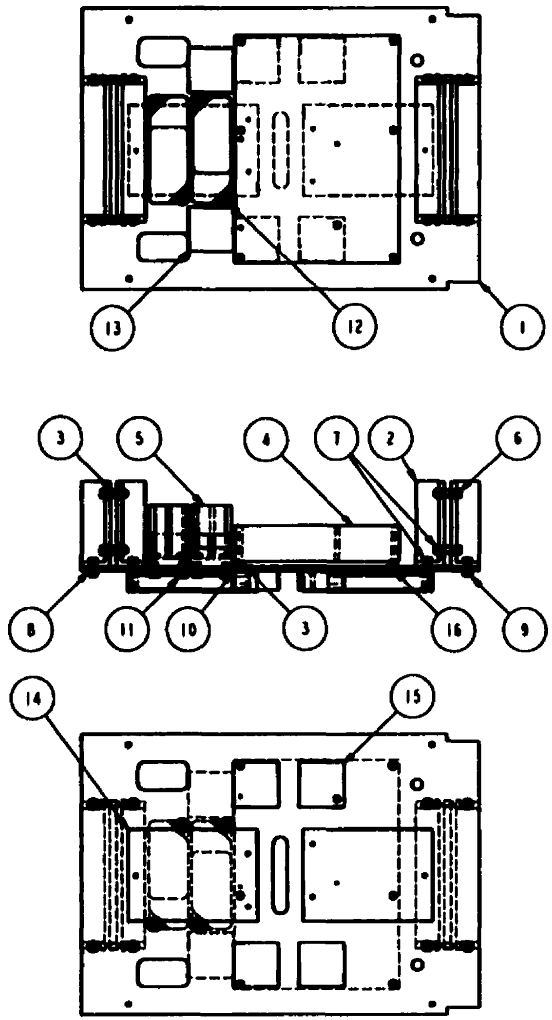

BILL OF MATERIALS					
INDEX	NAME	DESCRIPTION	MATERIAL	QTY	DWG NUMBER
1	TOP_ELEC_SUPPORT	SUPPORT BRACKET	LEXAN	1	SCII-023-A
2	SERVO_AMP	AMC PART# 12A8E	REF	4	REF
3	SERVO_AMP_SPACER	MERICAN PART# 56800 3.5X6X10	PLASTIC	14	REF
4	PC_BOARD	ADASTRA PART# VNS-486	REF	1	REF
5	LASER_CONTROLLER	AROMAT PART# LM10-250	REF	2	REF
6	SHCS_M4X20	M4X20 SHCS	STEEL	8	REF
7	NUT_M4	M4 NUT	STEEL	16	REF
8	WASHER_M4	4MM WASHER	STEEL	8	REF
9	SHCS_M4X12	M4X12 SHCS	STEEL	8	REF
10	WASHER_10	#10 WASHER	STEEL	4	REF
11	SHCS_10X5_8	#10X5/8" SHCS	STEEL	4	REF
12	NUT_10	#10 WASHER	STEEL	4	REF
13	GYRO_ADIO	ADIO BOARD FOR GYROS	REF	2	REF
14	SPPSPI	SPP/SPI BOARD	REF	2	REF
15	DAIO	DAIO BOARD FOR SERVO AMPS	REF	4	REF
16	SHCCS_M3X20	M3X20 SHCCS	STEEL	6	REF

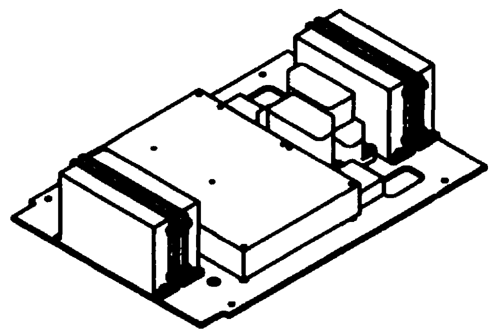

LINEAR TOLERANCE
X.X ±.1
X.XX ±.01
X.XXX ±.001

ANGULAR TOLERANCE
X. ±1°
X.X ±.5°
X.XX ±.25°

MAIN ELECTRONICS SUB-ASSEMBLY

SCII-A07-A

McGILL UNIVERSITY
DEPT. OF MECHANICAL ENGINEERING

CENTRE FOR INTELLIGENT MACHINES
AMBULATORY ROBOTICS LABORATORY

NTS
27-DEC-98
A
MM
1
2532 KG

REF
R. BATTAGLIA
SHEET 1 OF 2

A-format

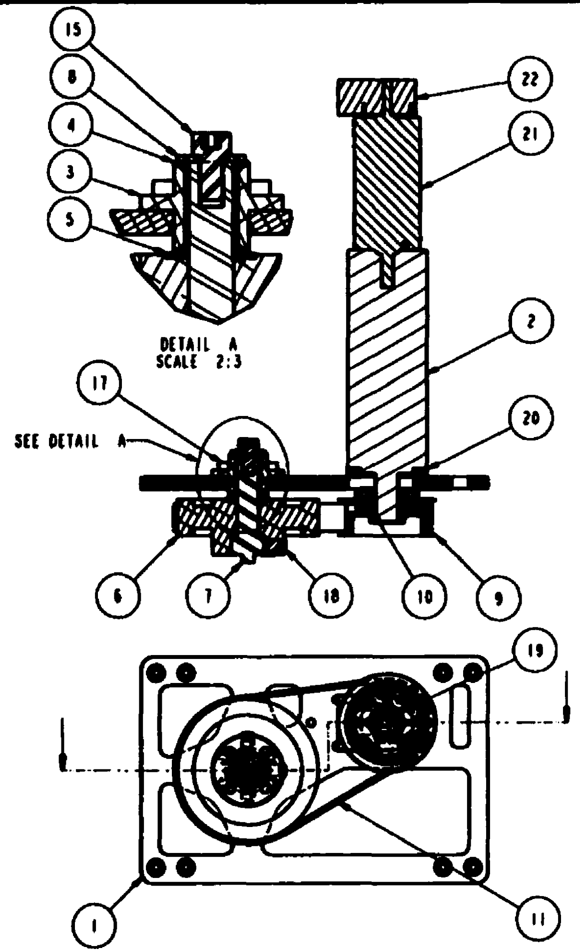

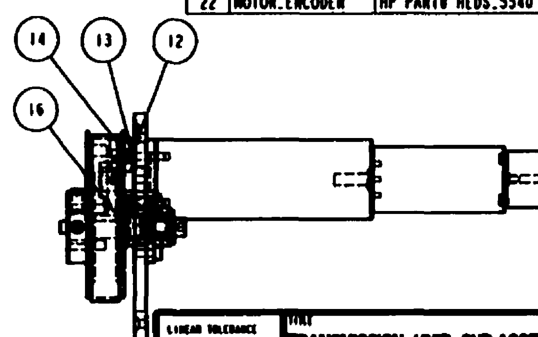

BILL OF MATERIALS					
INDEX	NAME	DECRIPTION	MATERIAL	QTY	DWG NUMBER
1	MOTOR_BRACKET	MOTOR BRACKET	AL-6061-T6	1	SCII-005-A
2	MOTOR-GEARHEAD	MAXON PART# 110404	REF	1	REF
3	LEG_BRACKET	LEG BRACKET	AL-6061-T6	1	SCII-001-A
4	SHAFT_BUSHING	GARLOCK PART# FMB1209DU	REF	2	REF
5	THRUST_BUSHING	GARLOCK PART# WC10DU	REF	1	REF
6	PULLEY_LG	SDP PART# A 6A25M04DNF1512	AL-6061-T6	1	SCII-006-A
7	LEG_SHAFT	LEG SHAFT	STEEL	1	SCII-004-A
8	WASHER_M6	6MM WASHER	STEEL	1	REF
9	PULLEY_SM	SDP PART# A 6A25M028DF1508	AL-6061-T6	1	SCII-003-A
10	SS_M4X8	M4X8 SET SCREW	STEEL	2	REF
11	BELT	SDP PART# A6R25M070150	REF	1	REF
12	WASHER_M4	4MM WASHER	STEEL	4	REF
13	SPLIT_WASHER_M4	4MM LOCK WASHER	STEEL	4	REF
14	MOTOR_BOLTS	M4X20 HEX CAP SCREWS	STEEL	4	REF
15	SHCS_M6X12	M6X12 SHCS	STEEL	1	REF
16	DOWEL_1_16X1_4	Ø1/16" X 1/4" DOWEL	STEEL	1	REF
17	SHCS_M4X10	M4X10 SHCS	STEEL	6	REF
18	SS_M6X12	M6X12 SET SCREW	STEEL	2	REF
19	GEAR_SLEEVE	GEARHEAD SHAFT SLEEVE	STEEL	1	SCII-027-A
20	MOTOR_SPACER	GEARHEAD SPACER	AL-6061-T6	1	SCII-002-A
21	MOTOR	MAXON PART# 118777	REF	1	REF
22	MOTOR_ENCODER	HP PART# HEDS_5540	REF	1	REF

LINEAR TOLERANCE
X.X ±.1
X.XX ±.01
X.XXX ±.001

ANGULAR TOLERANCE
X. ±1°
X.X ±.5°
X.XX ±.25°

TITLE: TRANSMISSION UNIT SUB-ASSEMBLY

DWG. NO. SCII-A08-A

McGILL UNIVERSITY
DEPT. OF MECHANICAL ENGINEERING
CENTRE FOR INTELLIGENT MACHINES
AMBULATORY ROBOTICS LABORATORY

SCALE: NTS
DATE: 23-DEC-98
SHEET SIZE: A
UNITS: MM
QTY: 4
CALC MASS: 1755 KG

REF
R. BATTAGLIA
SHEET 1 OF 2

A-format

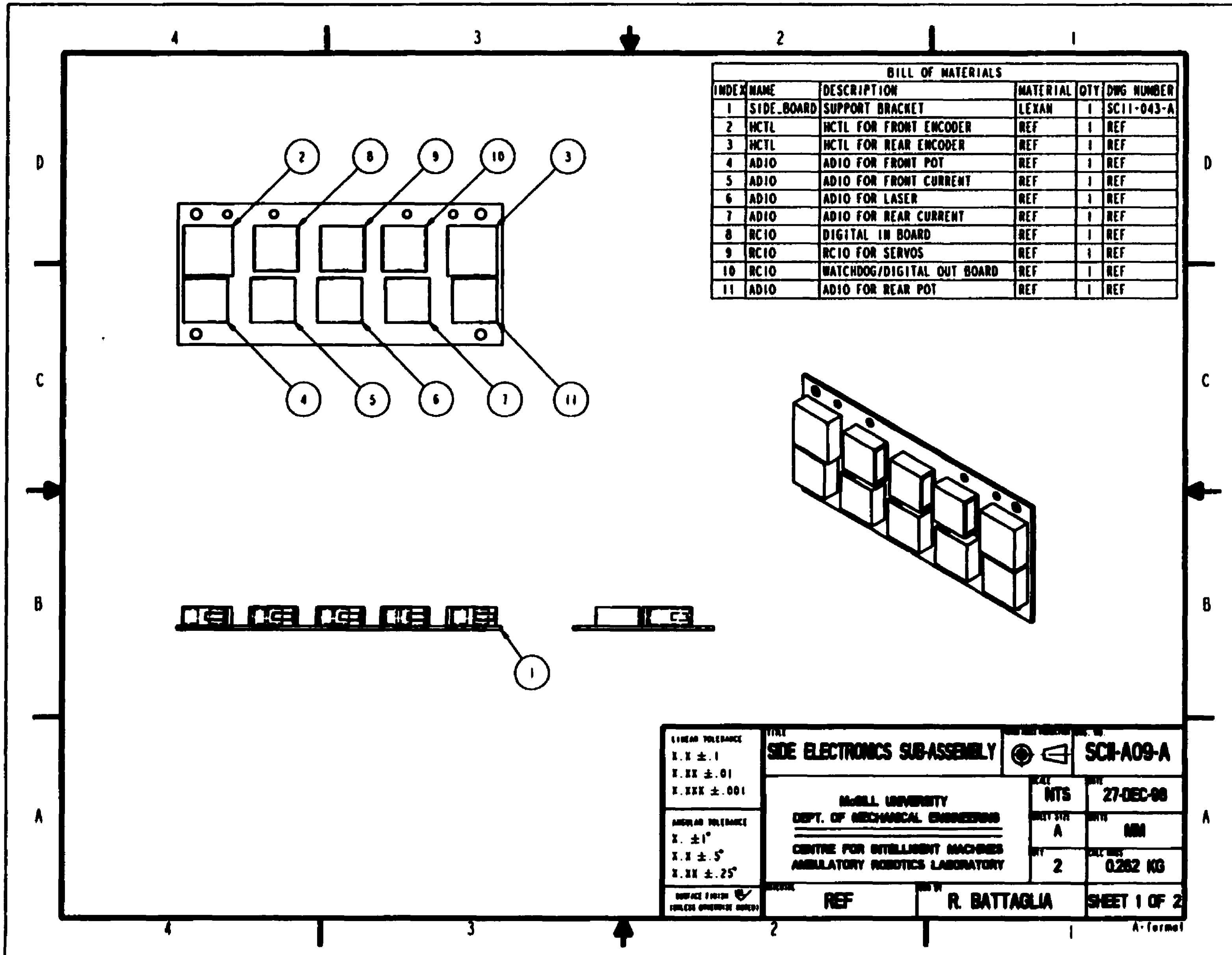

BILL OF MATERIALS

INDEX	NAME	DESCRIPTION	MATERIAL	QTY	DWG NUMBER
1	SIDE_BOARD	SUPPORT BRACKET	LEXAN	1	SCII-043-A
2	HCTL	HCTL FOR FRONT ENCODER	REF	1	REF
3	HCTL	HCTL FOR REAR ENCODER	REF	1	REF
4	ADIO	ADIO FOR FRONT POT	REF	1	REF
5	ADIO	ADIO FOR FRONT CURRENT	REF	1	REF
6	ADIO	ADIO FOR LASER	REF	1	REF
7	ADIO	ADIO FOR REAR CURRENT	REF	1	REF
8	RCIO	DIGITAL IN BOARD	REF	1	REF
9	RCIO	RCIO FOR SERVOS	REF	1	REF
10	RCIO	WATCHDOG/DIGITAL OUT BOARD	REF	1	REF
11	ADIO	ADIO FOR REAR POT	REF	1	REF

Appendix B

SCOUT II Circuit Diagrams

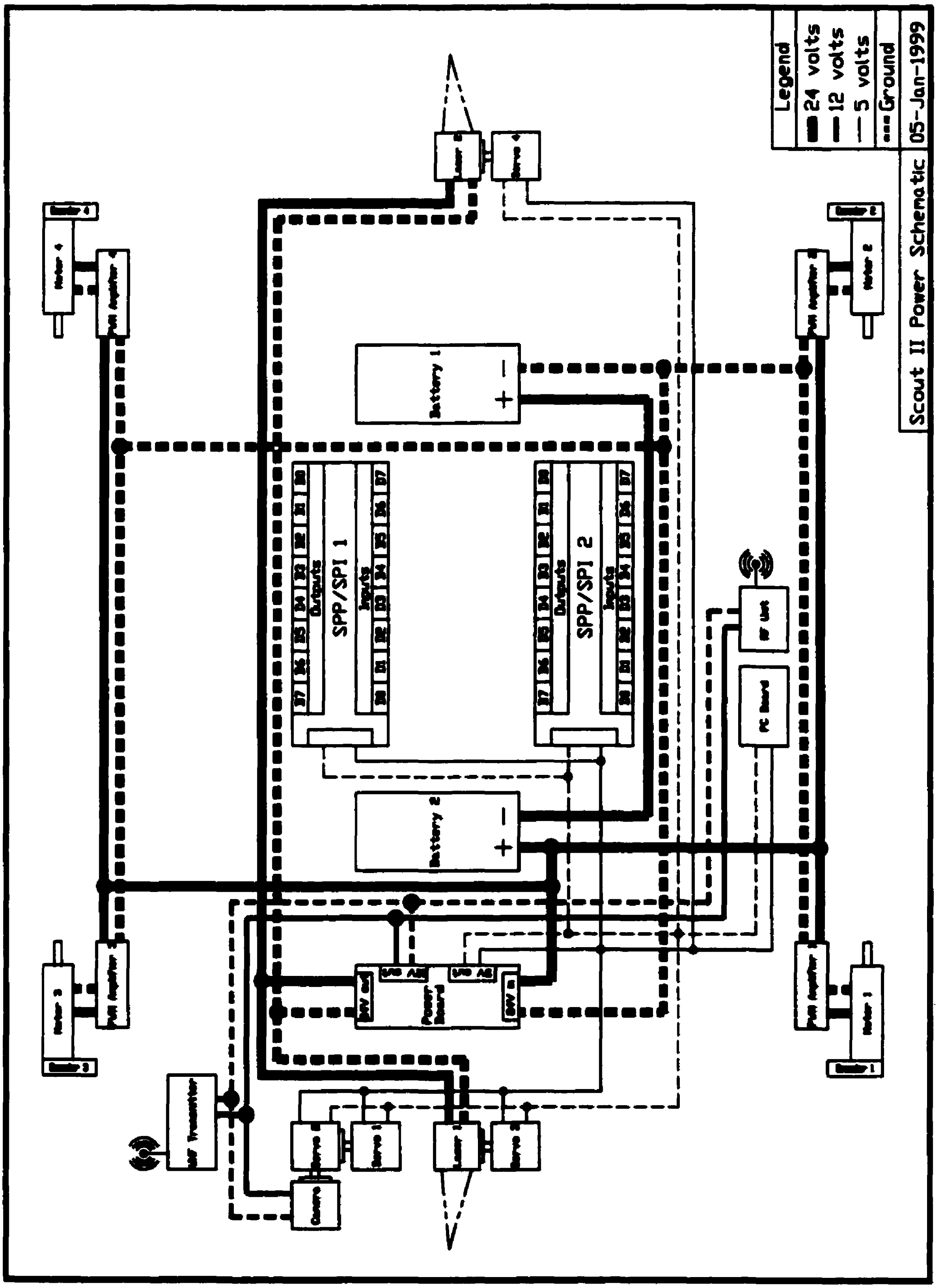
Legend
24 volts
12 volts
5 volts
Ground
05-Jan-1999
Scout II Power Schematic
Battery 1
Battery 2
SPP/SPI 1
SPP/SPI 2
Outputs
Inputs

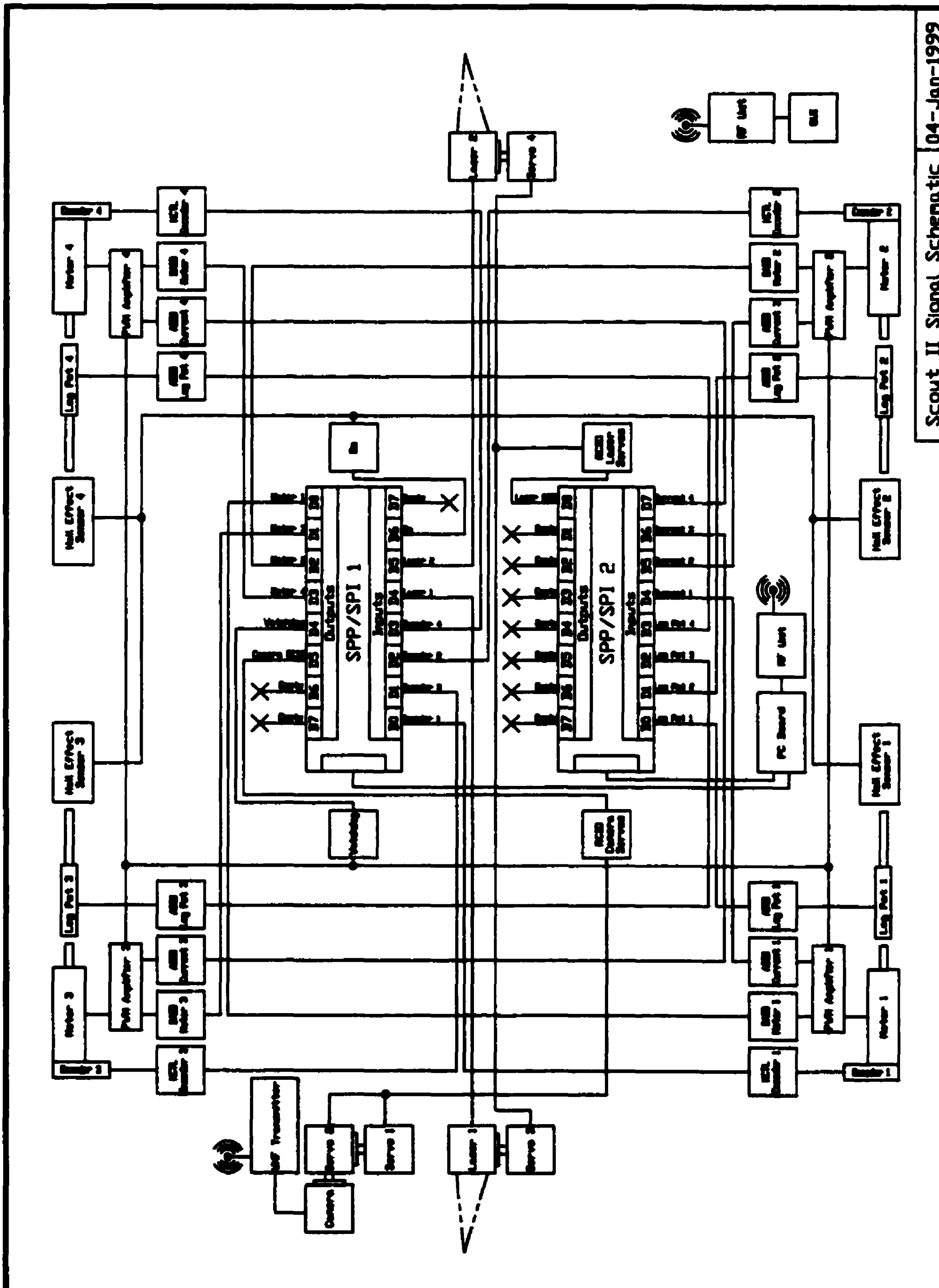
Scout II Signal Schematic
04-Jan-1999
SPP/SPI 1
SPP/SPI 2
Outputs
Inputs

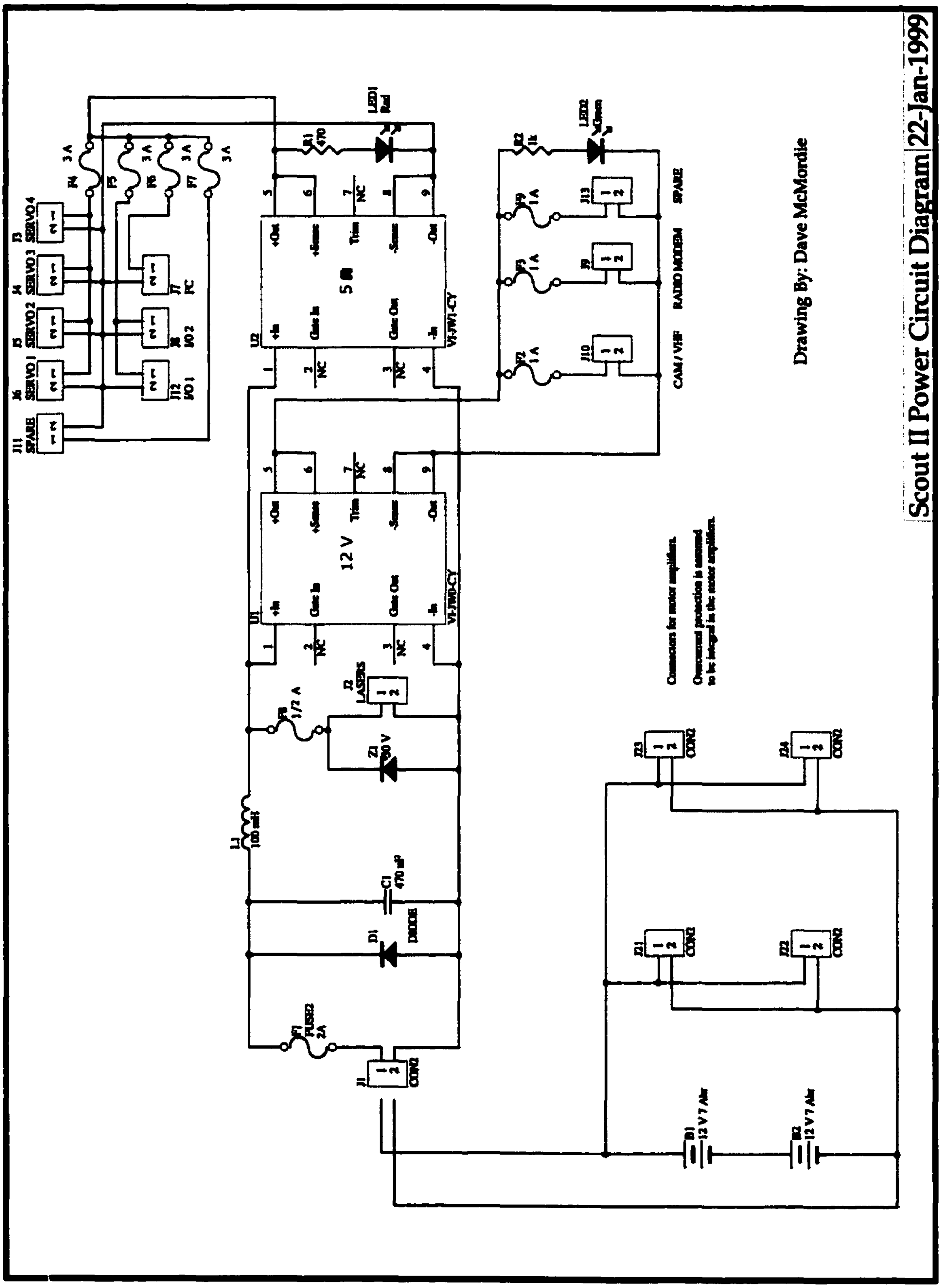
Scout II Power Circuit Diagram
22-Jan-1999
Drawing By: Dave McMordie
12 V
5 V
VI-JW0-CY
VI-JW1-CY
SERVO 1
SERVO 2
SERVO 3
SERVO 4
SPARE
CAM / VHF
RADIO MODEM
LASERS
DIODE
CON2

Appendix C

SCOUT II Stress Analysis

Almost every component of SCOUT II was analysed to ensure that it would resist the abuse of testing while at the same time be optimized to reduce its weight. Most components were simple enough that conventional methods were used. Two components, however, were more complex and required finite element modelling. This included the motor bracket and the upper leg. Both parts were made out of 6061-T6 aluminum whose relevant material properties are provided in Table C.1. The analyses were performed using Pro/Mechanica [60]. The results of these analyses is the subject of this appendix.

Poisson's Ratio (ν)	0.334†
Modulus of Elasticity (E)	10.3 GPa*
Ultimate tensile strength (σ_{ut})	310.5 MPa†
Yield tensile strength (σ_{yt})	276.0 MPa†
Ultimate shear strength (σ_{us})	207.0 MPa†

Table C.1: *Mechanical properties of aluminum 6061-T6. (*Taken from [65]. †Taken from [12].)*

C.1 Motor Bracket

The motor bracket was an important part of the transmission unit. Its function was to supply a base of support that the leg and motor were attached to. It also required slots at the motor mount to allow it to slide for the purpose of tensioning the belt. A picture of the final design is shown in Figure C.1. It is constructed out of 1/4" (6.35mm) 6061-T6 aluminum. Though numerous loading situations were examined, only the the major scenarios will be presented here. The bracket was analysed as a thin shell which significantly reduced the analysis time. Because of this, however, the chamfers were removed from the model. In all cases, the 8 bolt holes at the corners were fully constrained and the load was applied to a a 48mm diameter surface where the leg bracket attaches.

Figure C.1: *Motor bracket.*

Analysis 1: Impact Simulation

In this case a 1226N static load was applied to the foot simulating a 20G impact load at the leg (with the leg in the vertical position). In addition, a 70.8Nm moment was applied to account for the offset between the leg and bracket. Figure C.2 shows the Pro/Mechanica results with the maximum principal stress at the left and displacement at the right. Note that the displacement figure shows exaggerated deformations. The maximum stress was in the order of 245 MPa with displacements under 0.2mm.

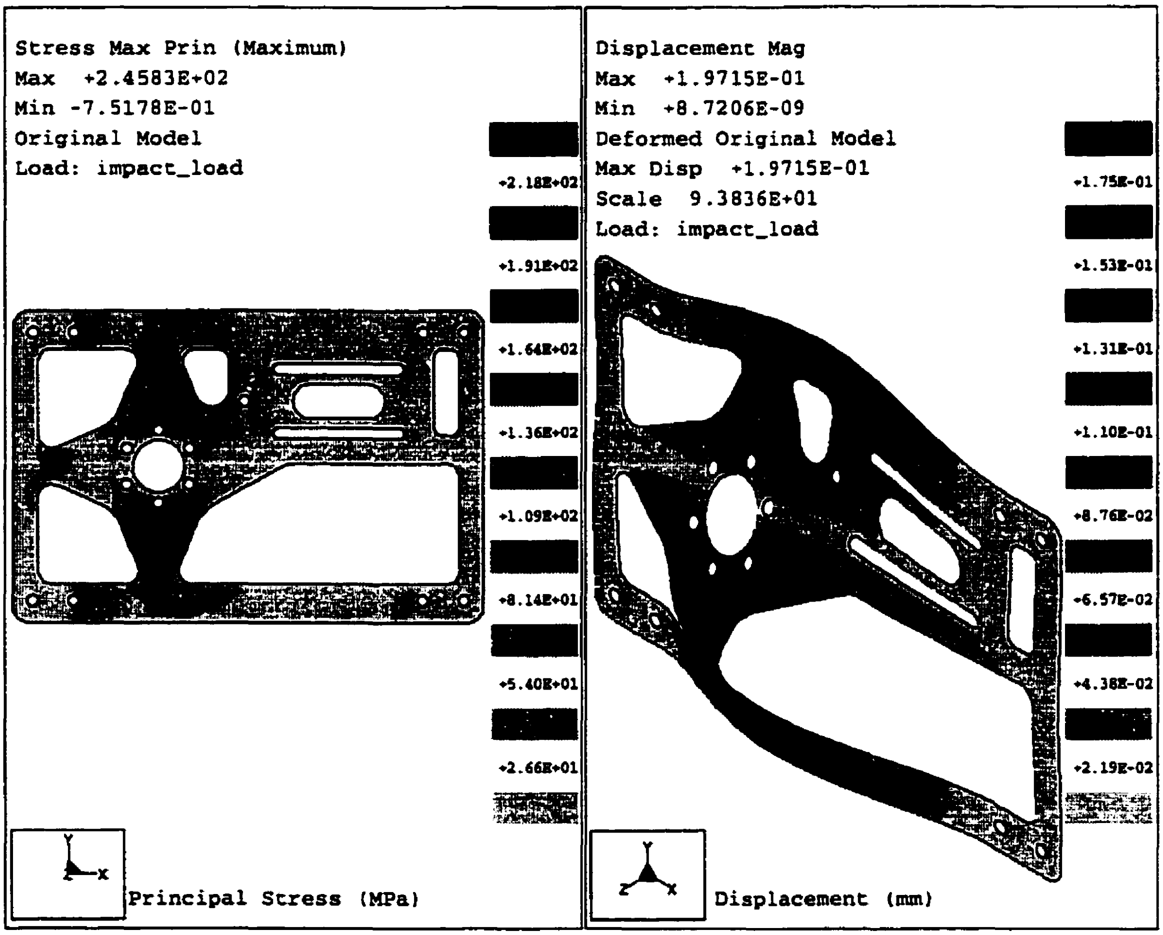

Figure C.2: *Pro/Mechanica results for motor bracket. (Analysis 1: 20G (1226N) load at the leg).*

Analysis 2: Side load - vertical leg

In this scenario, a 250N side load was applied to the foot while the leg was in the vertical position. This resulted in a force of 250N and a moment of 68.8Nm on the bracket. The resulting stresses and displacements are provided in in Figure C.3. The maximum stress was in the order of 271 MPa with displacements under 0.25mm.

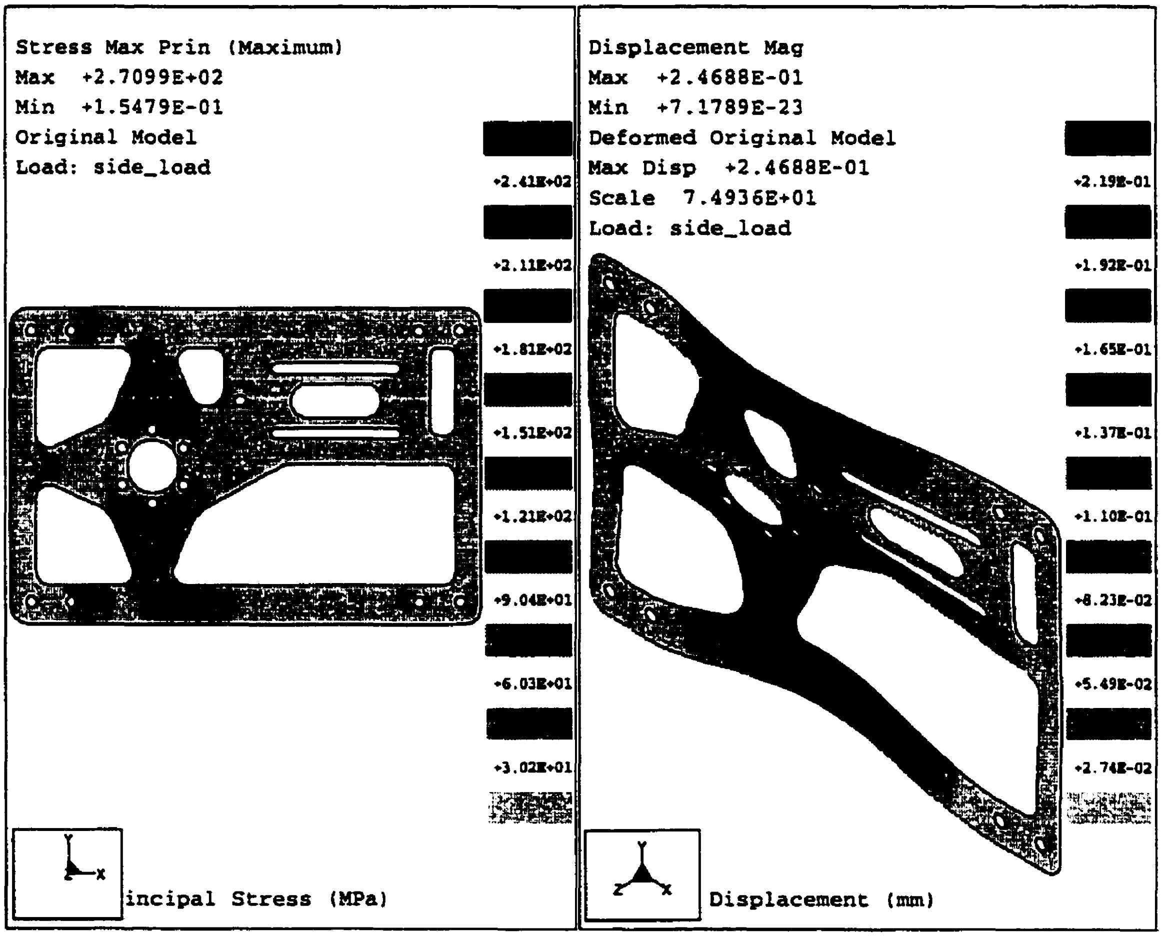

Figure C.3: *Pro/Mechanica results for motor bracket. (Analysis 2: 250N side load with leg in vertical position.)*

Analysis 3: Side load - extended leg

This final case had the same 250N side load at the foot, except that the leg was now in the fully extended position. The results, which can be found in Figure C.4, had stresses in the order of 196 MPa and displacements under 0.36mm.

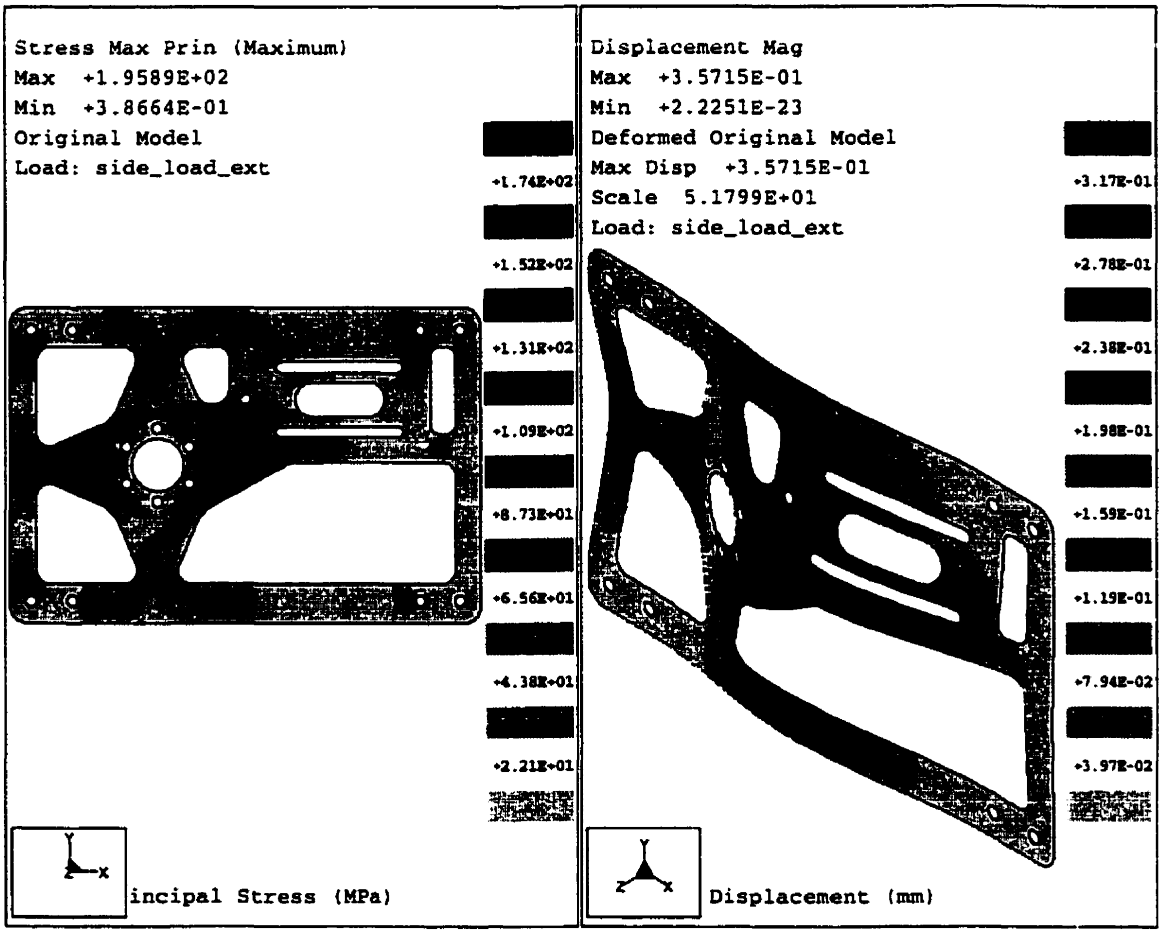

Figure C.4: *Pro/Mechanica results for motor bracket. (Analysis 3: 250N side load with leg in extended position.)*

Summary

Although only the maximum principal stresses were presented in the above analyses, other stresses, like Von Mises and maximum shear, were also verified. Numerous other loading scenarios were run with the legs at various angles and the loads from different directions. The three analyses described above were the main loading scenarios and also turned out to be the most severe.

C.2 Upper Leg

The upper leg served a dual function. First, it provided a support for the bushings that allowed the lower leg to slide. Second, it attached the leg to the transmission unit. It was made from a solid block of 6061-T6 aluminum and was machined on a milling machine. This model was analysed as a 3D solid. The loads were applied to the two holes that form the bushing surfaces. The constraints were the surfaces formed by the four washers and the surface that is in contact with the leg sprocket. Numerous scenarios were analysed using various loads from different angles with the upper leg constrained from various sets of holes. The scenario presented here has a 250N side load at the foot with a leg length of 275mm. Figure C.5 shows the principal stress results and Figure C.6 shows the deformations. Stresses were under 135MPa and displacements under 0.2mm.

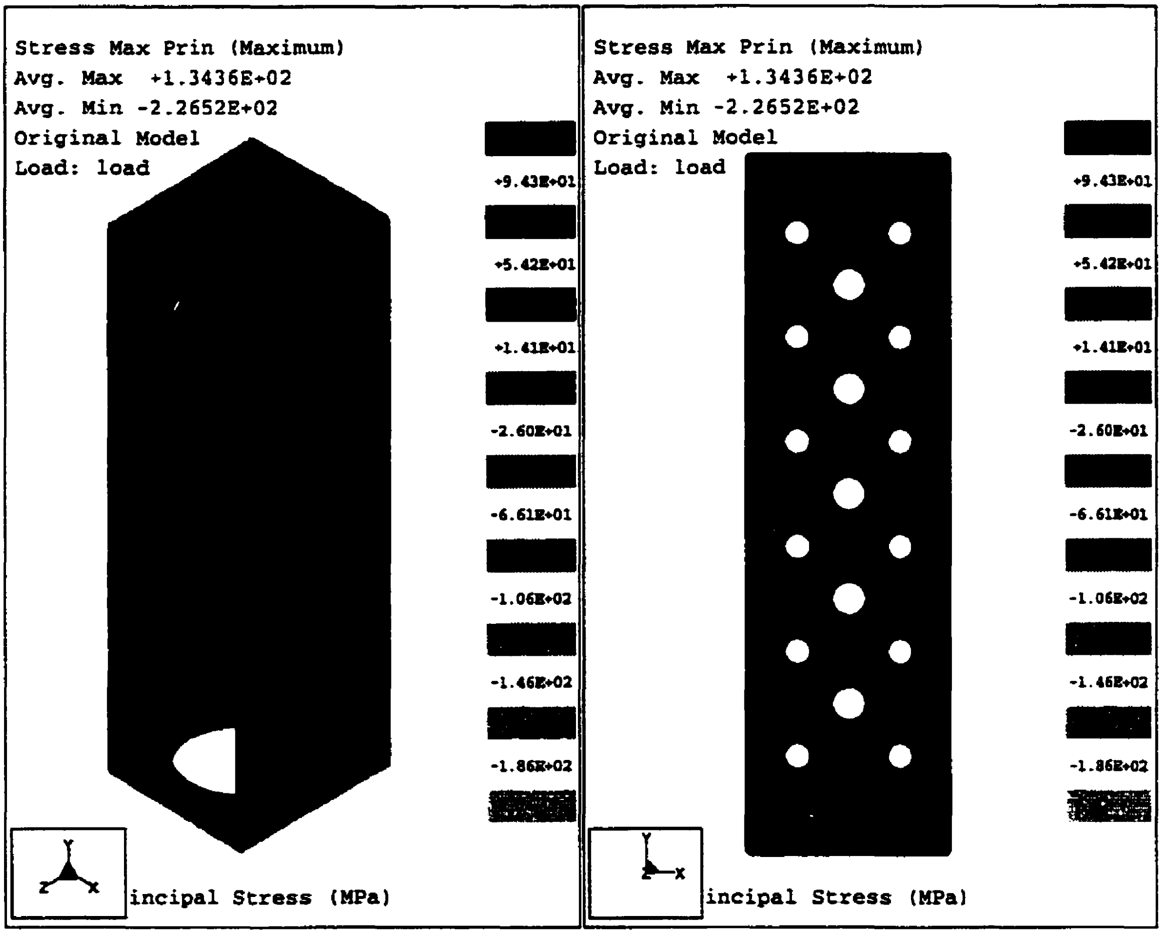

Figure C.5: *Pro/Mechanica stress results for upper leg (250N side load on the foot).*

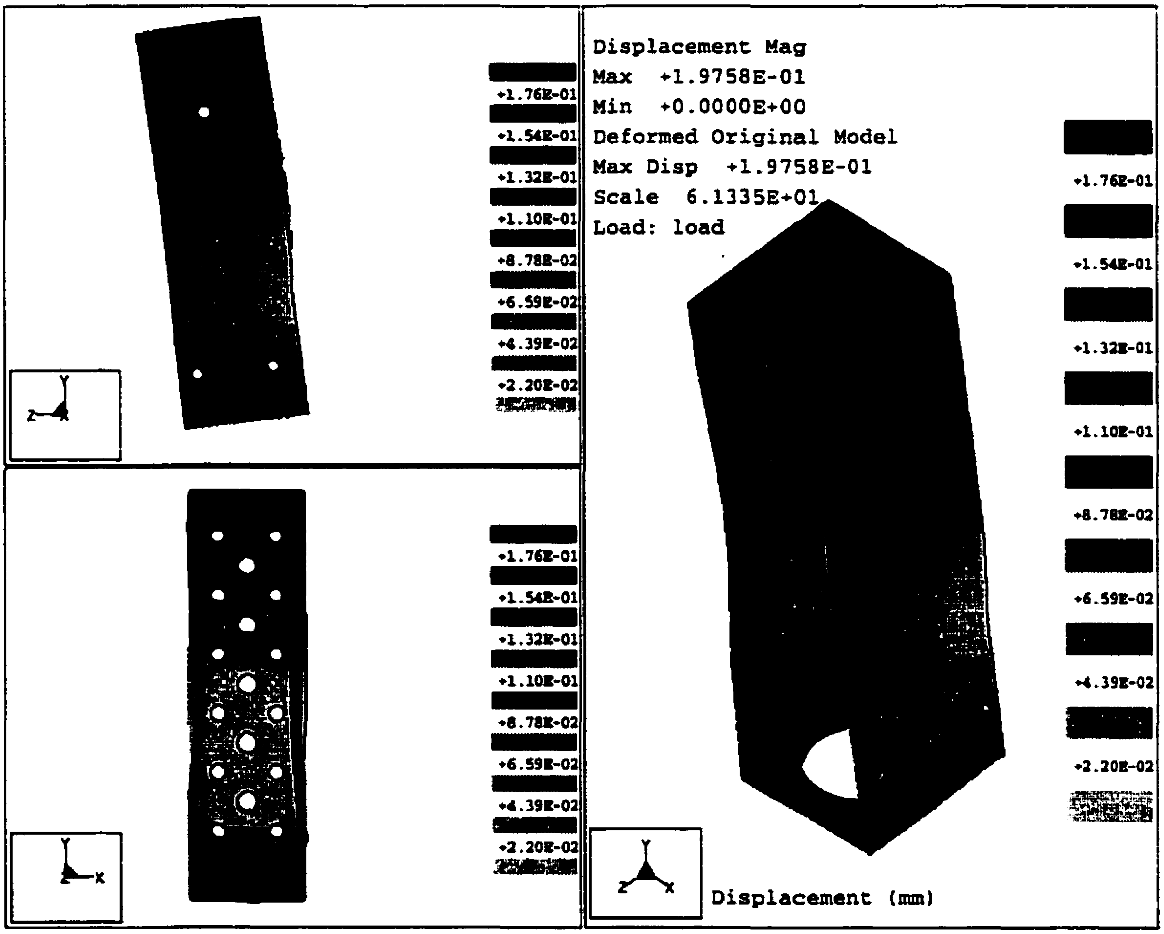

Figure C.6: *Pro/Mechanica displacement results for upper leg (250N side load on the foot).*

Appendix D

SCOUT II Parts List

Part Name	Index Number	Material	Item Mass [g]	Qty	Total Mass [g]
Transmission Unit (index numbers refer to drawing SCII-A08-A*)					
Maxon 118777 motor	21	Stock	340	4	1360
Maxon 110404 Gearhead	2	Stock	720	4	2880
HP HEDS 5540 Encoder	22	Stock	45	4	180
Gearhead Sleeve	19	Steel	1	4	4
Motor Spacer	20	Al-6061-T6	9	4	36
Motor Bracket	1	Al-6061-T6	233	4	932
Leg Bracket	3	Al-6061-T6	18	4	72
Leg Shaft	7	Steel	56	4	180
SDP A6R25M070150 Belt	11	Neoprene	21	4	84
SDP A6A25M048NF1215 Pulley	6	Al-6061-T6	209	4	836
SDP A6A25M034DF1508 Pulley	9	Al-6061-T6	77	4	308
Garlock FMB1209DU Bushing	4	Stock	4	8	32
Garlock WC10DU Thrust Bushing	5	Stock	4	4	16
M4x20 Hexagonal Cap Screw	14	Stock	2	16	32
M4x10 Socket Head Cap Screw	17	Stock	1	24	24
M6x12 Socket Head Cap Screw	15	Stock	5	4	5
M4x8 Set Screw	10	Stock	<1	8	5
M6x12 Set Screw	18	Stock	2	8	16
M4 Split Washer	13	Stock	<1	16	4
M4 Washer	12	Stock	<1	16	5
M6 Washer	8	Stock	2	4	8
ϕ1/16"x1/4" long Dowel	16	Stock	<1	4	<1
Front Hip Unit (index numbers refer to drawing SCII-A03-A*)					
Hip Bracket	1	Al-6061-T6	98	4	392
Angle Bracket	3	Al-6061-T6	9	8	72
Battery Bracket	20	Al-6061-T6	45	2	90
Battery Guide	21	Al-6061-T6	1	4	4
Laser/Camera Shield	12	Al-6061-T6	38	3	114
Shield Bracket	11	Al-6061-T6	4	6	24
Battery	19	Stock	2470	1	2470
M2x10 Socket Head Cap Screw	16	Stock	<1	20	6
M4x14 Socket Head CSK Cap Screw	7	Stock	1	16	16

Table D.1: *SCOUT II parts list: 1 of 5. (*Drawings can be found in Appendix A.)*

Part Name	Index Number	Material	Item Mass [g]	Qty	Total Mass [g]
Front Hip Unit - con't (index numbers refer to drawing SCII-A03-A*)					
M4x16 Socket Head CSK Cap Screw	4	Stock	1	16	16
M4x16 Socket Head Cap Screw	13	Stock	2	6	12
M5x16 Socket Head Cap Screw	18	Stock	4	8	32
M2 Washer	14	Stock	<1	20	<1
M4 Washer	5	Stock	<1	32	10
M5 Washer	17	Stock	<1	8	4
M2 Nut	15	Stock	<1	20	<1
M4 Nut	6	Stock	<1	32	24
Rear Hip Unit (index numbers refer to drawing SCII-A04-A*)					
Hip Bracket	1	Al-6061-T6	73	4	292
Angle Bracket	3	Al-6061-T6	9	8	72
Battery Bracket	19	Al-6061-T6	45	2	90
Battery Guide	20	Al-6061-T6	1	4	4
Laser/Camera Shield	11	Al-6061-T6	38	2	76
Shield Bracket	10	Al-6061-T6	4	4	16
Battery	18	Stock	2470	1	2470
M2x10 Socket Head Cap Screw	15	Stock	<1	16	5
M4x14 Socket Head CSK Cap Screw	7	Stock	1	16	16
M4x16 Socket Head CSK Cap Screw	4	Stock	1	16	16
M4x16 Socket Head Cap Screw	12	Stock	2	6	12
M5x16 Socket Head Cap Screw	17	Stock	4	8	32
M2 Washer	13	Stock	<1	16	<1
M4 Washer	5	Stock	<1	32	10
M5 Washer	16	Stock	<1	8	4
M2 Nut	14	Stock	<1	16	<1
M4 Nut	6	Stock	<1	32	24
Laser Unit (index numbers refer to drawing SCII-A05-A*)					
Main Laser Bracket	1	Al-6061-T6	47	2	94
Laser Servo Bracket	2	Al-6061-T6	14	2	28
Laser Bracket	5	Al-6061-T6	23	2	46
Laser Bushing	7	Plastic	<1	2	1
Laser Support	8	Plastic	10	2	20

Table D.2: *SCOUT II parts list: 2 of 5. (*Drawings can be found in Appendix A.)*

Part Name	Index Number	Material	Item Mass [g]	Qty	Total Mass [g]
Laser Unit - con't (index numbers refer to drawing SCII-A05-A*)					
Aromat LM10-250 Laser Sensor	6	Stock	318	2	636
Futaba S3003 Servo	3	Stock	66	2	132
M2x5 Socket Head Cap Screw	14	Stock	<1	4	1
M3x10 Socket Head Cap Screw	10	Stock	1	16	16
M5x16 Socket Head Cap Screw	12	Stock	4	4	16
M2 Washer	13	Stock	<1	4	<1
M3 Washer	9	Stock	<1	20	2
M5 Washer	11	Stock	<1	4	2
M3 Nut	15	Stock	<1	12	4
Camera Unit (index numbers refer to drawing SCII-A06-A*)					
Main Camera Bracket	1	Al-6061-T6	16	1	16
Camera Servo Bracket	1	Al-6061-T6	14	1	14
Camera Bracket	6	Al-6061-T6	23	1	23
Servo/Servo Bracket	5	Al-6061-T6	13	1	13
Futaba S3003 Servo	3	Stock	66	2	132
Camera	13	Stock	16	1	16
Camera Transmitter	16	Stock	204	1	204
Metrican 56800 3.5x6x5 Spacer	15	Plastic	<1	2	1
Metrican 56800 3.5x6x10 Spacer	12	Plastic	<1	4	2
M2x6 Socket Head Cap Screw	11	Stock	<1	4	1
M3x10 Socket Head Cap Screw	8	Stock	1	10	10
M3x20 Socket Head Cap Screw	14	Stock	2	4	8
M3x12 Socket Head CSK Cap Screw	17	Stock	1	2	2
M2 Washer	10	Stock	<1	4	<1
M3 Washer	7	Stock	<1	8	1
M3 Nut	9	Stock	<1	10	4
Main Electronics Unit (index numbers refer to drawing SCII-A07-A*)					
Support Bracket	1	Lexan	293	1	293
AMC 12A8E PWM Servo Amplifier	2	Stock	284	4	1136
Metrican 56800 3.5x6x10	3	Plastic	<1	14	7
Adastra VNS-486 PC Board	4	Stock	397	1	397
Aromat LM10-250 Controller	5	Stock	182	2	364

Table D.3: *SCOUT II parts list: 3 of 5. (*Drawings can be found in Appendix A.)*

Part Name	Index Number	Material	Item Mass [g]	Qty	Total Mass [g]
Main Electronics Unit - con't (index numbers refer to drawing SCII-A07-A*)					
Gyroscope ADIO Board	2	Stock	13	2	26
SPP/SPI Board	14	Stock	81	2	162
Servo Amp DAIO Board	15	Stock	13	4	52
M3x20 Socket Head CSK Cap Screw	16	Stock	2	6	12
M4x12 Socket Head Cap Screw	9	Stock	2	8	16
M4x20 Socket Head Cap Screw	6	Stock	3	8	24
#10x5/8" Socket Head Cap Screw	11	Stock	4	4	16
M4 Washer	8	Stock	<1	8	3
#10 Washer	10	Stock	1	4	4
M4 Nut	7	Stock	1	16	16
#10 Nut	12	Stock	1	4	4
Side Electronics Unit (index numbers refer to drawing SCII-A09-A*)					
Support Bracket	1	Lexan	135	2	270
HCTL for Motor Encoders	2	Stock	13	4	52
ADIO for Leg Potentimeters	4	Stock	13	4	52
ADIO for Current	5	Stock	13	4	52
ADIO for Lasers	6	Stock	13	2	26
Digital In	8	Stock	18	1	18
RCIO for Servos	9	Stock	18	2	36
Watchdog/Digital Out	10	Stock	18	1	18
Leg Unit (index numbers refer to drawing SCII-A02-A*)					
Upper Leg	1	Al-6061-T6	110	4	440
Spring Bracket	3	Al-6061-T6	10	8	80
Spring Support	6	Al-6061-T6	17	4	68
Leg Cap	8	Al-6061-T6	14	4	56
Lower Leg	9	Steel	328	4	1312
Foot	10	Al-6061-T6	38	4	152
Potentiometer Bushing	12	Steel	2	8	16
Potentiometer Shaft	13	Steel	3	4	12
Potentiometer Clamp	23	Al-6061-T6	4	8	32
Metrican 17420 M4x15x6 Screw Eye	4	Stock	3	16	48
Latex Rubber Spring	5	Latex	15	8	120

Table D.4: *SCOUT II parts list: 4 of 5. (*Drawings can be found in Appendix A.)*

Part Name	Index Number	Material	Item Mass [g]	Qty	Total Mass [g]
Leg Unit - con't (index numbers refer to drawing SCII-A02-A*)					
Garlock 16DU08 Bushing	2	Stock	15	8	120
SPAE-NAUR 600-055 Clamp	7	Stock	88	8	704
Midori LP-100FP Potentiometer	11	Al-6061-T6	35	4	140
Rubber Ball	21	Rubber	59	4	236
Aurora CW-M3 Rod End	24	Stock	9	4	36
M4x12 Socket Head Cap Screw	16	Stock	2	16	64
M5x16 Socket Head Cap Screw	19	Stock	4	4	16
M3x3 Set Screw	20	Stock	<1	16	2
ϕ3mm Retaining Ring	22	Stock	<1	8	<1
M3 Washer	14	Stock	<1	8	1
M4 Washer	15	Stock	<1	32	10
M5 Washer	18	Stock	<1	4	2
M4 Nut	17	Stock	<1	16	12
Main Body (index numbers refer to drawing SCII-A01-A*)					
Body Shaft	2	Al-6061-T6	81	4	324
Body Bracket	15	Al-6061-T6	19	8	152
Power Board Bracket	8	Al-6061-T6	155	1	155
RF Bracket	20	Lexan	54	1	54
Power Board	9	Stock	780	1	780
RF Unit	14	Stock	41	1	41
M3x30 Socket Head Cap Screw	12	Stock	2	4	8
M4x10 Socket Head Cap Screw	7	Stock	2	4	8
M4x16 Socket Head Cap Screw	5	Stock	3	16	48
M5x30 Socket Head Cap Screw	17	Stock	6	8	48
M3 Washer	10	Stock	<1	4	<1
M4 Washer	4	Stock	<1	20	6
M5 Washer	16	Stock	<1	8	4
M3 Nut	11	Stock	<1	4	1
M4 Nut	19	Stock	<1	16	12
M5 Nut	18	Stock	<1	8	4
Metrican 56800 3.5x6x10 Spacer	21	Plastic	<1	4	1
				Wiring and Cabling:	$\approx$500
				Total SCOUT II mass:	**23.77 kg**

Table D.5: *SCOUT II parts list: 5 of 5. (*Drawings can be found in Appendix A.)*

Assembly Name	Drawing Number*	Unit Mass† [kg]	Qty	Total Mass† [kg]
Leg Sub-Assembly	SCII-A02-A	0.920	4	3.679
Side Electronics Sub-Assembly	SCII-A09-A	0.262	2	0.524
Main Electronics Sub-Assembly	SCII-A07-A	2.532	1	2.532
Laser Sub-Assembly	SCII-A05-A	0.499	2	0.998
Camera Sub-Assembly	SCII-A06-A	0.447	1	0.447
Transmission Sub-Assembly	SCII-A08-A	1.755	4	7.020
Front Hip Sub-Assembly (incl. camera and laser units)	SCII-A03-A	9.580	1	9.580
Rear Hip Sub-Assembly (incl. laser unit)	SCII-A04-A	8.990	1	8.990
Scout II Assembly	SCII-A01-A	23.271	1	23.271

Table D.6: *SCOUT II sub-assembly mass. (*Drawings refered to can be found in Appendix A. † Mass does not include wiring and cabling.)*

Appendix E

SCOUT II Costs

Item	QTY	Material Costs($)		Machining Costs	
		Unit	Total	Time	Cost*($)
Maxon 118777 Motor	4	US 182.60	US 730.40	N/A	N/A
Maxon 110404 Gearhead	4	US 257.00	US 1028.00	N/A	N/A
HP HEDS 5540 Encoder	4	US 81.45	US 325.80	N/A	N/A
Gearhead Sleeve	4	‡	‡	5hrs	150
Motor Spacer	4	†	†	6hrs	180
Motor Bracket	4	†	†	11hrs	330
Leg Bracket	4	†	†	8hrs	240
Leg Shaft	4	‡	‡	13hrs	390
SDP A6R25M070150 Belt	4	US 12.45	US 49.80	N/A	N/A
SDP A6A25M048NF1215 Pulley	4	US 21.97	US 87.88	12hrs	360
SDP A6A25M034DF1508 Pulley	4	US 15.40	US 61.60	9hrs	270
Garlock FMB1209DU Bushing	8	3.27	26.16	N/A	N/A
Garlock WC10DU Thrust Bushing	4	2.16	8.64	N/A	N/A
Front Hip Bracket	4	†	†	3hrs	90
Rear Hip Bracket	4	†	†	3hrs	90
Angle Bracket	16	†	†	11hrs	330
Battery Bracket	4	†	†	3hrs	90
Battery Guide	8	†	†	1hr	30
Laser/Camera Shield	5	†	†	2hrs	60
Laser/Camera Shield Bracket	10	†	†	2hrs	60
Battery	2	21.60	43.20	N/A	N/A
Main Laser Bracket	2	†	†	7hrs	210
Laser Servo Bracket	2	†	†	3hrs	90
Laser Bracket	2	†	†	14hrs	420
Laser Bushing	2	≈0	≈0	2hrs	60
Laser Support	2	≈0	≈0	2hrs	60
Aromat LM10-250 Laser Sensor	2	2754.00	5508.00	N/A	N/A
Futaba S3003 Servo	4	17.00	68.00	N/A	N/A
Main Camera Bracket	1	†	†	2hrs	30
Camera Servo Bracket	1	†	†	1hr	30
Camera Bracket	1	†	†	5hrs	150
Camera Servo/Servo Bracket	1	†	†	4hrs	120
Camera	1	≈50.00	≈50.00	N/A	N/A

Table E.1: *SCOUT II costs dated July 1998: 1 of 4. (Exchange rate: 1 US$ = 1.5 CAN$. Canadian duties on imports and taxes not included. N/A: Not Applicable. *Machining costs $30/hr. †Al-6061-T6 material costs included as a whole. ‡Steel material costs included as a whole.)*

Item	QTY	Material Costs($)		Machining Costs	
		Unit	Total	Time	Cost*($)
Camera Transmitter	1	≈30.00	≈30.00	N/A	N/A
Main Electronics Support Bracket	1	10.00	10.00	2hrs	60
AMC 12A8E PWM Servo Amplifier	4	375.00	1500.00	N/A	N/A
Adastra VNS-486 PC Board	1	US 985.00	US 985.00	N/A	N/A
Side Electronics Support Bracket	2	5.00	10.00	0.5hrs	15
SPP/SPI Board	2	206.45	412.90	N/A	N/A
ADIO Board	12	104.74	1256.88	N/A	N/A
HCTL Board	4	43.26	173.04	N/A	N/A
DAIO Board	4	97.37	389.48	N/A	N/A
RCIO Board	2	60.21	120.42	N/A	N/A
Digital In Board	1	60.21	60.21	N/A	N/A
Digital Out/Watchdog Board	1	60.21	60.21	N/A	N/A
Upper Leg	4	†	†	20hrs	600
Spring Bracket	8	†	†	7hrs	210
Spring Support	4	†	†	4hrs	120
Leg Cap	4	†	†	4hrs	120
Lower Leg	4	‡	‡	7hrs	210
Foot	4	†	†	4hrs	120
Potentiometer Bushing	8	‡	‡	4hrs	120
Potentiometer Shaft	4	‡	‡	3hrs	90
Potentiometer Clamp	8	†	†	4hrs	120
Primeline 211BA Latex Tubing	8	7.53	60.20	N/A	N/A
Garlock 16DU08 Bushing	8	3.99	31.92	N/A	N/A
SPAE-NAUR 600-055 Clamp	8	12.60	100.80	N/A	N/A
Midori LP-100FP Potentiometer	4	134.00	536.00	N/A	N/A
Rubber Ball	4	2.00	8.00	1hr	30
Aurora CW-M3 Rod End	4	42.97	171.88	N/A	N/A
Body Shaft	4	†	†	2hrs	60
Body Bracket	8	†	†	10hrs	300
Power Board Bracket	1	†	†	1hr	30
RF Bracket	1	3.00	3.00	0.5hrs	15
Power Board	1	300.00	300.00	N/A	N/A
RF Units	2	375.60	751.20	N/A	N/A

Table E.2: *SCOUT II costs dated July 1998: 2 of 4. (Exchange rate: 1 US\$ = 1.5 CAN\$. Canadian duties on imports and taxes not included. N/A: Not Applicable. *Machining costs \$30/hr. †Al-6061-T6 material costs included as a whole. ‡Steel material costs included as a whole.)*

Item	QTY	Material Costs($)		Machining Costs	
		Unit	Total	Time	Cost*($)
Metrican 17420 M4x15x6 Screw Eye	16	0.32	5.12	N/A	N/A
Metrican 56800 3.5x6x5	2	0.15	0.30	N/A	N/A
Metrican 56800 3.5x6x10	22	0.18	3.96	N/A	N/A
M2x5 Socket Head Cap Screw	4	0.05	0.20	N/A	N/A
M2x6 Socket Head Cap Screw	4	0.05	0.20	N/A	N/A
M2x10 Socket Head Cap Screw	36	0.05	1.80	N/A	N/A
M2 Washer	44	0.01	0.44	N/A	N/A
M2 Nut	36	0.01	0.36	N/A	N/A
M3x10 Socket Head Cap Screw	36	0.07	2.52	N/A	N/A
M3x20 Socket Head Cap Screw	4	0.07	0.28	N/A	N/A
M3x30 Socket Head Cap Screw	4	0.07	0.28	N/A	N/A
M3x12 Socket Head CSK Cap Screw	2	0.06	0.12	N/A	N/A
M3x20 Socket Head CSK Cap Screw	6	0.06	0.36	N/A	N/A
M3x3 Set Screw	16	0.19	3.04	N/A	N/A
M3 Washer	40	0.01	0.40	N/A	N/A
M3 Nut	26	0.01	0.26	N/A	N/A
M4x20 Hexagonal Cap Screw	16	0.11	1.76	N/A	N/A
M4x10 Socket Head Cap Screw	28	0.08	2.24	N/A	N/A
M4x12 Socket Head Cap Screw	24	0.06	1.44	N/A	N/A
M4x16 Socket Head Cap Screw	28	0.07	1.96	N/A	N/A
M4x20 Socket Head Cap Screw	8	0.07	0.56	N/A	N/A
M4x14 Socket Head CSK Cap Screw	32	0.07	2.24	N/A	N/A
M4x16 Socket Head CSK Cap Screw	16	0.07	1.12	N/A	N/A
M4x8 Set Screw	8	0.06	0.48	N/A	N/A
M4 Washer	140	0.02	2.80	N/A	N/A
M4 Split Washer	16	0.02	0.32	N/A	N/A
M4 Nut	104	0.02	2.08	N/A	N/A
M5x16 Socket Head Cap Screw	24	0.14	3.36	N/A	N/A
M5x30 Socket Head Cap Screw	8	0.20	1.60	N/A	N/A
M5 Washer	32	0.05	1.60	N/A	N/A
M5 Nut	8	0.02	0.16	N/A	N/A
M6x12 Socket Head Cap Screw	4	0.15	0.60	N/A	N/A
M6x12 Set Screw	8	0.10	0.80	N/A	N/A

Table E.3: *SCOUT II costs dated July 1998: 3 of 4. (Exchange rate: 1 US$ = 1.5 CAN$. Canadian duties on imports and taxes not included. N/A: Not Applicable. *Machining costs $30/hr. †Al-6061-T6 material costs included as a whole. ‡Steel material costs included as a whole.)*

Item	QTY	Material Costs($)		Machining Costs	
		Unit	Total	Time	Cost*($)
M6 Washer	4	0.04	0.16	N/A	N/A
#10x5/8" Socket Head Cap Screw	4	0.07	0.28	N/A	N/A
#10 Washer	4	0.01	0.04	N/A	N/A
#10 Nut	4	0.01	0.04	N/A	N/A
ϕ3mm Retaining Ring	8	0.04	0.32	N/A	N/A
Al-6061-T6 Assorted Stock	1	≈200.00	≈200.00	N/A	N/A
Steel Assorted Stock	1	≈50.00	≈50.00	N/A	N/A
Wiring and Cabling	1	≈50.00	≈50.00	N/A	N/A
Total			16 938.46		8490.00

Total SCOUT II cost	**≈ $25 428.46**

Table E.4: *SCOUT II costs dated July 1998: 4 of 4. (Exchange rate: 1 US$ = 1.5 CAN$. Canadian duties on imports and taxes not included. N/A: Not Applicable. *Machining costs $30/hr. †Al-6061-T6 material costs included as a whole. ‡Steel material costs included as a whole.)*

Appendix F

Data Sheets

maxon motor

maxon DC motor
RE Ø35 mm, Graphite Brushes, 90 Watt

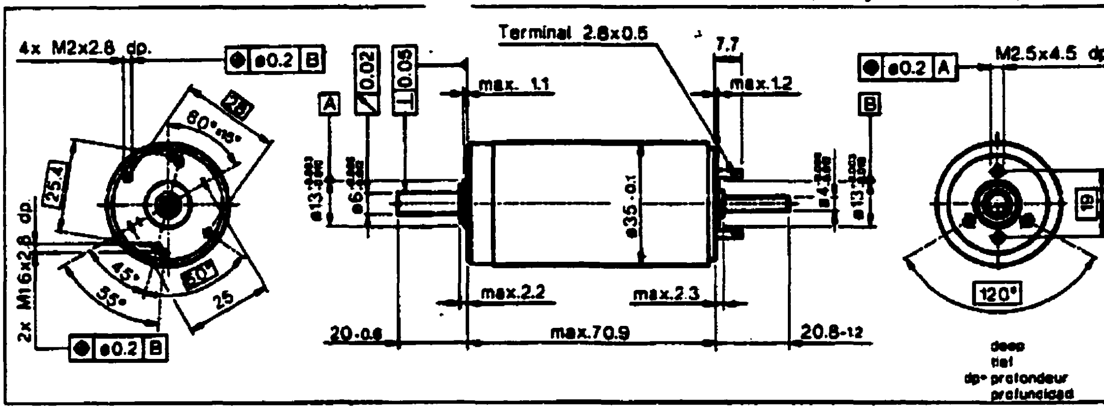

Motor Type:
maxon DC motor RE Ø35 mm . . .

Order Number
Motor Data

... Graphite Brushes, 90 W, ball bearings, 2 shafts		[illegible]	[illegible]	[illegible]	[illegible]	[illegible]	[illegible]	[illegible]	[illegible]	[illegible]	[illegible]	[illegible]	[illegible]	[illegible]	[illegible]	[illegible]
1 Assigned power rating	W	90	90	90	90	90	90	90	90	90	90	90	90	90	90	90
2 Nominal voltage	Volt	15.00	30.00	42.00	48.00	48.00	48.00	48.00	48.00	48.00	48.00	48.00	48.00	48.00	48.00	48.00
3 No load speed	rpm	7070	7220	7530	7270	6660	5870	4750	3810	3140	2570	2100	1620	1290	1060	856
4 Stall torque	mNm	672	849	1070	[illegible]	678	788	613	483	384	320	253	194	155	125	99.5
5 Speed/torque gradient	rpm/mNm	8.45	7.77	7.17	7.63	7.88	7.88	7.86	7.94	8.09	8.19	8.47	8.56	8.54	8.80	8.94
6 No load current	mA	245	124	92.8	77.4	68.7	58.7	44.7	34.2	27.2	21.8	17.2	13.0	10.1	8.27	6.82
7 Starting current	mA	44800	24400	20300	15500	12900	10100	6430	4180	2740	1830	1180	704	448	286	193
8 Terminal resistance	Ohm	0.334	1.23	2.07	3.09	3.72	4.75	7.46	11.5	17.5	28.2	40.5	68.2	107	161	248
9 Max. permissible speed	rpm	8200	8200	8200	8200	8200	8200	8200	8200	8200	8200	8200	8200	8200	8200	8200
10 Max. continuous current	mA	4000	2740	2150	1780	1620	1450	1170	944	768	620	508	382	313	256	206
11 Max. continuous torque	mNm	77.7	107	113	111	111	110	111	112	111	110	109	108	108	107	106
12 Max. power output at nominal voltage	mW	152000	176000	203000	161000	150000	116000	78000	48400	31800	21200	13700	8070	5100	3380	2150
13 Max. efficiency	%	80.6	84.1	85.5	85.2	84.8	84.2	83.1	81.9	80.4	78.6	76.8	74.3	71.8	68.2	65.1
14 Torque constant	mNm/A	18.4	35.9	52.5	62.2	68.0	76.8	95.2	119	144	175	214	276	348	416	516
15 Speed constant	rpm/V	481	248	182	154	140	126	100	80.5	66.4	54.6	44.7	34.6	27.5	22.9	18.5
16 Mechanical time constant	ms	5.60	5.38	5.29	5.19	5.18	5.18	5.17	5.15	5.15	5.14	5.13	5.12	5.11	5.11	5.11
17 Rotor inertia	gcm²	65.5	65.5	68.8	65.0	64.5	62.7	62.8	62.8	60.7	59.9	57.9	57.2	57.2	55.5	54.5
18 Terminal inductance	mH	0.08	0.34	0.62	0.87	1.04	1.29	2.04	3.16	4.65	6.80	10.3	17.1	26.9	38.3	59.7
19 Thermal resistance housing-ambient	K/W	6.20	6.20	6.20	6.20	6.20	6.20	6.20	6.20	6.20	6.20	6.20	6.20	6.20	6.20	6.20
20 Thermal resistance rotor-housing	K/W	2.00	2.00	2.00	2.00	2.00	2.00	2.00	2.00	2.00	2.00	2.00	2.00	2.00	2.00	2.00

Operating Range **Comments** (Details on page 38)

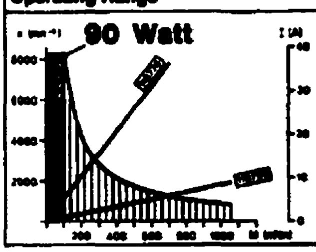

Recommended operating range

Continuous operation
In observation of above listed thermal resistances (lines 19 and 20) the maximum permissible rotor temperature will be reached during continuous operation at 25°C ambient.
= Thermal limit.

Short term operation
The motor may be briefly overloaded (recurring).

Stock program
Standard program
Special program (on request)

- Axial play 0.05 - 0.15 mm
- Max. ball bearing loads
  - axial (dynamic)
    - not preloaded 5.6 N
    - preloaded 2.4 N
  - radial (5 mm from flange) 28 N
  - Press-fit force (static) 110 N
  - same as above, shaft supported 1200 N
- Radial play ball bearings 0.025 mm
- Ambient temperature range -20/+100°C
- Max. rotor temperature +155°C
- Number of commutator segments 13
- Weight of motor 340 g
- Values listed in the table are nominal. For applicable tolerances (see page 33) and additional details please request our computer printout.

maxon Modular System

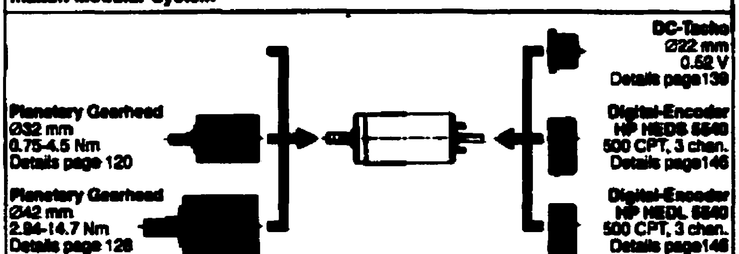

- Option: Hollow shaft as special design.

April 1997 edition / subject to change

maxon DC motor 77

Figure F.1: *Maxon 90W motor data sheet, from [37].*

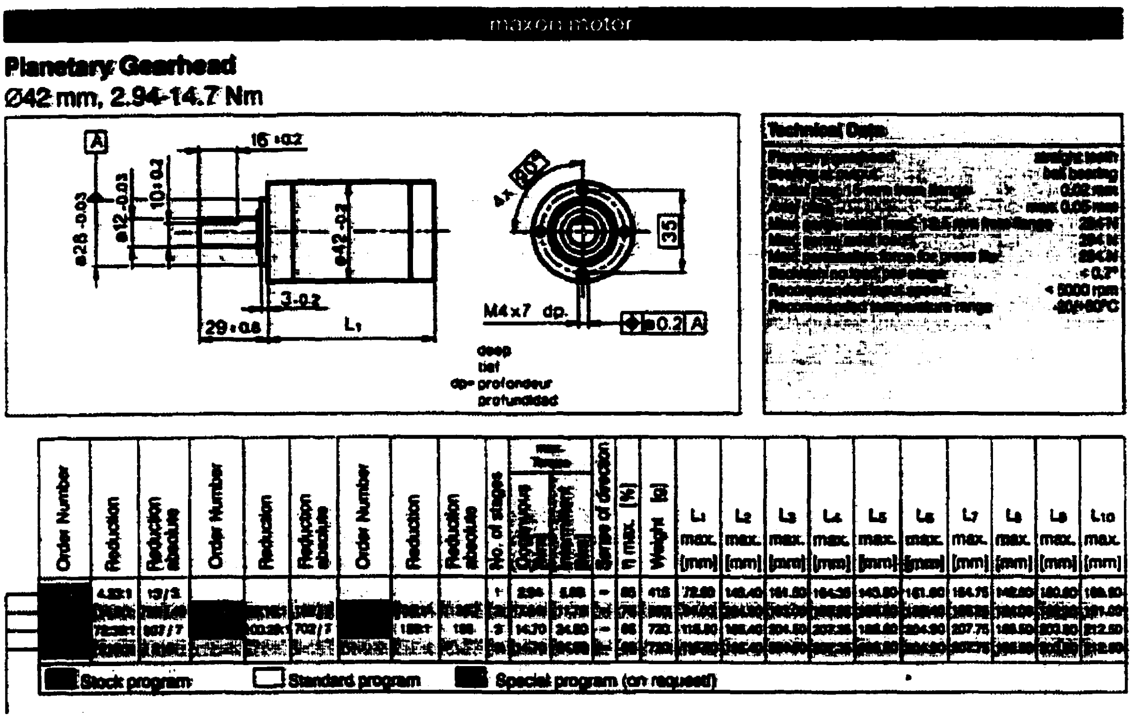

Figure F.2: *Maxon planetary gearhead data sheet, from [37].*